Norwegian University of Life Sciences
Faculty of Biosciences
Department of Animal and Aquacultural Sciences

Philosophiae Doctor (PhD)
Thesis 2017:36

Characterization of genes and gene products influencing carotenoid metabolism in Atlantic salmon

Karakterisering av gener og genprodukter involvert i karotenoidmetabolisme i Atlantisk laks

Nina Zoric

Characterization of genes and gene products influencing carotenoid metabolism in Atlantic salmon

Karakterisering av gener og genprodukter involvert i karotenoidmetabolisme i Atlantisk laks

Philosophiae Doctor (PhD) Thesis

Nina Zoric

Department of Animal and Aquacultural Sciences

Faculty of Biosciences

Norwegian University of Life Sciences

Ås, 2017

Thesis number 2017:36
ISSN 1894-6402
ISBN 978-82-575-1437-2

Acknowledgments

This thesis is funded by the Norwegian University of Life Sciences and support from the Research Council of Norway grant 221734/O30 and the breeding company AquaGen.

Firstly, I would like to express my sincere gratitude to Prof. Dr. Dag Inge Våge and Dr. Jacob Torgersen for the continuous support of my Ph.D. study and related research. Jacob guidance helped me in all the time of research and I appreciate all his contributions of time and ideas to make my Ph.D. experience productive and stimulating, especially during tough times in the Ph.D. pursuit. Dag Inge provided me with the tools that I needed for choosing the right direction and successfully completing my dissertation. I could not have imagined having better mentors for my Ph.D. study. It has been an honor to be your Ph.D. student.

I would like to express my special appreciation and thanks to my co-supervisors Prof. Dr. Sigbjørn Lien and Dr. Thomas Moen, for all their comments and suggestion on the last manuscript. I would also like to thank to Dr. Fabian Grammes for his brilliant work about the RNA sequencing data analysis, for his precious time and patience. The recombinant protein studies would not be possible without support of Dr. Kim Remans and entire Pep-Core at the EMBL in Heidelberg and Dr. Johannes Lintig, who helped me with the most challenging parts of my Ph.D. experimental work. I am grateful to Dr. Matthew Kent, whose comments greatly improved my work. I am also grateful to Dr. Siri Fjellheim, my master supervisor and an example of a strong and powerful woman, whose energy, joy and enthusiasm for research were contagious for me, even during my Ph.D. All the members of the CIGENE have contributed immensely to my personal and professional time at the NMBU. With a special mention to the lab-ladies, who have been a source of friendships, good advice and support. What a cracking place to work! Without you, CIGENE would never be as nice and prosperous as it is today.

Last but not the least; the greatest thanks goes to my forever interested, encouraging and always-enthusiastic parents, who supported me in all my pursuits. They were always keen to know what I was

doing and how I was proceeding, although it is likely that they never grasped what it was all about. You are my greatest inspiration, my motivation and energy.

Table of contents

Summary

Distinct red flesh color is a unique trait of the fish genera *Oncorhynchus*, *Salvelinus*, *Salmo* and *Parahucho*. In this thesis we have investigated its molecular basis in Atlantic salmon to better understand how and why it developed during the evolution in just these genera. In the aquaculture industry, the red muscle color in salmon is important for consumers perception of filet quality. The red flesh color is mainly caused by accumulation of the carotenoid astaxanthin in muscle tissue, obtained through a crustean rich diet in the wild, or by feed supplementation of syntetic astaxanthin in aquaculture.

Individual differences in salmon flesh color intensity in groups fed identical amounts of pigment, indicate variable uptake and metabolic processing between individuals. In order to improve or standardise the flesh coloration, genetic factors and molecular mechanisms responsible for the variation must be identified. Previous studies recognized that low absorption and/or high metabolic transformation rate are critical factors for the observed low retention of astaxanthin in muscle. Previous genome wide association studies have strongly indicated that the β-carotene oxygenases *bco1* and *bco1l* are involved in the flesh coloration. The aim of this thesis was to further investigate how *bco1* and its paralogue *bco1l* influence astaxanthin metabolism and to discover additional genes that might contribute to the flesh color variation.

In paper I, the fast freeze substitution tissue preservation method was developed as a useful tool for the experiments performed in paper II and paper III. The main advantage of this preservation method over the standardly used formalin fixation is that fixed tissues are suitable for more than only one type of analysis. Tissue morphology, RNA and proteins are very well preserved with freeze fixation and samples can be used for microscopy, but also for highly sensitive downstream analysis like RNA sequencing and protein and immunoblotting analysis.

In paper II, the functional roles of *bco1* and *bco1l* in carotenoid metabolism were investigated using molecular cloning and gene expression methods, western blotting and confocal microscopy. By immunostaining methods, we showed that Bco1 is a cytosolic enzyme primarily located in the subapical regions of enterocytes. These analyses also revealed that Bco1 is two folds more abundant in intestine of pale compared to red-fleshed fish. We did not manage to develop Bco1l specific antibodies, which explains the lack of corresponding analyses for Bco1l. By co-expressing either of the two genes with a β-carotene synthesizing cassette in *E. coli*, Bco1l showed a clear 15,15'-oxygenase activity on β-carotene, while Bco1 did not show any cleavage activity in this particular assay. Based on these experiments, we hypotheised that Bco1 is involved in astaxanthin degradation, while Bco1l degrades other carotenoids. RNA sequencing and gene set enrichment analysis (GSEA) showed that lipid-metabolism related genes, indicating that accumulation of astaxanthin in salmon is related to lipid metabolism.

In paper III a region on chromosome 2 containing SNPs strongly associated with salmon flesh coloration were identified by genome wide association mapping. Fine mapping of this region suggested that ATP binding cassette subfamily G member 2 (*abcg2-1a)* is another QTL for flesh color. A missense mutation in *abcg2-1a*, causing an amino acid substitution in amino acid position 230 (Asn230Ser), is proposed to be a causative mutation. Abcg2 is a known exporter of lipophilic molecules, and we suggest that Abcg2-1a is involved in salmon flesh coloration by translocating astaxanthin from enterocytes to the intestinal lumen, thus limiting the astaxanthin availability for muscle deposition. The Abcg2-1a protein was 2.5 folds more abundant in the pale-fleshed fish than in red-fleshed fish, supporting that this exporter plays a role in the flesh pigmentation.

List of papers

Paper I

Zoric N, Grammes F, Våge DI, Torgersen J. **Freeze substitution – Tissue fixation for preserving morphology and high quality RNA.** Manuscript

Paper II

Zoric N, Torgersen J, Grammes F, von Lintig J, Våge DI. **Functional divergence of beta-carotene oxygenase 1 enzymes after gene duplication in salmon (*Salmo salar*).** Manuscript

Paper III

Zoric N, Moen T, Korsvoll SA, Kjøglum S, Santi N, Lien S, Våge DI, Torgersen J. **A missense mutation in the *abcg2-1a* gene (ATP-binding cassette sub-family G member 2) is strongly associated with muscle color in Atlantic salmon (*Salmo salar*).** Manuscript

1. Literature review

1.1. Red coloration of salmon flesh

All species belonging to *Oncorhynchus*, *Salvelinus*, *Salmo*, and *Parahucho* genera of the Salmonidae family have a unique and characteristic red flesh color. The red colored muscle of these species is important for market acceptance, with only fillet freshness regarded as more important for consumer approval [1, 2]. The reddish muscle color originates from carotenoids ingested by the fish, but the underlying biology seems to be specialized since several other fish species that share the same habitat and have a similar diet do not have colored flesh (Fig. 1).

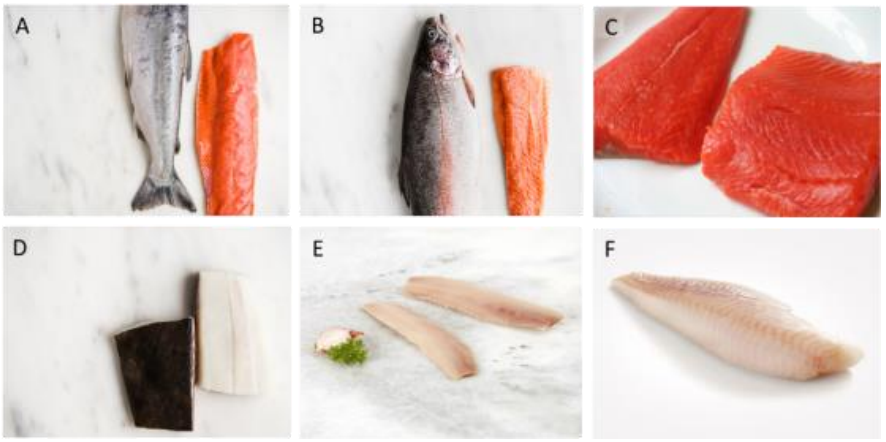

Figure 1. Different filet colors (A) Atlantic salmon (*Salmo salar*) (B) Rainbow trout (*Oncorhynchus mykiss*) (C) Sockeye salmon (*Oncorhynchus nerka*) and other commercial marine species (D) Atlantic halibut *(Hippoglossus hippoglossus*) (E) Atlantic herring *(Clupea harengus*) (F) Atlantic cod (*Gadus morhua*).

Vertebrates are incapable of *de novo* synthesis of carotenoids. The main source of these nutrients for wild salmon are aquatic organisms such as crustaceans, while farmed salmon receive a diet specifically supplemented with synthetic astaxanthin and to the lesser extent canthaxanthin [3, 4]. Optimal product quality is defined by an astaxanthin content above 6 mg/kg with minimal variation between fish. Levels in farmed Norwegian Atlantic salmon muscle vary from 5 to 8 mg/kg, with a trend towards decreasing astaxanthin content during the most recent years, for unclear reasons.

Furthermore, the deposition rate of carotenoids in organs and tissues differs among species such as Atlantic salmon (*Salmo salar*) and rainbow trout (*Oncorhynchus mykiss*) [5]. In addition to these, the difference between red-fleshed salmonids and fish species without pigmented flesh is also interesting from a biological and evolutionary aspect and further studies may also generate knowledge of carotenoid metabolism in general.

1.2. Carotenoids: colors with functions

Carotenoids are yellow or red organic pigments composed of polyene hydrocarbon chains, often with rings attached (Fig. 2).

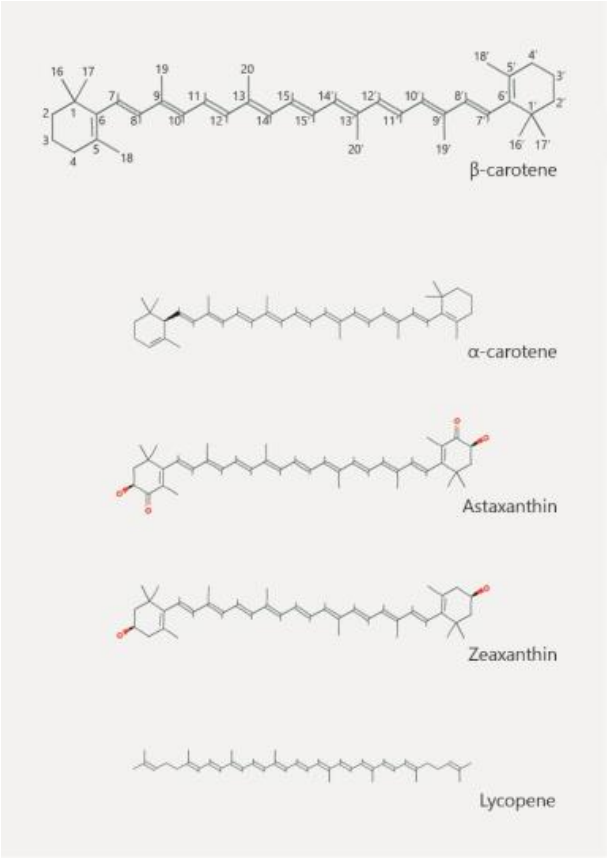

Figure 2. Chemical structures of carotenoids. The carbon-numbering scheme is shown for β-carotene. Carotenes are pure hydrocarbons and xanthophylls have oxygen groups attached (indicated in red).

Provitamin-A carotenoids are a particular subgroup of carotenoids that can be modified by oxidative cleavage at their central double-bond to yield two molecules of retinal (vitamin A aldehyde) (Fig. 2). Examples of provitamin-A includes β-carotene, β-cryptoxanthin and α-carotene, some of which are shown in Fig. 2.

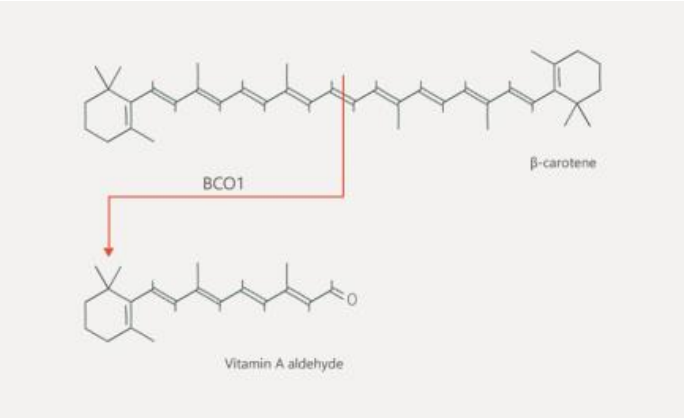

Figure 3. Oxidative cleavage of β-carotene by BCO1. BCO1 cleaves provitamin-A carotenoids at the central 15,15' double bond to yield two molecules of vitamin A aldehyde.

Provitamin-A carotenoids are pure hydrocarbons and are classified as carotenes [6]. These are distinct from oxygen containing carotenoids such as astaxanthin, canthaxanthin, zeaxanthin and lutein which are classified as xanthophylls [6] and are not typical provitamin-A source in mammals and birds [7]. The presence of oxygen groups affects the solubility of carotenoids, making xanthophylls more polar than carotenes [8] and more soluble in water.

Astaxanthin naturally exists in three stereoisomer forms namely (*3R,3'R*), (*3S,3'S*) and (*3R,3S*) (Fig. 4). The *3S,3'S* is the main form in wild salmon, while synthetic astaxanthin and thus farmed salmon contain more of *3S,3'R* and *3R,3'S all-trans* astaxanthin [9]. There are no evident differences in absorption and deposition between the stereoisomers [10].

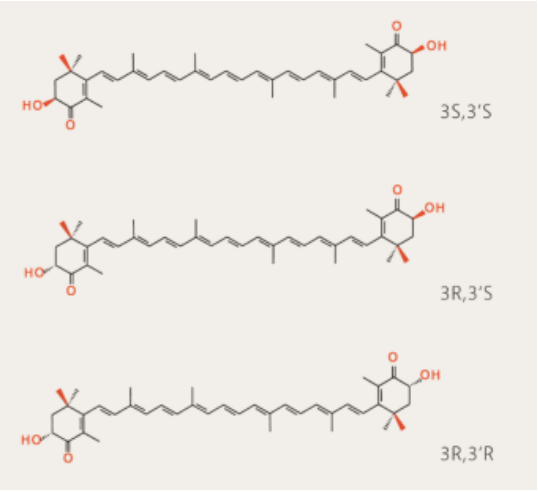

Figure 4. Chemical structures of astaxanthin stereoisomers: *(3S,3'S)-* ; *(3R,3'S)-* ; *(3R,3'R)-* astaxanthin.

The most common sources of astaxanthin are yeast *Phaffia rhodozyma*, the microalgae *Haematococcus pluvialis* or products based on crustaceans. The use of synthetic astaxanthin is justified because there is no significant difference in fillet color between trout fed on synthetic compared to those fed natural astaxanthin [9] and both forms also have similar biochemical and antioxidant properties [11-14]. The oxygen-containing groups in astaxanthin affect its solubility, but also orientation in cell membrane, in which they are important building blocks [15]. Namely, β-carotene (or other less polar carotenoids) are located deep within the hydrophobic lipid core, while astaxanthin (or other more polar carotenoids) span the membrane bilayer [16] (Fig. 5). Enzymes that utilize carotenoids, which have distinct orientation in the membrane lipid bilayer, might differ in the substrate binding sites, which ensures optimal activity of the cleavage reaction.

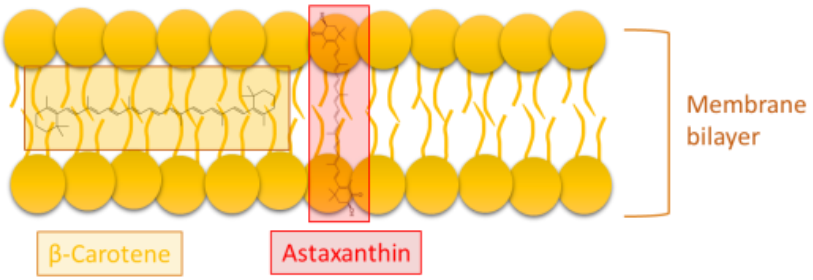

Figure 5. The localization of carotenoids in biological membranes.

The biological importance of carotenoids and their metabolites is evident in the fact that they participate in more than 1000 cellular processes involved in reproduction, embryonic development, vision, growth, cellular differentiation and proliferation, tissue maintenance and lipid metabolism [17]. β-carotene is a main source of vitamin A, and deficiencies can lead to blindness, decreased immune function, and even death [18]. Carotenoid metabolism also affects lipid metabolism, and several recent studies have focused on the crosstalk between retinoid and lipid metabolic pathways [19, 20]. Carotenoids are very potent antioxidants [21, 22] and free radical scavengers [23, 24] that prevent lipid oxidation [24-26] and affect immune status and reproduction [27, 28]. Circulating plasma levels of the xanthophylls lutein and zeaxanthin are associated with a decreased risk of age related macular degeneration [29, 30], and their accumulation in macula lutea of the primate eyes may provide protection by absorbing high energy light [31]. Finally, in a very wide range of organisms these pigments can accumulate in specific tissues, giving characteristic colors to many birds, marine invertebrates and fishes. This may have a role in species-specific camouflage and communication through coloration of integuments and plumage (Fig. 6) [32].

Figure 6. Examples of vivid coloration in different animals due to carotenoids.

Several evolutionary scenarios explaining flesh pigmentation in salmonids have been proposed, including linking astaxanthin deposition to somatic cell maintenance during long distance migrations under starvation, and proposing that red skin coloration is beneficial for reproduction [33]. Atlantic salmon accumulates astaxanthin in its skin, flesh, and (if female) eggs. At the young juvenile stage, astaxanthin is preferentially deposited in the skin, but as the fish matures deposition in the muscle increases [34]. Finally, upon sexual maturation, carotenoids are relocalized from muscle to skin and gonads [35-37]. Within these tissues, astaxanthin molecules can be deposited as protein conjugates or esterified with one or two fatty acids, retaining the antioxidant properties while being protected against spontaneous degradation [38].

Despite these studies characterizing the distribution of astaxanthin in Atlantic salmon, its biological role in fish physiology is unclear with several possible roles being proposed. One hypothesis suggests that increased astaxanthin levels in blood, recruited from the muscle during the energetically costly migration period, may contribute to normal tissue and organ functioning. An alternative suggestion is based on the observation that prior to spawning astaxanthin is

transported from muscle tissue to eggs and skin in females and males respectively [4]. Redder skin may function to attract females [39], while high carotenoid content in eggs may improve their viability [40, 41]. Another theory proposes that astaxanthin and its metabolites are important signaling and regulatory factors in fish metabolism that may improve viability during embryonic development, enhance growth, increase maturation rate and fecundity, particularly in harsh conditions of limited oxygen and intense light during spawning [42, 43].

The beneficial survival effects of astaxanthin are well documented with Atlantic salmon fed diets supplemented with less than 5.1 mg/kg astaxanthin dry diet showing reduced growth and lipid levels. Reducing astaxanthin concentrations further to below 1 mg/kg dry diet leads to 50% mortality of fry, which is significantly greater than fry fed with 5.1 mg/kg astaxanthin concentrations which demonstrated mortality rates <10% [44]. This study demonstrated that Atlantic salmon fries require astaxanthin in their diet for the growth and survival and strongly suggested a provitamin-A function for astaxanthin [44, 45].

1.4. Carotenoids as a source of provitamin-A

Carotenoids are a large class of pigments and more than 750 different chemical structures have been identified [46]. Humans obtain most or their carotenoids in the form of β-carotene, which is therefore the main source of provitamin-A [17] followed by β-cryptoxanthin and α-carotene [47]. Xanthophylls (oxygen containing carotenoids) are also an important carotenoid source, but they are not typical provitamin-A source in mammals and birds. They do not usually yield retinal by oxidative cleavage of the central bond and their role is still poorly understood [7]. However, they may be converted to vitamin A in retinol deficient rats [48]. In the aquatic ecosystem, carotenoid variation is particularly large, and while xanthophylls are notably abundant, β-

carotene is present at substantially lower levels compared to typical mammalian diets [6]. Different carotenoid profiles in the diets of aquatic and terrestrial species are likely to be related to the observed differences in carotenoid metabolism, and may explain why fish possess enzyme systems that can transform astaxanthin and canthaxanthin into vitamin A [5, 45, 49-54]. In addition to salmonids, a provitamin-A effect of astaxanthin has been reported in other fish species, suggesting that this metabolic conversion may be more widespread among fish than previously recognized [5, 50, 51, 53-55]. Astaxanthin can be converted to vitamin A in freshwater fishes like Guppies (*Lebistes reticulatus*) and Plaites (*Xiphophorus variatus*) [49], but also in marine fish Black brass (*Micropterus salmoides*) [52]. The intestinal lining and liver are quantitatively most important organs for catabolic conversion of carotenoids. The metabolic route for astaxanthin conversion into vitamin A is not known, but idoxanthin (3,3',4'-trihydroxy-β,β-carotene-4-one) (Fig. 7) is a metabolite detected in plasma rapidly after astaxanthin consumption in Atlantic salmon [35].

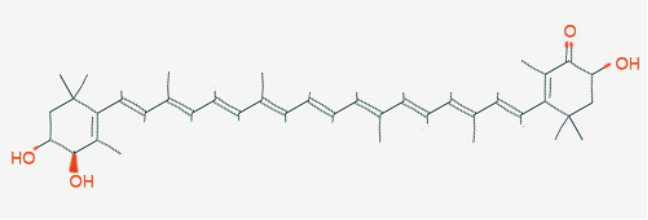

Figure 7. Structural formula of astaxanthin metabolite idoxanthin. Idoxanthin is formed by reduction of the keto group in astaxanthin.

The idoxanthin content of small fish is higher than in large fish suggesting that the metabolic capacity to transform absorbed astaxanthin decreases with age in salmonid fishes [5, 35].

Interestingly, if dietary retinol is available, these carotenoids are not metabolised to vitamin A [5].

These studies suggest there are alternative metabolic routes for conversion of carotenoids into vitamin A in different species, and these processes are very tightly regulated to ensure optimal vitamin A supply to tissues. The different mechanisms that govern the metabolic transformation remain to be elucidated.

1.5. Carotenoid metabolism: uptake, cleavage, transport, deposition

To understand the mechanisms driving salmonid flesh coloration, it is important to assimilate knowledge about astaxanthin absorption, enzymatic cleavage and muscle deposition. While only few studies have been carried out in fish (reviewed in [60]), these processes have been studied extensively in mammalian systems with a focus on mammalian provitamin-A carotenoids.

Carotenoid uptake begins in the gut with their release from ingesta, and is followed by their incorporation into lipid soluble mixed micelles, from where carotenoids can be absorbed into enterocytes [61-63]. In addition to passive diffusion [62], absorption in mammals is facilitated by several proteins including scavenger receptor BI (SCARB1) [64-68], cluster determinant type 36 (CD36) [66, 68, 69] and Niemann Pick C1 Like 1 (NPC1 [64, 66, 70] all of which mediate absorption of β-carotene, α-carotene, lutein and β-cryptoxanthin. Additionally, SCARB1 also transports lutein and lycopene [66, 70] while NPC1 transports lutein and zeaxanthin [64, 70]. In Atlantic salmon, Scarb1 and its paralog Scarb1-2 are highly expressed in the intestine and putatively facilitate carotenoid transport [71, 72]. ATP-binding cassette superfamily (ABC transporters) and fatty acid-binding proteins (FABPs) might also play a role as they display a

broad ligand specificity [62]. In the enterocyte, provitamin-A carotenoids are partially converted to a primary cleavage product, retinal (vitamin A aldehyde), by the enzyme β-carotene 15-15'-oxygenase (BCO1) (Fig. 3). Retinal can be converted to retinol which is esterified by lecithin:retinol acyltransferase (LRAT) and/or acyl-CoA-dependent transferases [73]. Next, retinyl esters together with non-cleaved carotenoids and fatty acids are packaged into chylomicrons for secretion into lymph or in case of fish, which do not have lymphatic system, directly into the blood [74]. Astaxanthin-containing chylomicrons can be stored in the liver, the major organ for storage of retinyl esters and carotenoids [75, 76]. The exact process of astaxanthin metabolism in the liver is unknown, as is the case with β-carotene metabolism. We do know, however, that the chylomicron-delivered astaxanthin that is not metabolized is repackaged into very low-density lipoproteins (VLDL) before being sent out into the blood once more. Astaxanthin is then assumed to be brought to the muscle by circulating albumin, which associates with astaxanthin after its release from astaxanthin-containing VLDL via lipoprotein lipase (LPL) [35, 77, 78]. The mechanism serving to keep astaxanthin in muscle is unclear, with binding to nonspecific targets [79, 80] and α-actinin [81] being proposed, together with the involvement of uncharacterized molecules [82]. Irrespective, astaxanthin remains in salmon muscle until the animal begins to sexually mature which induces relocalization of carotenoids from muscle to skin and gonads [34-37].

2. Interspecific vs. intraspecific color variation

Among the four genera of Salmonidae family with the unique red flesh coloration, there is a considerable variation in muscle retention of pigments, with Pink and Chum salmon reaching 5 mg/kg, Atlantic salmon 7 mg/kg and Sockeye more than 30 mg/kg astaxanthin. There is also a variation in response to dietary astaxanthin and muscle color among individuals belonging to the same species. It is thus important to explain the uniqueness of the pigmented muscle color in the four salmonid genera (Fig. 1), but also to determine factors causing the color variation within the species (Fig. 8). Different carotenoid digestibility and gastrointestinal absorption of ingested carotenoids, different metabolism of carotenoids or/and specific astaxanthin binding receptors in muscle uniquely present in the red-fleshed fish are some that might attribute to these.

Figure 8. Variation in flesh color between two Atlantic salmon individuals.

Muscle retention of dietary pigment in Atlantic salmon is around 10% [83-85], and there are several indications that low absorption and/or high metabolic transformation rate are critical factors for the observed low amount of astaxanthin available in intestine upon food ingestion [56,

59, 78]. Extreme increase in the astaxanthin plasma concentrations were acquired in Atlantic salmon, rainbow trout and Atlantic cod upon intraperitoneal injection of astaxanthin [57, 58]. In Atlantic salmon the pigment concentrations in plasma and muscle were correlated and increased linearly- 20 times in plasma and 15 times in muscle, compared to Atlantic salmon fed astaxanthin supplemented diets (Fig. 9) [57, 58, 83]. These are strong indications that neither muscle binding capacity nor transport can explain poor muscle retention of astaxanthin in Atlantic salmon. Low retention is rather due to low absorption of astaxanthin and/or high metabolic transformation.

Figure 9. Atlantic salmon with intraperitoneally injected (A) 0 and (B) 100 mg astaxanthin (Adapted with permission from the Trine Ytrestøyl PhD thesis).

The same experiment helped us to better understand the unique ability for accumulating carotenoids in species of the four salmonid genera. In contrast to Atlantic salmon, the muscle of

intraperitoneally injected white-fleshed Atlantic cod contained only 1 mg/kg, despite a high plasma concentration of about 20 mg/kg. This shows that the capacity of plasma to carry astaxanthin is not the limitation for retention of ingested astaxanthin. One possible explanation is that astaxanthin binding receptors present in the muscle of red-fleshed fish, but absent in the white-fleshed fish account for the observed color difference [57, 58]. Consequently, differences between red and white-fleshed fish species is linked to muscular astaxanthin binding molecules. A dynamic model of astaxanthin uptake, transport, utilization and metabolism in Atlantic salmon also predicted that the cellular incorporation mechanisms in the muscle will be an important source of variation in muscle color of these fish species [86].

3. Identification of genetic variation underlying flesh color variation in Atlantic salmon

The costs of astaxanthin supplementation have decreased over time due to the improvement in astaxanthin processing industry and synthetic astaxanthin production. In 2015 it counted for 3% of the total feed costs, which is much less compared to 10 years ago, but it still constitutes notable expense for salmon farming industry (pers. comm. C. Haraas, EWOS). Furthermore, in organic farming, synthetic astaxanthin is not currently allowed and the cost for natural sources are considerable. Salmon flesh color is a complex trait with heritability estimates ranging between (0.1-0.6) and a broad phenotypic variation [87, 88]. Astaxanthin concentrations in plasma are partially genetically determined and they vary greatly among individuals (<0.5-70% of the total carotenoid content) [89-91], and indicates that prospects for continued genetic improvement and cost reduction are high.

Two recent QTL studies on salmon linked flesh color to polymorphisms on chromosome 26 [92, 93]. More specifically, to a chromosomal region harboring two genes likely involved in degradation of carotenoids, beta-carotene-15-15'-oxygenase 1 (*bco1*) and beta-carotene-15-15'-oxygenase 1 like (*bco1l)*. Both genes also describe differential expression between red and pale fish, suggesting that carotenoid cleavage oxygenase (CCO) play important role in regulation of salmon flesh color. Additional genes might also be involved and their discovery is of a considerable interest.

3.1. beta-carotene-15-15'-oxygenase 1

Although carotenoids are known for the intensive color they confer to plants and animals, the cleavage products of carotenoids (apocarotenoids) are colorless. Thus, Bco1/Bco1l as putative carotenoid cleavage enzymes from CCO protein family, might affect salmon flesh coloration through controlling the amount of carotenoids available for muscle deposition. The molecular characterization of BCO1 was first reported in 2000 in an invertebrate, the fruit fly *Drosophila melanogaster* [94]. Since then it has been studied in humans [95, 96], chicken [97, 98], mice [99, 100] rat [101], cows [102], zebrafish [103] and *Caenorhabditis elegans* [104]. β-carotene has been shown to be the most efficient substrate for BCO1 [98, 105]. BCO1 interacts only with carotenoids containing minimum 30 carbons and at least one unmodified ionone ring, cleaving them centrally at the 15,15' double bond yielding two molecules of vitamin A [95, 97, 106]. The latter implies that astaxanthin is not typical substrate for BCO1. However, BCO1 cleavage of lycopene has been reported for the mouse ortholog [100], but the human and chicken homologs do not have this ability [98, 99, 105].

BCO1 is a cytosolic enzyme [105] and exists as a monomer [107, 108]. It is expressed in a variety of tissues [96]. Although BCO1 is mostly known for its role in vitamin A synthesis, tissue activity suggests a broader role for BCO1 than just breaking down carotenoids after a meal and generating retinal from dietary carotenoids. Recent studies tie BCO1 to lipid metabolism through esterification [20, 29, 109, 110] but the exact role and the underlying mechanism is elusive.

Non-provitamin A carotenoids, such as canthaxanthin and zeaxanthin fed to rats impeded BCO1 cleavage of β-carotene by 71 and 40%, respectively [111, 112]. Whether this is because they

have inhibiting effect on BCO1 function is not known. Astaxanthin has a similar structure to canthaxanthin and zeaxanthin, with hydroxyl and ketone groups in each β-ionone ring. These additional chemical groups were suggested to be crucial for the observed inhibitory effect. Astaxanthin might therefore have a broader role in carotenoid metabolism than initially assumed.

BCO1 knockout mice fed β-carotene as the only source for vitamin A became retinoid-deficient and accumulated large amounts of β-carotene in tissues like visceral adipose tissue, subcutaneous adipose tissue, and in the intestine [109]. A similar study in zebrafish showed that Bco1 is crucial for normal embryonic development, which cannot be substituted by Bco1l [103]. Mutations in the coding region and in the proximal promoter of BCO1 in chicken were associated with accumulation of carotenoids in the breast meat and consequently with the change of the breast meat color, mainly caused by accumulation of lutein and zeaxanthin [113]. Even though these two carotenoids are not considered to be substrates of the BCO1 enzyme, the observed results were explained by that they could be converted into β-carotene before symmetric cleavage by BCO1, as already described for related xanthophylls- canthaxanthin and astaxanthin [48, 53]. Lycopene accumulation was noted in mice lacking BCO2, another carotenoid cleavage enzyme that belongs to the same protein family as BCO1 [114]. Mutations in this gene were also detected to cause yellow skin in chicken [115], xanthophyll accumulation and yellow fat in sheep [116], and altered carotenoid content in serum and milk in cow [117]. BCO2 is the only known mammalian xanthophyll cleavage enzyme which cleaves substrate eccentrically (at 9',10' and 9,10 double bonds). Although it probably plays an important role in salmon carotenoid metabolism, it is beyond the scope of this study and will not be further discussed. Here, we focus on the *bco1/bco1l* paralogs, as the QTL studies suggested that these are the most likely candidates

underlying the color variation in Atlantic salmon. For a thorough review about the BCO2 function, reader can refer to [118].

4. Summary of introduction

The current knowledge illustrates that muscle color in Atlantic salmon is controlled by complex mechanisms that are affected by genetic variation. Potentially, a number of molecular mechanisms in several cell types and tissues affects the fate of dietary astaxanthin in Atlantic salmon. Despite the gaps in knowledge it seems like neither the muscle binding capacity, nor the plasma transport capacity limit the efficient utilization of astaxanthin in Atlantic salmon. Observed variation in muscle redness is therefore most likely due to individual differences in astaxanthin metabolism in the gastrointestinal tract. Previous findings emphasize that gene variants involved in enterocyte carotenoid metabolism are likely to explain individual phenotypic variation. The genes identified so far are *bco1*/*bco1l*, which degrade carotenoids.

On the other hand, interspecific contrasts in flesh color seems to be due to the specific mechanisms of astaxanthin uptake in muscle that are present in red but absent in pale-fleshed fish. Further studies are needed to understand astaxanthin deposition mechanisms unique to red-fleshed salmonids, to identify all the genes/proteins involved in astaxanthin/carotenoid metabolism and assess whether other types of genetic variation can modulate astaxanthin status among Atlantic salmon. Such research could be applied for developing Atlantic salmon fillet with increased astaxanthin retention, more even color, and yet at the reduced costs for feed supplementation. It would also shed the light on evolutionary scenario behind the salmonid pink muscle phenotype.

5. Aim of the thesis

The aim of the thesis was to provide a better understanding of factors causing differences in flesh color among Atlantic salmon. Of particular interest were the roles of *bco1* and *bco1l* but additional QTLs that contribute significantly to this trait were also explored.

6. Research outline and summary of work

The first part of this thesis copes with development of a tissue preservation method, called freeze substitution, for use in different downstream applications. Biological samples for laboratory analysis give the researcher a glimpse into the molecular processes occurring if prepared correctly. Secondly, my work focused on functional characterization of *bco1* and *bco1l*, paralogue genes that are known to be strongly associated with fillet color in Atlantic salmon. In the last part, the salmon *abcg2* was identified as a candidate gene influencing flesh pigmentation. A missense mutation causing an asparagine to serine substitution in this gene is identified as the most likely functional change (QTN). *Bco1*, *bco1l* and *abcg2* have profound roles in carotenoid metabolism, for which the intestine and liver are quantitatively important organs. Through specific mechanisms they determine the amount of dietary astaxanthin that will be available for muscle deposition, which in turn defines redness of salmon flesh. This research, together with the association studies [92, 93] revealed that gastrointestinal absorption and metabolic transformation of dietary carotenoids determine the retention of ingested astaxanthin. This work has progressed the understanding of these mechanisms and their role in color variation in Atlantic salmon.

6.1. Development of sample preparation method

Proper sample preparation is crucial for obtaining reliable data. There are various methods for sample fixation, and the choices depend on the purpose. Paper I describes the development of the fast freezing and substitution (FS) sample preservation method. This method is rapid, easy, cheap and safe. It satisfies the requirements for several applications and is especially beneficial when the amount of sample is limited and various analyses are to be performed. A protocol for freeze substitution was developed and optimized for Atlantic salmon intestine and liver tissues. Briefly, 0.5 cm^3 tissue pieces were rapidly frozen in isobutanol precooled to -100°C in a slurry of ethanol liquid, nitrogen and dry ice. Then, tissues were immersed into precooled isobutanol for few minutes, followed by storage at -80°C in pure ethanol. Main advantage of FS over other preservation methods is that tissues were appropriate for a variety of analysis and the tissue and cell morphology revealed high-quality histological details. High quality RNA with RIN values of 9.8 were also recovered from FS preserved tissue, allowing for highly sensitive downstream analyses like RNA sequencing. Proteins for immunostaining were better preserved than when using formalin fixation, as the signals were stronger and autofluorescence was weaker. Finally, FS preserved proteins better than formalin fixation, as judged by the total protein yield when comparing the two methods. All of this supports that FS is advantageous preservation method over standardly used formalin fixation and its application in this research ensured reliable data acquisition.

6.2. Metabolic transformation of carotenoids

A considerable interindividual variability in flesh color is observed in Atlantic salmon. Most studies measuring blood and tissue responses to diets supplemented with astaxanthin suggest this variability is due to differences in absorption efficiency and enzymatic degradation of astaxanthin, both of which profoundly occur in enterocyte cells in gastrointestinal tract and in the liver. Later QTL and GWAS studies suggested that this effect is probably due to variations in genes that encode proteins involved in carotenoid metabolism. The paralogs *bco1* and *bco1l* are examples of such candidate genes. *Bco1* and *bco1l* appear to derive from a duplication event prior to the teleost-tetrapod divergence, implying loss of the tetrapod *bco1l* paralog. Although the role of BCO1 in mammals has been well established as 15,15'- oxygenase, which cleaves provitamin-A carotenoids, the existence of the extended family of CCO in fish remains elusive. One possible explanation is that the extra copy of *bco1* in fish genome subfunctionalized and enabled fish to handle the broader variety of carotenoids present in aquatic ecosystems for vitamin A production, in particular astaxanthin, which is abundant in the salmon diet but hardly present in the mammalian diet. Lesser expression of *bco1* in red-fleshed compared to pale-fleshed fish supports this hypothesis. Here the two paralogs were functionally tested and showed that Bco1 and Bco1l are both translationally active, cytosolic enzymes, highly expressed in enterocytes of the small intestine. Bco1l from Atlantic salmon oxidatively cleaves β-carotene and zeaxanthin at the central 15,15' double bond, while the activity of Bco1 remains elusive due to technical issues.

As of the time of writing, there are three members of the CCO family with solved crystal structures: the apocarotenoid 15-15′-oxygenase (ACO) from the cyanobacterium *Synechocystis sp*. [119]; bovine RPE65 [120]; and maize VP14 [121]. To investigate the putative differences in

enzyme structure of salmon Bco1 and Bco1l, we modeled the two proteins using the crystal structure of bovine RPE65 as a template. Salmon Bco1 and Bco1l protein models are highly similar and both have highly conserved structure in the active site domain and active site with four conserved histidine residues that bind ferrous ion that are crucial for enzyme activity [122-124] [125]. In addition to the histidine residues five acidic residues D52, E140, E314, E405, E457 [122, 126] and F51, F93, E140, S139, T141, Y236, F307, Y325 [125] have been found to be vital for enzyme function in the mammalian BCO1 and are all found to be conserved in salmon Bco1 and Bco1l. Poor alignment between Bco1 and Bco1l was noticed only at the three periphery regions, which are suggested to be substrate binding.

Based on all information of salmon muscle pigmentation including the results from the current study, it is indicative that both Bco1 and Bco1l centrally cleave carotenoids, but might differ in substrate specificities. In that case Bco1 provides salmon with sufficient vitamin A through conversion of astaxanthin, the main provitamin A source in salmonid diet, while Bco1l finely regulates the vitamin A level in the body through cleavage of other less abundant provitamin A carotenoids. In order to resolve any doubts, additional efforts should be made to produce recombinant Bco1 and Bco1l and confirm their substrate specificities.

6.3. Novel QTL for salmon flesh coloration

Another QTL associated with flesh coloration was identified on ssa02 (Paper III). Fine mapping of the region revealed a missense mutation in an *abcg2* gene, that causes an amino acid substitution in position 230 (Asn230Ser). With respect to Abcg2 function in other species, the encoded salmon protein is a possible astaxanthin transporter, controlling efflux of the pigment from enterocytes back into the intestinal lumen [127].

ABCG2 belongs to the ATP binding cassette (ABC) protein superfamily, known for their role in pumping a broad array of chemical compounds from the cytosol outside the cell. ABCG2 is abundant in the intestine and can limit the uptake and availability of compounds that are their substrate [128-130]. The substrates recognized are chemotherapeutic agents but also natural products, some of which are lipids, bile salts, amino acids, peptides, proteins, or carbohydrates [131-133]. There is a growing evidence for the importance of ABC transporters in carotenoid metabolism and their influence on carotenoid status [134, 135]. β-carotene inhibits ABCG2 efflux function [134]. Another ABC transporter, the complex ABCG5/G8, was associated with lutein metabolism [136, 137]. Studies using knockout mice demonstrated that absence of ABCG2 could increase availability of certain drugs to the brain five- to 100-fold [138, 139].

There are no high-resolution structural data available for any of the eukaryotic ABC transporters, but by combining the computer-assisted predictions and biochemical experimental data the structure of ABCG2 was computed and revealed it is a half-transporter consisting of one nucleotide binding domain (NBD) and one membrane spanning domain (MSD). ABCG2 probably homodimerize to form the functional protein [140, 141]. The NBD of all ABC proteins contain Walker A, Walker B and C-motives that bind and hydrolyze ATP/GTP and play a critical role in transporter activation. MSD consists of six α- helices that form substrate-binding pocket (Fig. 10). Supposedly, ABCG2 activity is initiated when cargo binds to the binding-pocket on the cytoplasmic side, triggering protein dimerization and conformational change (driven by ATP binding and hydrolysis) and finally result in the release of the cargo outside the cell [142].

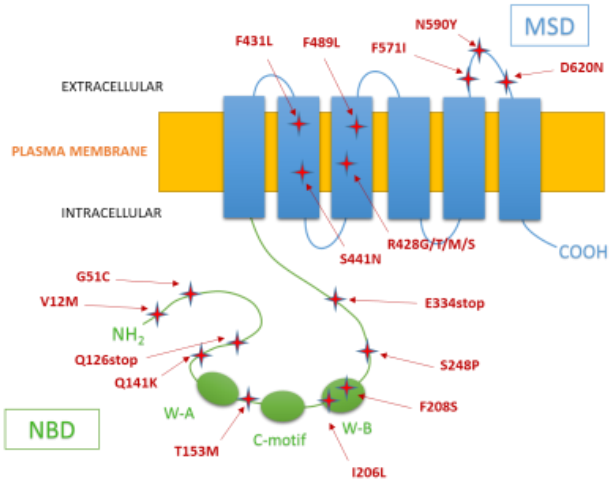

Figure 10. Schematic diagram of human ABCG2 domains showing functional single-nucleotide polymorphisms (red stars). ABCG2 is a 'half-transporter' presumed to homodimerize to form a functional transporter. A monomer of ABCG2 consists of intracellular N-terminal nucleotide binding domain (NBD) containing Walker A, Walker B and C-motifs that bind ATP/GTP and have catalytic function. Six membrane spanning domains (MSD), and associated intra- and extracellular loops that follow these are important for substrate binding. NBD: Nucleotide-binding domain; MSD: Membrane-spanning domain; W-A: Walker A motif; W-B: Walker B motif.

In humans, a number of functional ABCG2 polymorphisms have been identified (Fig. 10, red stars), resulting in altered activity through reduced expression and/or function [143-145]. Based on numerous functional studies [144, 146, 147] it seems that MSD is involved in the substrate recognition [148-150], while NBD is involved in Mg · ATP binding with a profound role in protein activity [151-154]. Position 230 in Abcg2 has not previously been assigned important in any species, but the mutation in salmon *abcg2-1a* is located in the proximity of an ATP binding site in the D-loop, important for protein activation in human. In order to investigate if Abcg2-1a

is involved in astaxanthin translocation, we compared the protein abundance in the intestine of red (fish homozygous for the favorable *abcg2-1a* allele for muscle color) and pale-fleshed fish (homozygous for the less favorable *abcg2-1a* allele for muscle color) using western blotting. Abcg2-1a was 2.5 fold more abundant in pale-fleshed compared to red-flesh fish, which is in line with the QTL genotype. This is the first study pointing on Abcg2 as a novel carotenoid transporter in Atlantic salmon, and further studies are required to assess the mechanism of the mutation and substrate specificity of Abcg2.

7. Concluding remarks and future perspectives

The importance of red flesh pigmentation for consumers, coupled with importance of understanding the evolutionary history of flesh coloration in salmonids, has led to increased interest in the molecular basis of carotenoid homeostasis. Functional genetics and biochemical characterization studies of genes involved in uptake, transport, deposition and degradation of carotenoids have advanced over the last years. Sequencing the Atlantic salmon genome has provided us with new tools like SNP-panels for GWAS-studies, detailed gene maps and access to RNA-sequencing. Emerging evidence suggest that efflux and metabolic breakdown of dietary carotenoids in small intestine significantly influence the amount of carotenoids deposed in the muscle of Atlantic salmon. *Bco1/bco1l* and *abcg2* are key components identified so far, although a more complete understanding of the mechanisms involved in carotenoid intestinal metabolism is still lacking. Selection for genetic variants of these genes is a strategy for more intensively colored fillet in Atlantic salmon. Fig. 11 shows current view of carotenoid metabolism in Atlantic salmon in enterocyte of small intestine. However, more remains to be learned about the roles of these proteins. Future studies should also assess the substrate specificities of these proteins, and developing Atlantic salmon enterocyte cell cultures will greatly contribute to the success. Also, additional searches for flesh coloration QTLs in Atlantic salmon should be performed. Understanding the mechanisms involved in astaxanthin binding to muscle would probably explain what is the criteria for red-flesh coloration and focus should also be set upon this topic. Cell culture together with proteome studies will continue to contribute to improve the understanding of an interesting life history trait in Atlantic salmon.

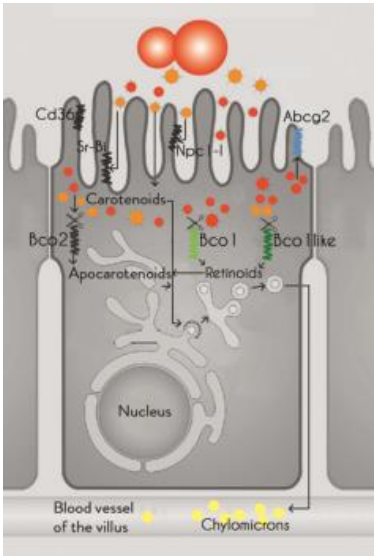

Figure 11. Proposed metabolism of carotenoids in enterocyte in Atlantic salmon. Proteins studied in this thesis are colored, while other proteins supposedly involved in the pathway are non-colored. Food containing β-carotene and other typical provitamin-A carotenoids (orange spheres) and astaxanthin (red spheres) is ingested and the pigments are taken up into the enterocyte in small intestine by membrane protein transporters (Cd36, Sr-Bi, Npci-1l). Astaxanthin can be symmetrically cleaved by Bco1 into retinoids, effluxed back into the intestinal lumen through Abcg2, or remain intact. Other provitamin A carotenoids can be symmetrically cleaved by Bco1l into retinoids or remain intact. Some carotenoids can be asymmetrically cleaved into apocarotenoids by Bco2. Apocarotenoids, retinoids and intact carotenoids combine into chylomicrons (yellow spheres), which are secreted into circulation and delivered to the different tissues.

5. List of figures

Figure 10. Schematic diagram of human ABCG2 domains showing functional single-nucleotide polymorphisms (red stars). ABCG2 is a 'half-transporter' presumed to homodimerize to form a functional transporter. A monomer of ABCG2 consists of intracellular N-terminal nucleotide binding domain (NBD) containing Walker A, Walker B and C-motifs that bind ATP/GTP and have catalytic function. Six membrane spanning domains (MSD), and associated intra- and extracellular loops that follow these are important for substrate binding. NBD: Nucleotide-binding domain; MSD: Membrane-spanning domain; W-A: Walker A motif; W-B: Walker B motif.

Figure 11. Proposed metabolism of carotenoids in enterocyte in Atlantic salmon. Proteins studied in this thesis are colored, while other proteins supposedly involved in the pathway are non-colored. Food containing β-carotene and other typical provitamin-A carotenoids (orange spheres) and astaxanthin (red spheres) is ingested and the pigments are taken up into the enterocyte in small intestine by membrane protein transporters (Cd36, Sr-Bi, Npci-1l). Astaxanthin can be symmetrically cleaved by Bco1l into retinoids, effluxed back into the intestinal lumen through Abcg2, or remain intact. Other provitamin A carotenoids can be symmetrically cleaved by Bco1 into retinoids or remain intact. Some carotenoids can be asymmetrically cleaved into apocarotenoids by Bco2. Apocarotenoids, retinoids and intact carotenoids combine into chylomicrons (yellow spheres), which are secreted into circulation and delivered to the body.

6. Literature

1. Moe, N.H., *Key factors in marketing farmed salmon.* Proceedings of the Nutrition Society of New Zealand 1990. **15**: p. 16-22
2. Sjofn Sigurgisladottir , O.Ø., Øyvind Lie , Magny Thomassen & Hannes Hafsteinsson, *Salmon quality: Methods to determine the quality parameters.* Reviews in Fisheries Science 1997. **5**(3): p. 223-252.
3. Rahman, M.M., et al., *Effects of Dietary Inclusion of Astaxanthin on Growth, Muscle Pigmentation and Antioxidant Capacity of Juvenile Rainbow Trout (Oncorhynchus mykiss).* Prev Nutr Food Sci, 2016. **21**(3): p. 281-288.
4. W., G.T., *The Biochemistry of the Carotenoids*. Vol. Vol. II. Animals. 1984: Chapman and Hall, London.
5. Schiedt, K., et al., *Absorption, Retention and Metabolic Transformations of Carotenoids in Rainbow-Trout, Salmon and Chicken.* Pure and Applied Chemistry, 1985. **57**(5): p. 685-692.
6. Matsuno, T., *Aquatic animal carotenoids.* Fisheries Science, 2001. **67**(5): p. 771-783.
7. Jyonouchi, H., et al., *Astaxanthin, a Carotenoid without Vitamin-a Activity, Augments Antibody-Responses in Cultures Including T-Helper Cell Clones and Suboptimal Doses of Antigen.* Journal of Nutrition, 1995. **125**(10): p. 2483-2492.
8. Zaripheh, S. and J.W. Erdman, *Factors that influence the bioavailablity of xanthophylls.* Journal of Nutrition, 2002. **132**(3): p. 531s-534s.
9. Moretti, V.M., et al., *Determination of astaxanthin stereoisomers and colour attributes in flesh of rainbow trout (Oncorhynchus mykiss) as a tool to distinguish the dietary pigmentation source.* Food Additives and Contaminants, 2006. **23**(11): p. 1056-1063.
10. Foss, P., et al., *Carotenoids in Diets for Salmonids .1. Pigmentation of Rainbow-Trout with the Individual Optical Isomers of Astaxanthin in Comparison with Canthaxanthin.* Aquaculture, 1984. **41**(3): p. 213-226.
11. Seabra, L.M.J. and L.F.C. Pedrosa, *Astaxanthin: structural and functional aspects.* Revista De Nutricao-Brazilian Journal of Nutrition, 2010. **23**(6): p. 1041-1050.
12. Gross, G.J. and S.F. Lockwood, *Cardioprotection and myocardial salvage by a disodium disuccinate astaxanthin derivative (Cardax (TM)).* Life Sciences, 2004. **75**(2): p. 215-224.
13. Miki, W., *Biological Functions and Activities of Animal Carotenoids.* Pure and Applied Chemistry, 1991. **63**(1): p. 141-146.
14. Oliveros, E., et al., *Quenching of Singlet Oxygen (1-Delta-G) by Carotenoid Derivatives - Kinetic-Analysis by near-Infrared Luminescence.* New Journal of Chemistry, 1994. **18**(4): p. 535-539.
15. Kidd, P., *Astaxanthin, Cell Membrane Nutrient with Diverse Clinical Benefits and Anti-Aging Potential.* Alternative Medicine Review, 2011. **16**(4): p. 355-364.
16. George Britton, S.L.-J., Hanspeter Pfander, *Carotenoids, Vol. 4: Natural Functions*. 2008 Springer Science & Business Media.

17. Eroglu, A. and E.H. Harrison, *Carotenoid metabolism in mammals, including man: formation, occurrence, and function of apocarotenoids.* J Lipid Res, 2013. **54**(7): p. 1719-30.
18. Organization, W.H., *Global prevalence of vitamin A deficiency in populations at risk 1995-2005 : WHO global database on vitamin A deficiency*. 2009: Geneva : World Health Organization.
19. Lee, S.A., et al., *Cardiac dysfunction in beta-carotene-15,15'-dioxygenase-deficient mice is associated with altered retinoid and lipid metabolism.* Am J Physiol Heart Circ Physiol, 2014. **307**(11): p. H1675-84.
20. Kim, Y.K., et al., *Tissue- and sex-specific effects of beta-carotene 15,15' oxygenase (BCO1) on retinoid and lipid metabolism in adult and developing mice.* Arch Biochem Biophys, 2015. **572**: p. 11-8.
21. McNulty, H.P., et al., *Differential effects of carotenoids on lipid peroxidation due to membrane interactions: X-ray diffraction analysis.* Biochimica Et Biophysica Acta-Biomembranes, 2007. **1768**(1): p. 167-174.
22. Sharoni, Y., et al., *Carotenoids and apocarotenoids in cellular signaling related to cancer: a review.* Mol Nutr Food Res, 2012. **56**(2): p. 259-69.
23. Rodrigues, E., L.R. Mariutti, and A.Z. Mercadante, *Scavenging capacity of marine carotenoids against reactive oxygen and nitrogen species in a membrane-mimicking system.* Mar Drugs, 2012. **10**(8): p. 1784-98.
24. Dose, J., et al., *Free Radical Scavenging and Cellular Antioxidant Properties of Astaxanthin.* Int J Mol Sci, 2016. **17**(1).
25. Chiste, R.C., et al., *Carotenoids inhibit lipid peroxidation and hemoglobin oxidation, but not the depletion of glutathione induced by ROS in human erythrocytes.* Life Sci, 2014. **99**(1-2): p. 52-60.
26. Pike, T.W., et al., *Carotenoids, oxidative stress and female mating preference for longer lived males.* Proceedings of the Royal Society B-Biological Sciences, 2007. **274**(1618): p. 1591-1596.
27. Leclaire, S., et al., *Carotenoids increase immunity and sex specifically affect color and redox homeostasis in a monochromatic seabird.* Behavioral Ecology and Sociobiology, 2015. **69**(7): p. 1097-1111.
28. Ruhl, R., *Effects of dietary retinoids and carotenoids on immune development.* Proceedings of the Nutrition Society, 2007. **66**(3): p. 458-469.
29. Carpentier, S., M. Knaus, and M.Y. Suh, *Associations between Lutein, Zeaxanthin, and Age-Related Macular Degeneration: An Overview.* Critical Reviews in Food Science and Nutrition, 2009. **49**(4): p. 313-326.
30. Hammond, B.R. and L.M. Fletcher, *Influence of the dietary carotenoids lutein and zeaxanthin on visual performance: application to baseball.* American Journal of Clinical Nutrition, 2012. **96**(5): p. 1207s-1213s.
31. Eisenhauer, B., et al., *Lutein and Zeaxanthin-Food Sources, Bioavailability and Dietary Variety in Age-Related Macular Degeneration Protection.* Nutrients, 2017. **9**(2).
32. McGraw, K.J. and G.E. Hill, *Plumage color as a dynamic trait: carotenoid pigmentation of male house finches (Carpodacus mexicanus) fades during the breeding season.* Canadian Journal of Zoology-Revue Canadienne De Zoologie, 2004. **82**(5): p. 734-738.
33. Rajasingh, H., et al., *Why are salmonids pink?* Canadian Journal of Fisheries and Aquatic Sciences, 2007. **64**(11): p. 1614-1627.

34. Bjerkeng, B., T. Storebakken, and S. Liaaenjensen, *Pigmentation of Rainbow-Trout from Start Feeding to Sexual-Maturation.* Aquaculture, 1992. **108**(3-4): p. 333-346.
35. Aas, G.H., et al., *Blood appearance, metabolic transformation and plasma transport proteins of (14)C-astaxanthin in Atlantic salmon (Salmo salar L.).* Fish Physiology and Biochemistry, 1999. **21**(4): p. 325-334.
36. March, B.E., et al., *Intestinal-Absorption of Astaxanthin, Plasma Astaxanthin Concentration, Body-Weight, and Metabolic-Rate as Determinants of Flesh Pigmentation in Salmonid Fish.* Aquaculture, 1990. **90**(3-4): p. 313-322.
37. Steven, D.M., *Studies on Animal Carotenoids .2. Carotenoids in the Reproductive Cycle of the Brown Trout.* Journal of Experimental Biology, 1949. **26**(3): p. 295-303.
38. Hussein, G., et al., *Astaxanthin, a carotenoid with potential in human health and nutrition.* Journal of Natural Products, 2006. **69**(3): p. 443-449.
39. Amundsen, T. and E. Forsgren, *Male mate choice selects for female coloration in a fish.* Proceedings of the National Academy of Sciences of the United States of America, 2001. **98**(23): p. 13155-13160.
40. Craik, J.C.A. and S.M. Harvey, *The Carotenoids of Eggs of Wild and Farmed Atlantic Salmon, and Their Changes during Development to the Start of Feeding.* Journal of Fish Biology, 1986. **29**(5): p. 549-565.
41. Shahidi, F., Metusalach, and J.A. Brown, *Carotenoid pigments in seafoods and aquaculture.* Critical Reviews in Food Science and Nutrition, 1998. **38**(1): p. 1-67.
42. Christiansen, R. and O.J. Torrissen, *Growth and survival of Atlantic salmon, Salmo salar L. fed different dietary levels of astaxanthin. Juveniles.* Aquaculture Nutrition, 1996. **2**(1): p. 55-62.
43. Torrissen, O.J., *Pigmentation of Salmonids - Effect of Carotenoids in Eggs and Start-Feeding Diet on Survival and Growth-Rate.* Aquaculture, 1984. **43**(1-3): p. 185-193.
44. Christiansen, R., O. Lie, and O.J. Torrissen, *Growth and survival of Atlantic salmon, Salmo salar L., fed different dietary levels of astaxanthin. First-feeding fry.* Aquaculture Nutrition, 1995. **1**(3): p. 189-198.
45. Christiansen, Ø.L., O.J. Torrissen, *Effect of astaxanthin and vitamin A on growth and survival during first feeding of Atlantic salmon, Salmo salar L.* Aquaculture research, 1994. **25**(9): p. 903–914.
46. Takaichi, S., *Distributions, biosyntheses and functions of carotenoids in algae.* Agro Food Industry Hi-Tech, 2013. **24**(1): p. 55-58.
47. vanVliet, T., et al., *In vitro measurement of beta-carotene cleavage activity: Methodological considerations and the effect of other carotenoids on beta-carotene cleavage.* International Journal for Vitamin and Nutrition Research, 1996. **66**(1): p. 77-85.
48. Sangeetha, R.K. and V. Baskaran, *Retinol-deficient rats can convert a pharmacological dose of astaxanthin to retinol: antioxidant potential of astaxanthin, lutein, and beta-carotene.* Canadian Journal of Physiology and Pharmacology, 2010. **88**(10): p. 977-985.
49. Gross, J. and P. Budowski, *Conversion of Carotenoids into Vitamins A1 and A2 in 2 Species of Freshwater Fish.* Biochemical Journal, 1966. **101**(3): p. 747-&.
50. Alkhalifa, A.S. and K.L. Simpson, *Metabolism of Astaxanthin in the Rainbow-Trout (Salmo-Gairdneri).* Comparative Biochemistry and Physiology B-Biochemistry & Molecular Biology, 1988. **91**(3): p. 563-568.

51. Guillou, A., et al., *Bioconversion Pathway of Astaxanthin into Retinol-2 in Mature Rainbow-Trout (Salmo-Gairdneri Rich).* Comparative Biochemistry and Physiology B-Biochemistry & Molecular Biology, 1989. **94**(3): p. 481-485.
52. Yamashita, E., S. Arai, and T. Matsuno, *Metabolism of xanthophylls to vitamin A and new apocarotenoids in liver and skin of black bass, Micropterus salmoides.* Comparative Biochemistry and Physiology B-Biochemistry & Molecular Biology, 1996. **113**(3): p. 485-489.
53. Moren, M., T. Naess, and K. Hamre, *Conversion of beta-carotene, canthaxanthin and astaxanthin to vitamin A in Atlantic halibut (Hippoglossus hippoglossus L.) juveniles.* Fish Physiology and Biochemistry, 2002. **27**(1-2): p. 71-80.
54. Katsuyama, M. and T. Matsuno, *Carotenoid and Vitamin-a, and Metabolism of Carotenoids, Beta-Carotene, Canthaxanthin, Astaxanthin, Zeaxanthin, Lutein and Tunaxanthin in Tilapia Tilapia-Nilotica.* Comparative Biochemistry and Physiology B-Biochemistry & Molecular Biology, 1988. **90**(1): p. 131-139.
55. White, D.A., R. Ornsrud, and S.J. Davies, *Determination of carotenoid and vitamin A concentrations in everted salmonid intestine following exposure to solutions of carotenoid in vitro.* Comparative Biochemistry and Physiology a-Molecular & Integrative Physiology, 2003. **136**(3): p. 683-692.
56. Bjerkeng, B. and G.M. Berge, *Apparent digestibility coefficients and accumulation of astaxanthin E/Z isomers in Atlantic salmon (Salmo salar L.) and Atlantic halibut (Hippoglossus hippoglossus L.).* Comparative Biochemistry and Physiology B-Biochemistry & Molecular Biology, 2000. **127**(3): p. 423-432.
57. Ytrestoyl, T. and B. Bjerkeng, *Intraperitoneal and dietary administration of astaxanthin in rainbow trout (Oncorhynchus mykiss)--plasma uptake and tissue distribution of geometrical E/Z isomers.* Comp Biochem Physiol B Biochem Mol Biol, 2007. **147**(2): p. 250-9.
58. Ytrestoyl, T. and B. Bjerkeng, *Dose response in uptake and deposition of intraperitoneally administered astaxanthin in Atlantic salmon (Salmo salar L.) and Atlantic cod (Gadus morhua L.).* Aquaculture, 2007. **263**(1-4): p. 179-191.
59. Ytrestoyl, T., et al., *Astaxanthin digestibility as affected by ration levels for Atlantic salmon, Salmo salar.* Aquaculture, 2006. **261**(1): p. 215-224.
60. Chimsung, N., et al., *Effects of various dietary factors on astaxanthin absorption in Atlantic salmon (Salmo salar).* Aquaculture Research, 2014. **45**(10): p. 1611-1620.
61. Harrison, E.H., *Mechanisms involved in the intestinal absorption of dietary vitamin A and provitamin A carotenoids.* Biochimica Et Biophysica Acta-Molecular and Cell Biology of Lipids, 2012. **1821**(1): p. 70-77.
62. Reboul, E., *Absorption of Vitamin A and Carotenoids by the Enterocyte: Focus on Transport Proteins.* Nutrients, 2013. **5**(9): p. 3563-3581.
63. Shete, V. and L. Quadro, *Mammalian Metabolism of beta-Carotene: Gaps in Knowledge.* Nutrients, 2013. **5**(12): p. 4849-4868.
64. During, A., H.D. Dawson, and E.H. Harrison, *Carotenoid transport is decreased and expression of the lipid transporters SR-BI, NPC1L1, and ABCA1 is downregulated in Caco-2 cells treated with ezetimibe.* Journal of Nutrition, 2005. **135**(10): p. 2305-2312.
65. Kiefer, C., et al., *A class B scavenger receptor mediates the cellular uptake of carotenoids in Drosophila.* Proceedings of the National Academy of Sciences of the United States of America, 2002. **99**(16): p. 10581-10586.

66. Moussa, M., et al., *Lycopene absorption in human intestinal cells and in mice involves scavenger receptor class B type I but not Niemann-Pick C1-like 1.* J Nutr, 2008. **138**(8): p. 1432-6.
67. Reboul, E., et al., *Lutein transport by Caco-2 TC-7 cells occurs partly by a facilitated process involving the scavenger receptor class B type I (SR-BI).* Biochemical Journal, 2005. **387**: p. 455-461.
68. van Bennekum, A., et al., *Class B scavenger receptor-mediated intestinal absorption of dietary beta-carotene and cholesterol.* Biochemistry, 2005. **44**(11): p. 4517-25.
69. Sakudoh, T., et al., *A CD36-related Transmembrane Protein Is Coordinated with an Intracellular Lipid-binding Protein in Selective Carotenoid Transport for Cocoon Coloration.* Journal of Biological Chemistry, 2010. **285**(10): p. 7739-7751.
70. Sato, Y., et al., *Involvement of Cholesterol Membrane Transporter Niemann-Pick C1-Like 1 in the Intestinal Absorption of Lutein.* Journal of Pharmacy and Pharmaceutical Sciences, 2012. **15**(2): p. 256-264.
71. Kleveland, E.J., et al., *Characterization of scavenger receptor class B, type I in Atlantic salmon (Salmo salar L.).* Lipids, 2006. **41**(11): p. 1017-1027.
72. Sundvold, H., et al., *Characterisation of a novel paralog of scavenger receptor class B member I (SCARB1) in Atlantic salmon (Salmo salar).* Bmc Genetics, 2011. **12**.
73. O'Byrne, S.M., et al., *Retinoid absorption and storage is impaired in mice lacking lecithin : retinol acyltransferase (LRAT).* Journal of Biological Chemistry, 2005. **280**(42): p. 35647-35657.
74. D'Ambrosio, D.N., R.D. Clugston, and W.S. Blaner, *Vitamin A metabolism: an update.* Nutrients, 2011. **3**(1): p. 63-103.
75. Blomhoff, R., *Transport and metabolism of vitamin A.* Nutr Rev, 1994. **52**(2 Pt 2): p. S13-23.
76. Shmarakov, I., et al., *Hepatic stellate cells are an important cellular site for beta-carotene conversion to retinoid.* Arch Biochem Biophys, 2010. **504**(1): p. 3-10.
77. Trigatti, B.L. and G.E. Gerber, *A direct role for serum albumin in the cellular uptake of long-chain fatty acids.* Biochem J, 1995. **308 (Pt 1)**: p. 155-9.
78. Bjerkeng, B., et al., *Quality parameters of the flesh of Atlantic salmon (Salmo salar) as affected by dietary fat content and full-fat soybean meal as a partial substitute for fish meal in the diet.* Aquaculture, 1997. **157**(3-4): p. 297-309.
79. Henmi, H., M. Hata, and M. Hata, *Combination of Astaxanthin and Canthaxanthin with Fish Muscle Actomyosins Associated with Their Surface Hydrophobicity.* Nippon Suisan Gakkaishi, 1990. **56**(11): p. 1821-1823.
80. Henmi, H., M. Hata, and M. Takeuchi, *Studies on the Carotenoids in the Muscle of Salmon .5. Combination of Astaxanthin and Canthaxanthin with Bovine Serum-Albumin and Egg-Albumin.* Comparative Biochemistry and Physiology B-Biochemistry & Molecular Biology, 1991. **99**(3): p. 609-612.
81. Matthews, S.J., et al., *Astaxanthin binding protein in Atlantic salmon.* Comp Biochem Physiol B Biochem Mol Biol, 2006. **144**(2): p. 206-14.
82. Saha, M.R., et al., *Development of a method to assess binding of astaxanthin to Atlantic salmon Salmo salar L. muscle proteins.* Aquaculture Research, 2005. **36**(4): p. 336-343.
83. Bjerkeng, B., B. Hatlen, and E. Wathne, *Deposition of astaxanthin in fillets of Atlantic salmon (Salmo salar) fed diets with herring, capelin, sandeel, or Peruvian high PUFA oils.* Aquaculture, 1999. **180**(3-4): p. 307-319.

84. Torrissen, O.J., et al., *Astaxanthin deposition in the flesh of Atlantic Salmon, Salmo salar L., in relation to dietary astaxanthin concentration and feeding period.* Aquaculture Nutrition, 1995. **1**(2): p. 77-84.
85. Wathne, E., et al., *Pigmentation of Atlantic salmon (Salmo salar) fed astaxanthin in all meals or in alternating meals.* Aquaculture, 1998. **159**(3-4): p. 217-231.
86. Rajasingh, H., et al., *Carotenoid dynamics in Atlantic salmon.* Bmc Biology, 2006. **4**.
87. Neira, R., et al., *Studies on carcass quality traits in two populations of Coho salmon (Oncorhynchus kisutch): phenotypic and genetic parameters.* Aquaculture, 2004. **241**(1-4): p. 117-131.
88. Odegard, J., et al., *Genomic prediction in an admixed population of Atlantic salmon (Salmo salar).* Front Genet, 2014. **5**: p. 402.
89. Schiedt, K., et al., *Metabolism of Carotenoids in Salmonids .1. Idoxanthin, a Metabolite of Astaxanthin in the Flesh of Atlantic Salmon (Salmo-Salar, L) under Varying External Conditions.* Comparative Biochemistry and Physiology B-Biochemistry & Molecular Biology, 1989. **92**(2): p. 277-281.
90. Schiedt, K., et al., *Metabolism of Carotenoids in Salmonids .2. Distribution and Absolute-Configuration of Idoxanthin in Various Organs and Tissues of One Atlantic Salmon (Salmo-Salar, L) Fed with Astaxanthin.* Helvetica Chimica Acta, 1988. **71**(4): p. 881-886.
91. Schiedt, K., et al., *Metabolism of Carotenoids in Salmonids .3. Metabolites of Astaxanthin and Canthaxanthin in the Skin of Atlantic Salmon (Salmo-Salar, L).* Helvetica Chimica Acta, 1988. **71**(4): p. 887-896.
92. Baranski, M., T. Moen, and D.I. Vage, *Mapping of quantitative trait loci for flesh colour and growth traits in Atlantic salmon (Salmo salar).* Genetics Selection Evolution, 2010. **42**.
93. Sodeland M, H.H., Torgersen J, Moen T, Kjøglum, S, Våge DI, Lien S, *Gene and genome duplications allowed for the evolution of the characteristic red color of salmon flesh* in *Manuscript in preparation*. 2017.
94. von Lintig, J. and K. Vogt, *Filling the gap in vitamin A research. Molecular identification of an enzyme cleaving beta-carotene to retinal.* J Biol Chem, 2000. **275**(16): p. 11915-20.
95. Lindqvist, A. and S. Andersson, *Biochemical properties of purified recombinant human beta-carotene 15,15'-monooxygenase.* Journal of Biological Chemistry, 2002. **277**(26): p. 23942-23948.
96. Lindqvist, A. and S. Andersson, *Cell type-specific expression of beta-carotene 15,15 '-mono-oxygenase in human tissues.* Journal of Histochemistry & Cytochemistry, 2004. **52**(4): p. 491-499.
97. Wyss, A., et al., *Cloning and expression of beta,beta-carotene 15,15 '-dioxygenase.* Biochemical and Biophysical Research Communications, 2000. **271**(2): p. 334-336.
98. Kim, Y.S. and D.K. Oh, *Substrate specificity of a recombinant chicken beta-carotene 15,15'-monooxygenase that converts beta-carotene into retinal.* Biotechnology Letters, 2009. **31**(3): p. 403-408.
99. Paik, J., et al., *Expression and characterization of a murine enzyme able to cleave beta-carotene - The formation of retinoids.* Journal of Biological Chemistry, 2001. **276**(34): p. 32160-32168.
100. Redmond, T.M., et al., *Identification, expression, and substrate specificity of a mammalian beta-carotene 15,15'-dioxygenase.* J Biol Chem, 2001. **276**(9): p. 6560-5.

101. Takitani, K., et al., *Molecular cloning of the rat beta-carotene 15,15'-monooxygenase gene and its regulation by retinoic acid.* Eur J Nutr, 2006. **45**(6): p. 320-6.
102. Morales, A., et al., *Cloning of the bovine beta-carotene-15,15'-oxygenase and expression in gonadal tissues.* Int J Vitam Nutr Res, 2006. **76**(1): p. 9-17.
103. Lampert, J.M., et al., *Provitamin A conversion to retinal via the beta,beta-carotene-15,15 '-oxygenase (bcox) is essential for pattern formation and differentiation during zebrafish embryogenesis.* Development, 2003. **130**(10): p. 2173-2186.
104. Cui, Y.X. and J.H. Freedman, *Cadmium Induces Retinoic Acid Signaling by Regulating Retinoic Acid Metabolic Gene Expression.* Journal of Biological Chemistry, 2009. **284**(37): p. 24925-24932.
105. Lindqvist, A. and S. Andersson, *Biochemical properties of purified recombinant human beta-carotene 15,15'-monooxygenase.* J Biol Chem, 2002. **277**(26): p. 23942-8.
106. von Lintig, J. and K. Vogt, *Filling the gap in vitamin A research - Molecular identification of an enzyme cleaving beta-carotene to retinal.* Journal of Biological Chemistry, 2000. **275**(16): p. 11915-11920.
107. Kowatz, T., et al., *Characterization of human beta,beta-carotene-15,15 '-monooxygenase (BCMO1) as a soluble monomeric enzyme.* Archives of Biochemistry and Biophysics, 2013. **539**(2): p. 214-222.
108. Lindqvist, A., et al., *Loss-of-function mutation in carotenoid 15,15'-monooxygenase identified in a patient with hypercarotenemia and hypovitaminosis A(1-3).* Journal of Nutrition, 2007. **137**(11): p. 2346-2350.
109. Hessel, S., et al., *CMO1 deficiency abolishes vitamin A production from beta-carotene and alters lipid metabolism in mice.* J Biol Chem, 2007. **282**(46): p. 33553-61.
110. Kim, Y.K., et al., *beta-Carotene and its cleavage enzyme beta-carotene-15,15 '-oxygenase (CMOI) affect retinoid metabolism in developing tissues.* Faseb Journal, 2011. **25**(5): p. 1641-1652.
111. Grolier, P., et al., *In vitro and in vivo inhibition of beta-carotene dioxygenase activity by canthaxanthin in rat intestine.* Archives of Biochemistry and Biophysics, 1997. **348**(2): p. 233-238.
112. Nagao, A., et al., *Inhibition of beta-carotene-15,15 '-dioxygenase activity by dietary flavonoids.* Journal of Nutritional Biochemistry, 2000. **11**(6): p. 348-355.
113. Le Bihan-Duval, E., et al., *Detection of a Cis [corrected] eQTL controlling BCMO1 gene expression leads to the identification of a QTG for chicken breast meat color.* PLoS One, 2011. **6**(7): p. e14825.
114. Ziouzenkova, O., et al., *Asymmetric cleavage of beta-carotene yields a transcriptional repressor of retinoid X receptor and peroxisome proliferator-activated receptor responses.* Mol Endocrinol, 2007. **21**(1): p. 77-88.
115. Eriksson, J., et al., *Identification of the yellow skin gene reveals a hybrid origin of the domestic chicken.* PLoS Genet, 2008. **4**(2): p. e1000010.
116. Vage, D.I. and I.A. Boman, *A nonsense mutation in the beta-carotene oxygenase 2 (BCO2) gene is tightly associated with accumulation of carotenoids in adipose tissue in sheep (Ovis aries).* BMC Genet, 2010. **11**: p. 10.
117. Berry, S.D., et al., *Mutation in bovine beta-carotene oxygenase 2 affects milk color.* Genetics, 2009. **182**(3): p. 923-6.
118. Amengual, J., et al., *Two carotenoid oxygenases contribute to mammalian provitamin A metabolism.* J Biol Chem, 2013. **288**(47): p. 34081-96.

119. Kloer, D.P., et al., *The structure of a retinal-forming carotenoid oxygenase.* Science, 2005. **308**(5719): p. 267-9.
120. Kiser, P.D., et al., *Crystal structure of native RPE65, the retinoid isomerase of the visual cycle.* Proc Natl Acad Sci U S A, 2009. **106**(41): p. 17325-30.
121. Messing, S.A.J., et al., *Structural Insights into Maize Viviparous14, a Key Enzyme in the Biosynthesis of the Phytohormone Abscisic Acid.* Plant Cell, 2010. **22**(9): p. 2970-2980.
122. Poliakov, E., et al., *Key role of conserved histidines in recombinant mouse beta-carotene 15,15 '-monooxygenase-1 activity.* Journal of Biological Chemistry, 2005. **280**(32): p. 29217-29223.
123. Redmond, T.M., et al., *Mutation of key residues of RPE65 abolishes its enzymatic role as isomerohydrolase in the visual cycle.* Proceedings of the National Academy of Sciences of the United States of America, 2005. **102**(38): p. 13658-13663.
124. Takahashi, Y., et al., *Identification of conserved histidines and glutamic acid as key residues for isomerohydrolase activity of RPE65, an enzyme of the visual cycle in the retinal pigment epithelium.* Febs Letters, 2005. **579**(24): p. 5414-5418.
125. Sui, X.W., et al., *Key Residues for Catalytic Function and Metal Coordination in a Carotenoid Cleavage Dioxygenase.* Journal of Biological Chemistry, 2016. **291**(37): p. 19401-19412.
126. Redmond, T.M., et al., *Identification, expression, and substrate specificity of a mammalian beta-carotene 15,15 '-dioxygenase.* Journal of Biological Chemistry, 2001. **276**(9): p. 6560-6565.
127. Choubert, G. and T. Storebakken, *Digestibility of astaxanthin and canthaxanthin in rainbow trout as affected by dietary concentration, feeding rate and water salinity.* Annales De Zootechnie, 1996. **45**(5): p. 445-453.
128. Glavinas, H., et al., *The role of ABC transporters in drug resistance, metabolism and toxicity.* Curr Drug Deliv, 2004. **1**(1): p. 27-42.
129. Horsey, A.J., et al., *The multidrug transporter ABCG2: still more questions than answers.* Biochemical Society Transactions, 2016. **44**: p. 824-830.
130. Maliepaard, M., et al., *Subcellular localization and distribution of the breast cancer resistance protein transporter in normal human tissues.* Cancer Research, 2001. **61**(8): p. 3458-3464.
131. Borel, P., *Genetic variations involved in interindividual variability in carotenoid status.* Molecular Nutrition & Food Research, 2012. **56**(2): p. 228-240.
132. Dean, M., Y. Hamon, and G. Chimini, *The human ATP-binding cassette (ABC) transporter superfamily.* J Lipid Res, 2001. **42**(7): p. 1007-17.
133. Mao, Q. and J.D. Unadkat, *Role of the breast cancer resistance protein (BCRP/ABCG2) in drug transport--an update.* AAPS J, 2015. **17**(1): p. 65-82.
134. Teng, Y.N., et al., *beta-carotene reverses multidrug resistant cancer cells by selectively modulating human P-glycoprotein function.* Phytomedicine, 2016. **23**(3): p. 316-23.
135. Eid, S.Y., M.Z. El-Readi, and M. Wink, *Carotenoids reverse multidrug resistance in cancer cells by interfering with ABC-transporters.* Phytomedicine, 2012. **19**(11): p. 977-987.
136. Fernandez, M.L., et al., *ABCG5 Polymorphism Contributes to the Individual Response to Dietary Cholesterol and to Carotenoids Present in Eggs.* Journal of Nutrigenetics and Nutrigenomics, 2009. **2**(4-5): p. 211-211.

137. Herron, K.L., et al., *The ABCG5 polymorphism contributes to individual responses to dietary cholesterol and carotenoids in eggs.* Journal of Nutrition, 2006. **136**(5): p. 1161-1165.
138. Breedveld, P., et al., *The effect of Bcrp1 (Abcg2) on the in vivo pharmacokinetics and brain penetration of imatinib mesylate (Gleevec): implications for the use of breast cancer resistance protein and P-glycoprotein inhibitors to enable the brain penetration of imatinib in patients.* Cancer Res, 2005. **65**(7): p. 2577-82.
139. Schinkel, A.H., *P-Glycoprotein, a gatekeeper in the blood-brain barrier.* Adv Drug Deliv Rev, 1999. **36**(2-3): p. 179-194.
140. Wakabayashi, K., et al., *Identification of cysteine residues critically involved in homodimer formation and protein expression of human ATP-binding cassette transporter ABCG2: a new approach using the flp recombinase system.* J Exp Ther Oncol, 2006. **5**(3): p. 205-22.
141. Ozvegy, C., et al., *Functional characterization of the human multidrug transporter, ABCG2, expressed in insect cells.* Biochem Biophys Res Commun, 2001. **285**(1): p. 111-7.
142. Rosenberg, M.F., et al., *Three-dimensional structure of the human breast cancer resistance protein (BCRP/ABCG2) in an inward-facing conformation.* Acta Crystallogr D Biol Crystallogr, 2015. **71**(Pt 8): p. 1725-35.
143. Kondo, C., et al., *Functional analysis of SNPs variants of BCRP/ABCG2.* Pharmaceutical Research, 2004. **21**(10): p. 1895-1903.
144. Tamura, A., et al., *Re-evaluation and functional classification of non-synonymous single nucleotide polymorphisms of the human ATP-binding cassette transporter ABCG2.* Cancer Science, 2007. **98**(2): p. 231-239.
145. Yanase, K., et al., *Functional SNPs of the breast cancer resistance protein - therapeutic effects and inhibitor development.* Cancer Letters, 2006. **234**(1): p. 73-80.
146. Mizuarai, S., N. Aozasa, and H. Kotani, *Single nucleotide polymorphisms result in impaired membrane localization and reduced atpase activity in multidrug transporter ABCG2.* Int J Cancer, 2004. **109**(2): p. 238-46.
147. Morisaki, K., et al., *Single nucleotide polymorphisms modify the transporter activity of ABCG2.* Cancer Chemother Pharmacol, 2005. **56**(2): p. 161-72.
148. Hazai, E. and Z. Bikadi, *Homology modeling of breast cancer resistance protein (ABCG2).* Journal of Structural Biology, 2008. **162**(1): p. 63-74.
149. Li, Y.F., et al., *Towards understanding the mechanism of action of the multidrug resistance-linked half-ABC transporter ABCG2: A molecular modeling study.* Journal of Molecular Graphics & Modelling, 2007. **25**(6): p. 837-851.
150. Sarkadi, B., et al., *ABCG2 - a transporter for all seasons.* Febs Letters, 2004. **567**(1): p. 116-120.
151. Chen, J., et al., *A tweezers-like motion of the ATP-binding cassette dimer in an ABC transport cycle.* Mol Cell, 2003. **12**(3): p. 651-61.
152. Hou, Y.X., et al., *Effects of putative catalytic base mutation E211Q on ABCG2-mediated methotrexate transport.* Biochemistry, 2009. **48**(38): p. 9122-31.
153. Smith, P.C., et al., *ATP binding to the motor domain from an ABC transporter drives formation of a nucleotide sandwich dimer.* Mol Cell, 2002. **10**(1): p. 139-49.
154. Verdon, G., et al., *Crystal structures of the ATPase subunit of the glucose ABC transporter from Sulfolobus solfataricus: nucleotide-free and nucleotide-bound conformations.* J Mol Biol, 2003. **330**(2): p. 343-58.

Papers I-III

Paper I

Zoric N, Grammes F, Våge DI, Torgersen J. **Freeze substitution – Tissue fixation for preserving morphology and high quality RNA.** Manuscript

Paper II

Zoric N, Torgersen J, Grammes F, von Lintig J, Våge DI. **Functional divergence of β-carotene oxygenase 1 enzymes after gene duplication in salmon.** Manuscript

Paper III

Zoric N, Moen T, Korsvoll SA, Kjøglum S, Santi N, Lien S, Våge DI, Torgersen J. **A missense mutation in the abcg2-1a gene (ATP-binding cassette sub-family G member 2) is strongly associated with muscle color in Atlantic salmon (*Salmo salar*).** Manuscript

Paper I

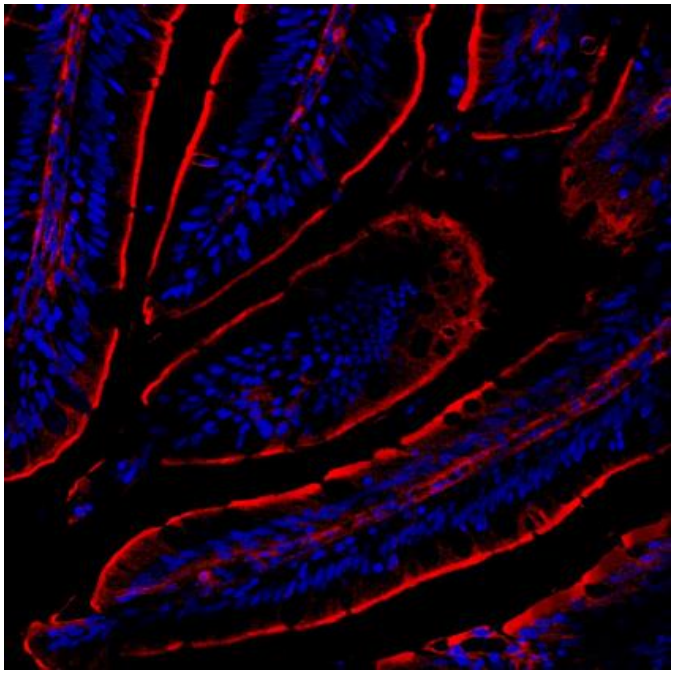

Image: Nina Zoric

Freeze substitution – Tissue fixation for preserving morphology and high quality RNA

Zoric Nina[1], Grammes Fabian[1], Dag Inge Våge[1], Torgersen Jacob[2*]

[1]Centre for Integrative Genetics (CIGENE), Department of Animal and Aquacultural Sciences (IHA), Faculty of Biosciences (BIOVIT), Norwegian University of Life Sciences (NMBU), P.O. Box 5003, N-1432 Ås, Norway.

[2]AquaGen, Postboks 1240, 7462 Trondheim, Norway.

[*]Corresponding author

Abstract

The ideal tissue fixative should preserve a good morphological tissue structure and allow downstream analysis of proteins, lipids and nucleic acids. Commonly, tissues are fixated in formalin followed by paraffin embedding, which preserves tissue structures well. However, the chemical crosslinking of proteins often affects antigen accessibility and the quality of nucleic acids, which is unsatisfactory for subsequent transcriptome analysis. Freeze substitution (FS) is an alternative fixation method that has been used for many years. In order to evaluate the potential of this preservation method for analysis of both protein and RNA quality, freeze-substituted tissues from Atlantic salmon (*Salmo salar*) were subjected to histological inspection, immunohistochemistry analysis, protein yield measurements and RNA sequencing. Compared to formalin-fixed tissues, FS preserved tissue and cell morphology well and outperformed formalin-fixation in immunofluorescence analysis, as the signal was stronger and autofluorescence was weaker. Compared to formalin fixation, FS samples had higher protein yield and better RNA quality, which is particularly important for downstream analysis such as SDS-PAGE and RNA sequencing, respectively.

In conclusion, freeze substitution is a reliable, highly stable, cheap, non-toxic, and fast tissue preservation method that produces high-quality histological detail and permits recovery of RNA and proteins suitable for highly sensitive downstream analyses.

Introduction

Recent advances in large-scale analysis of biomolecules including proteomics and next-generation sequencing together with improvements in microscopy enable the congregation of vast amounts of data from single tissue samples. A prerequisite is the presence of intact biomolecules and retained tissue morphology. However, to date no single tissue fixation method has been reported that ensures both preservation of morphology and provides high yields of intact nucleic acids and proteins. Consequently, different fixation methods are used for different purposes. It is therefore of considerable interest to develop a simple, standardized tissue preservation method which satisfies these different demands in one single preparation procedure.

Typically, tissues for histology are preserved using 10% neutral-buffered formalin fixation (FF), followed by paraffin embedding. Formalin is cheap, preserves morphologic features well and it also permits histologic staining and enables long-term storage of material. Unfortunately formalin is toxic and, as a cross-linking fixative introduces methylene bridges and compromises the quality of the macromolecules making specimens less suitable for down-stream proteomics and nucleic acid studies [1, 2]. FF also alters protein structure, and masks antigen epitopes restricting their association to antibodies [3]. Finally, formalin fixes tissue rather slowly due to a slow penetrance rate through the tissue, of approximately 1 mm per hour [4]. Hence, formalin does not give a true snapshot in time of a tissue because of the lack of immediate arrest of cellular processes throughout the tissue. Because of the strong crosslinking of proteins in FF tissue, antigen retrieval methods (chemical, enzymatic, physical) must often be applied to restore antigenicity [5]. However, retrieval methods require optimization and are not always successful

as they can result in degenerated tissue, false-positive results, and destruction of interesting molecules like mRNA [6, 7].

Of the alternative fixatives, such as F-Solv (Adamas, Rhenen, the Netherlands), FineFIX (Milestone, Bergamo, Italy), RCL2 (Alphelys, Plaisir, France), and many others [1, 8-11], none has gained a greater acceptance than FF. Coagulant fixatives, such as alcohol, alcohol-based fixatives, and acetone have been reported to be superior to formalin with respect to retaining RNAs and proteins, but inferior in morphological quality compared to formalin [6, 12]. Paxgene is a commercial fixative introduced most recently and is perhaps the most promising alternative, albeit at a high cost [39]. Snap-freezing of tissues followed by cryo-sectioning avoids chemical fixatives and ensures good biomolecule quality. However, such preparation is technically challenging and can often result in suboptimal tissue morphology, and preparing thick sections for 3D confocal microscopy is impossible. Biomolecule quality also heavily depends upon keeping the tissue well frozen throughout the procedure. For electron microscopy, tissue fixation by freezing is considered superior to chemical fixatives because of the immediate arrest of cell processes [13].

Paraffin embedding may be an additional limitation for antigen detection and macromolecule preservation [14]. There are many embedding/sectioning procedures available each with their own advantages and disadvantages. Both, the choice of the preservation method as well as embedding/sectioning strategy is determined by the goal of the study. Paraffin embedding/microtome sectioning is widely used and allows for very thin sections <5µm, however other alternatives such as polyester wax/stedmans wax [15] and various plastic resins are available. High temperatures and solvents are included in these protocols, leading to tissue shrinkage and distortion and making it difficult to maintain the original sample's 3D architecture

[16-18]. As an alternative, agar-embedding combined with vibratome slicing can help circumvent these difficulties.

In this study we used neighboring sections from liver and intestine tissue samples of Atlantic salmon to compare freeze-substitution (FS) to FF, with regard to the tissue morphology, immunofluorescence labelling, total protein concentration, the integrity of RNA, and the subsequent performance of RNA in sequencing based transcriptome analysis.

Materials and methods

Tissue samples and experimental design

Atlantic salmons were euthanized in accordance with the Norwegian Regulation on Animal Experimentation (http://oslovet.norecopa.no/statute.html), before tissues were sampled for downstream applications.

Fixation of tissues

Two methods, FS and FF were compared, using liver (hematoxylin and eosin (H&E) staining, protein yield, and RNA quality analysis), and the anterior part of the distal intestine (H&E staining, immunofluorescence, RNA quality, and transcriptomics analysis). After dissection, the tissue samples were washed with ice-cold phosphate buffered saline (PBS; Sigma-Aldrich) and cut into 0.5 cm^3 cubes. For FF, the biopsies were fixated with 10% neutral buffered formalin for 20 hrs, before being washed with 1xPBS and successively dehydrated to 70% ethanol. The samples were then stored in 70% ethanol at -20^{o}C until use.

For FS, tubes containing either 40 ml of pure isobutanol or 96% ethanol were cooled to approximately -100ºC by placing them in a slurry of liquid nitrogen, ethanol and dry ice. Tissue cubes were immersed into the precooled isobutanol for 4 minutes, before being transferred to the precooled ethanol tubes for 5 min. The frozen tissue samples were then stored in 96% ethanol at -80°C for at least 7 days, to allow water to be substituted by ethanol.

Embedding and sectioning

Paraffin embedding combined with microtome sectioning was used for H&E staining and morphology analysis, while agar embedding and vibratome slicing were used for immunofluorescence, protein and RNA isolation. For paraffin embedding, FF tissues were successively dehydrated to 96% ethanol, whereas the FS tissues were slowly brought to room temperature, before a 30 min incubation in fresh 96% ethanol. Next, tissues from both fixation methods were cleared in Clear Rite (3 x 3 min, Richard-Allan Scientific, Kalamazoo, MI) and then infiltrated and embedded in paraffin (3 x 1 hr, Paraplast, Sigma) at 61°C. Prepared paraffin blocks were stored at 4°C. For all paraffin embedded samples, 7 µm serial slices were prepared using a Leica RM2245 microtome (Leica Gmbh, Wetzlar, Germany) and mounted onto Superfrost Plus slides (Fisher Scientific, Pittsburgh, PA). Vibratome sections were cut on agarose embedded tissue after successive hydration in 1x PBS. Both liver and intestine were embedded in 3% low melting agarose (40°C) and prepared at 100 µm for immunofluorescence. Neighboring slices for RNA isolation were cut at 300 µm using a Compresstome VF-200 vibratome (Precisionary Instruments, NC, USA).

Tissue storage and RNA quality

Total RNA was extracted using Qiagen RNeasy kit (Qiagen, Venlo, Netherlands) from single 300 µm vibratome sections of FS and FF tissues immediately after slicing. The slicing and isolation of RNA were repeated after 3 and 6 months storage at -80oC. The RNA integrity number (RIN value) was obtained by analyzing each sample on a 2100 BioAnalyser capillary electrophoresis using an RNA 6000 Nano LabChip (Agilent Technologies, California, USA).

Library preparation and sequencing

In comparison to snap frozen material, FS also enables the possibility to isolate total RNA from dissected areas of interest. In this experiment, the mucosa layer of the intestine from 11 individuals were isolated from the intestinal folds, enabling us study genes involved in uptake and transport of nutrients. Briefly, intestinal slices (300 µm) were placed in ice cold RNAse free 1 x PBS and dissected manually under a microscope, total RNA was extracted as described above. Stranded libraries were produced from 2 µg total RNA using the TruSeq Stranded Total RNA Sample Prep Kit (Illumina, USA) according to the manufacturer's instructions (Guide:15031048 Rev.E). Sequencing was performed on a MiSeq instrument using the v3 MiSeq Reagent Kit (Illumina) and pooling 10-12 samples per lane, generating 2 x 300bp of strand specific, paired-end reads. Raw sequencing files (.fastq) were subjected to adapter and quality trimming using cutadapt [19] followed by quality control with FastQC before aligning the trimmed reads to the Atlantic salmon genome (GenBank Accession number: GCA_0002333375.4) [20] using STAR [21]. Read alignments, recorded in BAM format, were subsequently used to count uniquely mapped reads per gene using the HTseq-count script [22] and provisional genome annotation [20]. The resulting data were then compared against a dataset

prepared in an earlier study using snap frozen intestines. Gene counts for all samples were imported into R and analyzed with the edgeR package [23]. Genes from more than 3 samples with at least one count per million (CPM) were considered to be expressed. The sequencing data is publicly available through the ArrayExpress Database at EBI (https://www.ebi.ac.uk/arrayexpress/; accession E-MTAB-3821).

Protein extraction and total protein concentration measurement

To avoid anatomical or regional tissue heterogeneity total proteins were extracted and the concentration was measured in liver samples, but not in intestine. Five replicates of each FS and FF liver neighbouring pieces, originating from the same fish were used (20 mg wet weight per sample). Briefly, 1 ml of RIPA buffer (150 mM NaCl, 50 mM Tris-Cl, 1% Triton X-100, 1% sodium-deoxycholate, 0.1% SDS, 10 mM EDTA, pH 7.4) was added to 20 mg of sample before homogenizing for 20 seconds using TissueLyser LT (Qiagen, CA, USA). The samples were then incubated on ice with gentle periodical shaking for 30 minutes. The resultant lysate was centrifuged at 10 000 g for 20 min at 4°C. The supernatant was collected and re-centrifuged under the same conditions before using a bicinchoninic acid assay (BCA, Pierce, Rockford, IL) to determine total protein yield. A standard curve was prepared using serially diluted bovine serum albumin (BSA; 2.0 µg/µl 1.5, 1.0, 0.75, 0.5, 0.25, 0.125, 0.025, 0). Aliquots of each standard and sample (25 µl) were mixed with 200 µl of BCA working reagent (Pierce), and then incubated at 37°C for 30 minutes. Absorbance at 526 nm (NanoDrop 2000, Thermo Fisher Scientific, Massachusetts) was then measured at room temperature.

Hematoxylin and Eosin staining (H&E)

For H&E staining the sections were deparaffinized by bathing 3 times (15 min each) in Clear Rite 3 (Richard-Allan Scientific, Kalamazoo, MI). They were subsequently rehydrated by soaking in series of diluted graded ethanol solutions (96%, 70%, 50%, 3min each) and then in 1 x PBS. Sections were stained with hematoxylin (Sigma-Aldrich; St Louis, MO) for 1.5 minutes, rinsed with the tap water for 30 sec, stained with eosin (Sigma-Aldrich; St Louis, MO) for 2.5 minutes, and dehydrated in ethanol and xylene. Finally, samples were mounted with Poly-Mount Xylene (Polysciences, Inc).

Immunofluorescence

Vibratome sections from FS and FF intestine tissues were prepared for immunofluorescence and the signal intensities and background fluorescence were compared. The procedure was performed in 24-well plates with gentle agitation using free floating sections. Slices were first hydrated in 1 x PBS containing 0.5% Triton-X 100 (PBST) and then permeabilized for 20 minutes with 1 x PBST. Blocking was performed by soaking samples for 1 hour in 1 x PBST containing 2% dry milk powder (Sigma-Aldrich; St Louis, MO). Samples were exposed to the primary antibodies (Table 1) in PBS containing 2% dry milk powder and 0.02% Triton overnight at 4°C. Following a series of washes (using 0.02% Triton X-100 in PBS), samples were incubated for 2 hours with secondary antibodies diluted in 2% dry milk and 0.02% Triton in PBS. Samples were washed repeatedly in 1 x PBST, before nuclear staining with DAPI and clearing in 2,2'-thiodiethanol (Sigma-Aldrich; St Louis, MO). Vibratome slices were also stained with Alexa Fluor 488-conjugated phalloidin (1:200 in PBS) or Alexa Fluor 488-conjugated wheat germ agglutinin (1:

500 in PBS) (Sigma). Samples were incubated at room temperature for 30 minutes with gentle rocking, before DAPI staining and 3 x 20 minute washes with 1 x PBS.

Samples were imaged using confocal microscope (Leica TCS LSI-III). Immunofluorescence was evaluated by applying excitation and emission filters adapted for the fluorochromes used, recommended by the manufacturer. ImageJ (http://imagej.nih.gov/ij/; NIH; Bethesda, MD) was used for image analysis and processing.

Table 1. List of antibodies and fluorescent stains* used to test antigen preservation in freeze-fixed and formalin-fixed intestine tissues

Antigen / Ready probe	Species and Isotype	Source	Secondary Antibody
CDH1	Mouse IgG2a	610182, BD Transduction Laboratories	647 goat anti-mouse IgG (H+L) (Life Technologies)
Na, K-ATPase	Mouse IgG	II-20/5.75.36, DSHB Hybridoma Product	647 goat anti-mouse IgG (H+L) (Life Technologies)
WGA*	Alexa Fluor 488-conjugated wheat germ aglutinin	W11261, Life Technologies	
Phalloidin*	Alexa Fluor 488-conjugated Phalloidin	A12379, Life Technologies	

Antigenes and cell structures, with corresponding antibodies and ReadyProbes (*) used to compare fluorescent staining between freeze-substitued and formalin-fixed small intestine tissue samples from Atlantic salmon (Salmo salar) are shown. Agar embedded, 100 µm vibratome sectioned samples were used.
Abbreviations: Cdh1, cadherin. WGA, Wheat Germ Agglutinin.
* denoting ReadyProbes® Reagents

Results

RNA integrity

Analysis of RNA quality showed that the choice of fixation method has a profound effect on the extent of RNA degradation (Table 2). The quality of FS samples was high, as judged by intact 28s and 18s ribosomal RNA bands, whereas these bands were lost and the RNA appeared as a smear on the gel when RNA from FF tissues was analyzed. RNA with the highest RIN scores (10) was isolated from FS liver tissue. RINs for RNA from FS tissue were in the range of 9.6 – 10.0, while for FF tissue were predominantly in the range of 0.0 – 3.3. As expected, RNA was slightly better preserved in liver than in the small intestine samples. The mean fragment length obtained by the FS and FF was approximately 2200 and 100 nucleotides, respectively.

Table 2. Chromatogram representation of Bioanalyzer RIN values, showing quality of RNA isolated at three time points, from freeze-fixed and formalin-fixed intestine and liver tissue.

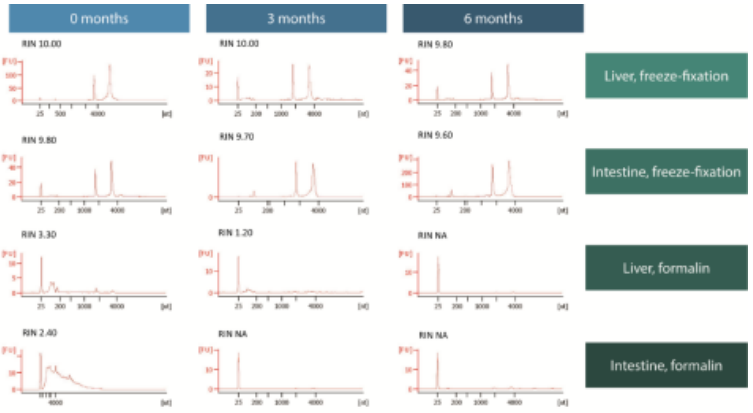

In order to determine how storage influences the RNA integrity of fixated tissue, RNA was isolated from the liver and intestine at the three time points: soon after the fixation, after 3 and 6 months of storage. Over the time, the quality of RNA in freeze-fixed tissues only slightly decreased from 10.00 to 9.80 in liver and from 9.80 to 9.60 in intestine. FF seems not to provide such storage possibilities, as there was a larger drop in the quality of the RNA extracted after equivalent times (3.30-0 in liver and 2.40-0 in intestine samples).

Gene expression

The gene expression from manually dissected slices (11 specimens), prepared from FS intestines, was analyzed using RNAseq. The results from this experiment were compared with an existing RNAseq dataset (ArrayExpress accession: E-MTAB-3822) consisting of two Atlantic salmon intestinal samples that were fixed by snap freezing the tissues samples in liquid nitrogen. Comparing the average mapping statistics between samples that were FS and samples which were snap-frozen showed highly similar percentages for the number of unique reads as well as for multi-mapping reads (Table 3). To verify that gene expression measurements were not affected by the fixation method, we compared the identities as well as the expression levels of all genes found in both datasets. The majority of genes (86.4%) could be identified in both datasets (Fig. 1). However, a considerable proportion (10.2%) were found to be expressed only in the dataset of the snap-frozen samples.

Table 3. Average mapping/counting statistics for samples from reference intestine compared to samples from freeze-substituted intestine slices.

	Intestine freeze	Intestine reference
Average input read length	530,27	435,5
UNIQUE READS:		
Uniquely mapped reads %	76,61	75,63
Average mapped length	530,89	437,14
Mismatch rate per base, %	0,55	0,39
MULTI-MAPPING READS:		
% of reads mapped to multiple loci	6,94	6,03
% of reads mapped to too many loci	1,54	1,43
UNMAPPED READS:		
% of reads unmapped: too many mismatches	0	0
% of reads unmapped: too short	13,49	15,74
% of reads unmapped: other	1,42	1,18

Protein concentration

Total protein concentrations from 5 fish livers prepared by FS or FF were analyzed. Preparation of proteins from FS tissue showed more than two fold higher protein yield compared to formalin (Table 4).

Table 4. Total protein concentrations isolated from freeze-substituted and formalin-fixed samples.

Sample	Freeze-fixed [µg/µl]	Formalin-fixed [µg/µl]
1	5.5	1.3
2	4.3	2.8
3	6.2	3.1
4	3.4	0.93
5	5.9	2.1
Mean	5.06 ± 1.18	2.046 ± 0.93

Sectioning and tissue morphology of paraffin embedded tissues

Cell and tissue morphology of liver and intestine was compared between sections of FS and FF tissues. No differences in the ease of paraffin sectioning were apparent with respect to tissue hardness, curling, stretching and adhesion to the slides. Rapid freezing is of importance to avoid freeze artefacts from ice crystals and was rarely seen as long as the tissue sample was kept sufficiently small. Larger tissue samples can also be prepared without freeze artifacts as long as the thickness is ≤ 5 mm. Microscopic examination of H&E stained intestine showed no visible differences between FF and FS intestine (Fig. 1C and D). Microscopy of sectioned livers revealed some differences with respect to morphology. The FS tissue appeared denser, with more intimately connected hepatocytes. In the FF liver, tissue shrinkage was apparent for both cells and nuclei (Fig. 1A and B).

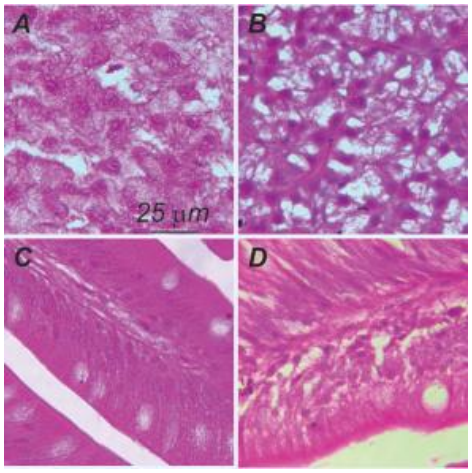

Figure 1. Hematoxylin and eosin stained sections of A. Freeze-fixated liver (40x magnification) B. Formalin-fixated liver (40x) C. Freeze-fixated intestine (40x) D. Formalin-fixated intestine (50x) of Atlantic salmon. Paraffin sections, 7 µm.

Microscopy & immunofluorescence

Immunofluorescence was carried out to assess antigen accessibility for vibratome slices of both FF and FS intestine. Notably, FF tissues exhibited a broad-spectrum autofluorescence. Summary of FF and FS performance in immunofluorescence is shown in Table 5 and Fig. 2 - 3. Cdh1 was detected in the tight junctions and showed a similar spatial distribution for both fixation methods. Signal intensity was considerable stronger in sample fixated by FS. Signal of NaK-ATPase was not detectable in FF intestines, whereas tissue prepared by FS showed intense staining. Intestinal integrity was also visualized by Phalloidin and WGA, staining filamentous actin and cell membranes/mucus, respectively. No differences in morphology was visible between the two fixation methods and both stains showed a similar distribution and fluorescence intensity.

Table 5. Results of fluorescent staining of freeze-substituted and formalin fixed samples.

Antigen	Freeze-substitution	Formalin-fixation
Cdh	+	+
Na,K-ATPase	+	-
Phalloidin*	+	+
WGA*	+	+

Freeze-substituted and formalin-fixed small intestine samples were evaluated for their performance in fluorescence staininig. + indicates that the fluorescent signal was detected, while - indicates absence of signal.
Abbreviations: Cdh1, cadherin. WGA, Wheat Germ Agglutinin.
* denoting ReadyProbes® Reagents

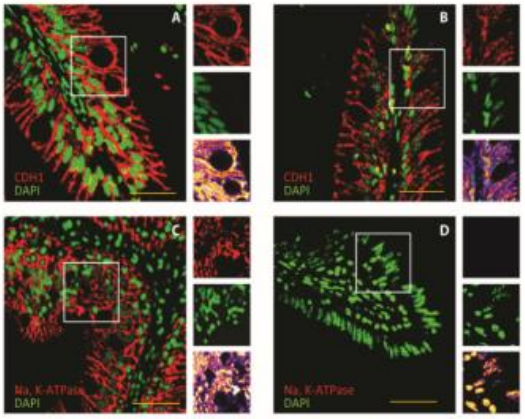

Figure 2. Immunofluorescence microscopy of freeze-substituted (A, C) and formalin-fixed (B, D) intestine using indirect immunofluorescence. Bars 20 µm. Nuclei were labelled with DAPI (green). Section of villus stained with antibodies to CDH1 (red) in freeze-substituted (A) and formalin-fixed (B) sample. Section of villus stained with antibodies to Na,K-ATPase (red) in freeze-substituted (C) and formalin-fixed (D) sample. Na,K-ATPase signal was not detected in formalin-fixed sample (D). Heat map images were made using fire option in ImageJ and indicate stronger signal under the same imaging conditions in freeze-substituted compared with formalin-fixed samples.

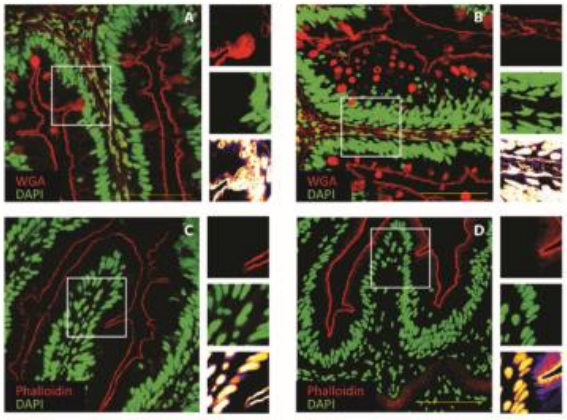

Figure 3. Confocal fluorescence microscopy of freeze-substituted (A, C) and formalin-fixed (B, D) villi stained using ReadyProbes® Reagents. Bars 20 µm. Nuclei were labelled with DAPI (green). Section of villus stained with WGA ReadyProbes (red) in freeze-substituted (A) and formalin-fixed (B) samples. F-actin ReadyProbes® stained villus (red) in freeze-substituted (C) and formalin-fixed (D) samples. Heat map images were made using fire option in ImageJ and indicate stronger signal under the same imaging conditions in freeze-substituted compared with formalin-fixed samples.

Discussion and Conclusions

Preserving tissue integrity is the primary objective of fixation procedures, and FF has established itself as the gold standard in histology. However, this approach has limitations when it comes to transcriptomic studies, protein analysis and immunohistochemistry. We have investigated FS as an alternative to FF and asserted important parameters including tissue morphology, and the ability to isolate high quality proteins and nucleic acids.

During FS, tissue is rapidly frozen at the temperatures below -80°C to avoid formation of ice crystals, which would deteriorate tissue morphology. Tissue is then immersed in cold absolute ethanol which dehydrates and fixes the tissue at the same low temperature. The effect of this is that fixed tissue and cells maintain their native morphology and preserve some classes of molecules such as nucleic acids and proteins. FS tissue can be embedded in paraffin and then easily sectioned. We observed that finer tissue morphology can be affected by formation of freeze artefacts when tissue pieces used for fixation are too thick; this is probably due to the slow water thermal conductivity of cellular water during the fast freezing. Thus, we recommend keeping tissue thickness less than 5 mm. Microscopy of H&E stained intestines revealed a similar morphology, whereas the liver appeared more compact with enlarged nuclei in the FF material.

Thus, FS is not entirely comparable to formalin and should be used with care for histopathological examination.

In order to compare epitope preservation of FS samples with FF samples two polyclonal antibodies using indirect immunofluorescence and two fluorochrome-conjugated stains were tested (Table 1). The goal of applying these different antibodies and stains was not to address the biology of the antigen, but to evaluate the relative degree of antigenicity when using the two preservation methods. Through immunofluorescence assays we demonstrated that FS combined with agar embedding is an excellent protocol that preserves antigens and allows antigen detection, overcoming protein cross-linking, one of the major limitations of FF. The results of the present study showed that FS in addition to preserving the structure of the tissue also allows a uniform immunolabeling. Tissue antigenicity was well maintained for the antibodies we tested and showed a better overall preservation of epitopes than FF. NaK-ATPase antigens were detected in FS, but not in FF samples. In addition, the strong immunofluorescence signal and weaker background in FS compared to FF samples indicated the suitability and higher sensitivity of this fixation method in immunolabeling. The tissues analyzed were embedded in low melting agar and sliced on vibratome, instead of the commonly used paraffin embedding followed by microtome slicing. Thus, any adverse effects of high temperatures during the paraffin embedding procedure were avoided [30]. Besides, low point melting agar followed by vibratome slicing enabled us to prepare sections up to 300 μm thick, allows investigation of the 3D organization of the tissue. New available techniques for 3D imaging make this an interesting option [32, 33]. For sections thinner than 20 μm wax embedding and microtome sectioning still is the preferable method. However, it is important to emphasize that FS is not a panacea. Not all antigens can be detected by antibodies after FS due to their inaccessibility or inactivation by alcohols or if

proteins are extracted by the solvent [34, 35]. Using low concentrations of glutaraldehyde rather than the pure solvent might be a possible solution for this [35]. However, some targets are better preserved in formalin or other fixation chemistry and retention of antigenicity is antigen-dependent; therefore, it is important to compare different sample preparation techniques to determine which is optimal for a specific antigen or application.

Long term storage of FS tissues is not recommended for immunolabeling, and it has been reported that prolonged incubation in absolute ethanol removes not only free water, but also water bound to molecules, causing excessive tissue drying which may result in weaker signal, stronger autofluorescence and poor antibody detection [36, 37]. Most likely this problem can be overcome by storing frozen samples dry and adding ethanol for water substitution at a later stage when the samples are to be analyzed. As described, storage had negligible effects on the RNA integrity in FS tissue, whereas storage of FF tissues contributed to considerable degradation of RNA after 3 and 6 months, pointing that FF does not have such protective capabilities.

Studies that compare protein concentrations in tissues fixed in various ways are few and to our knowledge there are none that investigate protein concentration in FS samples. In the present study total protein concentration measured in FF was lower compared to FS samples. These findings are most likely related to the cross-linking effect of formalin, which reduces protein solubility and extractability from a tissue sample [38].

RNA quality has been reported superior in FS samples, as detected by RNA in situ hybridization [24]. The possibility to carry out RNA sequencing on tissue sections is of importance for small and valuable samples but requires high-quality RNA to provide reliable data. Our results on RNAseq describe similar read count and mapping statistics, as well as a high expression correlation between the RNA samples from FS and standard liquid-nitrogen frozen tissues. This suggests that FS is a suitable protocol for the preservation of RNA for highly sensitive

downstream applications, such as sequencing. The portion of the genes (10.2%) that were not detected in the FS dataset maybe related to the fact that we microdissected FS samples, removed serosa, muscle and submucosa tissue layers and that RNA from only a subsection of the organ was analyzed. The difference could also be explained by our classification of expressed genes (see M&M), and the smaller number of samples in snap-frozen dataset. Regardless, comparing the average gene expression of all genes that were found in both datasets showed a high, significant correlation (r = 0.8927; p-value < 2.2e-16 , Fig. 4), thus confirming FS as a reliable fixation method for gene expression measurements.

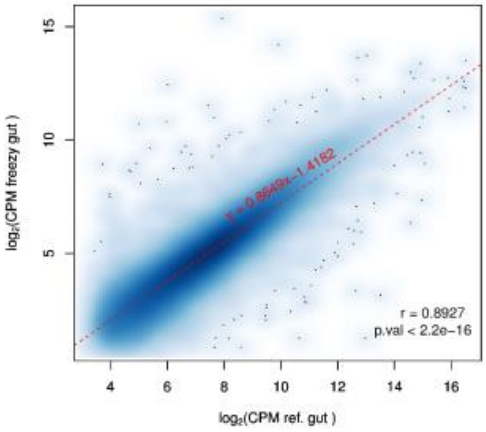

Figure 4. Scatterplot displaying the average gene expression (as log2 counts per million CPM) for samples from snap-frozen intestine samples (ref. gut) compared to freeze-fixed intestine (freezy gut). Pearson correlation (r) displayed in the plot.

Despite some shortcomings, FS is a sample preservation method that renders samples suitable for both morphological and molecular studies. There are a variety of FS protocols which combine

different coolant and substitution media. In our study we chose isobutanol and ethanol, but alternatives include sequential immersion in isopentane and methanol [24]. Even though isobutanol has a higher melting point it is a suitable replacement for isopentane: it freezes tissue equally rapid; is not explosive and is safe for the working environment. Main advantages of FS are that it circumvents protein-crosslinking, deterioration of biomolecules and nucleic acid degradation so that neighboring tissue slices of the same sample can be used for histological and several downstream molecular applications. Thus, FS is a reliable, highly stable, cheap, non-toxic, and fast tissue preservation method, which provides good quality of histological detail, preserve tissue antigenicity, permit recovery of proteins and RNA of high quality, and is a recommended alternative to the commonly used FF.

References

1. Delfour, C., et al., *RCL2, a new fixative, preserves morphology and nucleic acid integrity in paraffin-embedded breast carcinoma and microdissected breast tumor cells.* J Mol Diagn, 2006. **8**(2): p. 157-69.
2. Gallego Romero, I., et al., *RNA-seq: impact of RNA degradation on transcript quantification.* BMC Biol, 2014. **12**: p. 42.
3. Srinivasan, M., D. Sedmak, and S. Jewell, *Effect of fixatives and tissue processing on the content and integrity of nucleic acids.* Am J Pathol, 2002. **161**(6): p. 1961-71.
4. Thavarajah, R., et al., *Chemical and physical basics of routine formaldehyde fixation.* J Oral Maxillofac Pathol, 2012. **16**(3): p. 400-5.
5. Shi, S.R., R.J. Cote, and C.R. Taylor, *Antigen retrieval immunohistochemistry: past, present, and future.* J Histochem Cytochem, 1997. **45**(3): p. 327-43.
6. Howat, W.J., et al., *Antibody validation of immunohistochemistry for biomarker discovery: recommendations of a consortium of academic and pharmaceutical based histopathology researchers.* Methods, 2014. **70**(1): p. 34-8.
7. Shi, S.R., Y. Shi, and C.R. Taylor, *Antigen retrieval immunohistochemistry: review and future prospects in research and diagnosis over two decades.* J Histochem Cytochem, 2011. **59**(1): p. 13-32.
8. Mueller, C., et al., *One-step preservation of phosphoproteins and tissue morphology at room temperature for diagnostic and research specimens.* PLoS One, 2011. **6**(8): p. e23780.
9. Stanta, G., et al., *A novel fixative improves opportunities of nucleic acids and proteomic analysis in human archive's tissues.* Diagn Mol Pathol, 2006. **15**(2): p. 115-23.
10. Vincek, V., et al., *A tissue fixative that protects macromolecules (DNA, RNA, and protein) and histomorphology in clinical samples.* Lab Invest, 2003. **83**(10): p. 1427-35.
11. Gillespie, J.W., et al., *Evaluation of non-formalin tissue fixation for molecular profiling studies.* Am J Pathol, 2002. **160**(2): p. 449-57.
12. Hostein, I., et al., *Nucleic acid quality preservation by an alcohol-based fixative: comparison with frozen tumors in a routine pathology setting.* Diagn Mol Pathol, 2011. **20**(1): p. 52-62.
13. McDonald, K.L., *Out with the old and in with the new: rapid specimen preparation procedures for electron microscopy of sectioned biological material.* Protoplasma, 2014. **251**(2): p. 429-48.
14. Accart, N., F. Sergi, and R. Rooke, *Revisiting fixation and embedding techniques for optimal detection of dendritic cell subsets in tissues.* J Histochem Cytochem, 2014. **62**(9): p. 661-71.
15. Steedman, H.F., *Polyester wax; a new ribboning embedding medium for histology.* Nature, 1957. **179**(4574): p. 1345.
16. Nelson, C.M. and M.J. Bissell, *Of extracellular matrix, scaffolds, and signaling: tissue architecture regulates development, homeostasis, and cancer.* Annu Rev Cell Dev Biol, 2006. **22**: p. 287-309.
17. Xu, R., A. Boudreau, and M.J. Bissell, *Tissue architecture and function: dynamic reciprocity via extra- and intra-cellular matrices.* Cancer Metastasis Rev, 2009. **28**(1-2): p. 167-76.

18. Daley, W.P., S.B. Peters, and M. Larsen, *Extracellular matrix dynamics in development and regenerative medicine.* J Cell Sci, 2008. **121**(Pt 3): p. 255-64.
19. Marcel, M., *Cutadapt removes adapter sequences from high-throughput sequencing reads.* EMBnet.journal 17.1, 2011. **17**(1).
20. Lien, S., et al., *The Atlantic salmon genome provides insights into rediploidization.* Nature, 2016. **533**(7602): p. 200-+.
21. Dobin, A., et al., *STAR: ultrafast universal RNA-seq aligner.* Bioinformatics, 2013. **29**(1): p. 15-21.
22. Anders, S., P.T. Pyl, and W. Huber, *HTSeq--a Python framework to work with high-throughput sequencing data.* Bioinformatics, 2015. **31**(2): p. 166-9.
23. Robinson, M.D., D.J. McCarthy, and G.K. Smyth, *edgeR: a Bioconductor package for differential expression analysis of digital gene expression data.* Bioinformatics, 2010. **26**(1): p. 139-40.
24. Duran, I., et al., *Freeze substitution followed by low melting point wax embedding preserves histomorphology and allows protein and mRNA localization techniques.* Microsc Res Tech, 2011. **74**(5): p. 440-8.
25. Kellenberger, E., *The potential of cryofixation and freeze substitution: observations and theoretical considerations.* J Microsc, 1991. **161**(Pt 2): p. 183-203.
26. Paul, T.R. and T.J. Beveridge, *Reevaluation of envelope profiles and cytoplasmic ultrastructure of mycobacteria processed by conventional embedding and freeze-substitution protocols.* J Bacteriol, 1992. **174**(20): p. 6508-17.
27. Hedegaard, J., et al., *Next-generation sequencing of RNA and DNA isolated from paired fresh-frozen and formalin-fixed paraffin-embedded samples of human cancer and normal tissue.* PLoS One, 2014. **9**(5): p. e98187.
28. Azimzadeh, O., M.J. Atkinson, and S. Tapio, *Qualitative and Quantitative Proteomic Analysis of Formalin-Fixed Paraffin-Embedded (FFPE) Tissue.* Methods Mol Biol, 2015. **1295**: p. 109-15.
29. Do, H. and A. Dobrovic, *Sequence artifacts in DNA from formalin-fixed tissues: causes and strategies for minimization.* Clin Chem, 2015. **61**(1): p. 64-71.
30. Otali, D., et al., *Combined effects of formalin fixation and tissue processing on immunorecognition.* Biotech Histochem, 2009. **84**(5): p. 223-47.
31. Paavilainen, L., et al., *The impact of tissue fixatives on morphology and antibody-based protein profiling in tissues and cells.* J Histochem Cytochem, 2010. **58**(3): p. 237-46.
32. Provenzano, P.P., K.W. Eliceiri, and P.J. Keely, *Multiphoton microscopy and fluorescence lifetime imaging microscopy (FLIM) to monitor metastasis and the tumor microenvironment.* Clin Exp Metastasis, 2009. **26**(4): p. 357-70.
33. Weninger, W.J. and T.J. Mohun, *Three-dimensional analysis of molecular signals with episcopic imaging techniques.* Methods Mol Biol, 2007. **411**: p. 35-46.
34. Ripper, D., H. Schwarz, and Y.D. Stierhof, *Cryo-section immunolabelling of difficult to preserve specimens: advantages of cryofixation, freeze-substitution and rehydration.* Biol Cell, 2008. **100**(2): p. 109-23.
35. Sobol, M.A., et al., *Quantitative evaluation of freeze-substitution effects on preservation of nuclear antigens during preparation of biological samples for immunoelectron microscopy.* Histochem Cell Biol, 2012. **138**(1): p. 167-77.
36. Warmington, A.R., J.M. Wilkinson, and C.B. Riley, *Evaluation of ethanol-based fixatives as a substitute for formalin in diagnostic clinical laboratories.* Journal of Histotechnology, 2000. **23**(4): p. 299-308.

37. Ramos-Vara, J.A. and M.A. Miller, *When tissue antigens and antibodies get along: revisiting the technical aspects of immunohistochemistry--the red, brown, and blue technique.* Vet Pathol, 2014. **51**(1): p. 42-87.
38. Grantzdorffer, I., et al., *Comparison of different tissue sampling methods for protein extraction from formalin-fixed and paraffin-embedded tissue specimens.* Exp Mol Pathol, 2010. **88**(1): p. 190-6.
39. Liu Y1 and Edward D.P, *Assessment of PAXgene Fixation on Preservation of Morphology and Nucleic Acids in Microdissected Retina Tissue*. Curr Eye Res, 2017. **42**(1): p. 104-110.

Paper II

Online image, retrieved June 2017, from http://mentalfloss.com/article

Functional divergence of beta-carotene oxygenase 1 enzymes after gene duplication in salmon (*Salmo salar*)

Nina Zoric[1], Jacob Torgersen[2], Fabian Grammes[1], Johannes von Lintig[3], Dag Inge Våge[1]

[1]Centre for Integrative Genetics (CIGENE), Department of Animal and Aquacultural Sciences (IHA), Faculty of Biosciences (BIOVIT), Norwegian University of Life Sciences (NMBU), P.O. Box 5003, N-1432 Ås, Norway.

[2]AquaGen, Postboks 1240, 7462 Trondheim, Norway.

[3]Case Western Reserve University, 2109 Adelbert Rd. Wood 341, Cleveland, OH 44106, USA.

Abstract

The red coloration of muscle tissue is a unique biological trait of salmonids, and is also an important factor influencing consumers' perception of filet quality. Red flesh color is caused by the accumulation of the dietary carotenoid pigment astaxanthin in muscle tissue, however only a small amount of astaxanthin absorbed from feed is finally deposited in muscle. Genome wide association studies in salmon have shown that beta-carotene-15,15'-monooxygenase 1 (*bco1*) and its paralog β-carotene-15,15'-monooxygenase 1 like (*bco1l*) are strong candidate genes for explaining variation in filet coloration. Here we investigated the functional roles of these two enzymes in carotenoid metabolism and consequently in salmon flesh coloration. We showed that Bco1 is a cytosolic enzyme mostly localized to subapical regions of enterocytes. Plasmids carrying either *bco1* or *bco1l* were transfected into an E. coli strain capable of synthesizing β-carotene. Bco1l showed a clear 15,15'-oxygenase activity, while Bco1 did not show any cleavage activity in this particular assay. This study represents the first functional characterization of candidate genes involved in salmon flesh coloration and creates opportunities for further analysis of this important salmon trait.

Introduction

Pink-red coloration of muscle tissue is striking feature of several salmonid genera, including Atlantic salmon and is caused chiefly by the accumulation of a specific carotenoid; astaxanthin. In wild salmon this is obtained from a crustacean rich diet, while in farmed salmon its synthetic counterparts are provided as a dietary supplement [1]. Intensity of flesh color varies depending on the pigment content in the diet, but is also affected by genetic variation [2]. Genome-wide association studies (GWAS) have identified a region on salmon chromosome 26, which is tightly associated with salmon flesh color [3, 4]. This region harbors both β-carotene oxygenase 1 (*bco1*) and its paralog β-carotene oxygenase 1 like (*bco1l*), which are members of the carotenoid cleavage oxygenases (CCO) family. Studies of BCO1 activity from drosophila, chickens, mice, rat, and humans have shown that BCO1 has a very narrow substrate specificity and converts carotenoids with at least one unsubstituted β-ionone ring, such as β-carotene, into retinaldehyde (vitamin A - aldehyde). Other non-provitamin A carotenoids such as astaxanthin and zeaxanthin remain intact, since BCO1 is unable to cleave such carotenoids [5-11].

In mammals, another member of the CCO-family, β-carotene oxygenase 2 (BCO2), has been found to have a broad substrate specificity and cleaves provitamin-A and non-provitamin A carotenoids into apocarotenoids [12, 13]. The function of these compounds in mammals is unknown, but studies in mice suggest that BCO2 cleavage prevents oxidative stress from carotenoid accumulation [14]. In addition to generating retinoids, BCO1 has recently been shown to also influence lipid metabolism. There is evidence that BCO1 is involved in retinyl ester formation [15-17], and in mouse embryo it contributed to retinyl as well as cholesteryl ester production [15]. Whether this alternative BCO1 function is exerted by its direct involvement in

the esterification process or indirectly (through secondary metabolites of carotenoids, such as retinoic acid and regulation of transcription) remains to be elucidated.

A relationship between genetic variation and carotenoid metabolism has been demonstrated in several species. In human, SNPs 5′ upstream from the *BCO1* gene correlate with decreased catalytic activity of BCO1 and increased circulatory levels of β-carotene [18, 19]. In the chicken, two fully linked SNPs, positioned within the proximal promoter of the *BCO1* gene, are associated with differential expression of the *BCO1* in the muscle and with variations in breast meat lutein and zeaxanthin content and yellow color [20]. The importance of CCO activity in carotenoid catabolism is also evident in sheep, where a non-sense mutation in BCO2 leads to xanthophyll deposition in adipose tissue and the phenomenon of yellow fat [21]. Together these studies provide evidence of a genetic effect on carotenoid bioavailability and carotenoid deposition and coloration of various tissues.

The role of CCO in the metabolism of Atlantic salmon has not been described and high expression of both *bco1* paralogs in intestine and liver, organs important for carotenoid metabolism, point they might be involved in the carotenoid metabolic pathways [22]. In mammals vitamin A is generated mostly by BCO1 mediated cleavage of β-carotene, α-carotene and β-cryptoxanthin substrates. However, in both wild and farmed salmon dietary astaxanthin is the most abundant carotenoid, with β-carotene, α-carotene and β-cryptoxanthin being present at relatively lower levels. Unlike mammals, fish produce vitamin A from astaxanthin [23-27], but the molecular pathway is not known. Retention of the two *bco1* copies in salmon genome could enable fish to utilize astaxanthin as a novel provitamin-A source, in addition to common BCO1 substrates, thus broadening the enzyme substrate specificity in Atlantic salmon.

Based on the facts that BCO1 is a carotenoid cleavage enzyme and that astaxanthin is the most abundant carotenoid available in salmon diet, we hypothesize that the two salmon paralogs *bco1*

and *bco1l* developed different substrate specificities, which enables more efficient processing of carotenoids.

In the present study we have investigated the potential role of the two *bco1* paralogs in Atlantic salmon flesh coloration, as indicated by GWA and gene expression studies [4]. We have cloned and expressed *bco1* and *bco1l* coding sequences using both *E. coli* and baculovirus expression systems, purified the gene products, and tested the enzyme activities *in vitro*. Substrate specificities of the salmon Bco1 and Bco1l were tested by expressing them in an *E. coli* strain capable of synthesizing and accumulating β-carotene and zeaxanthin. Appropriate antibodies were developed to assess the subcellular distribution of Bco1 in intestine using an immunofluorescence assay and compare its abundance between red and pale-fleshed fish. RNAseq was used to compare intestinal gene expression profiles in intestines from red and pale flesh colored fish, and to investigate the expression of *bco1* alternative splicing variants.

Materials and Methods

Western blotting

Total protein lysates were prepared from intestinal tissue collected from pale and red-fleshed individuals as defined by the genotype of rs863785818 SNP. Five homozygous individuals with red T allele and six homozygous individuals with pale G allele was analysed. The SNP falls within the 3'UTR of bco1l and is informative with regard to flesh color [4]. Protein lysates were prepared from 10 mg tissue using RIPA buffer (Tris-Cl, 50 mM; pH 8.0, 150 mM NaCl, 0.1% SDS, 1% NP-40, 0.5% deoxycholate and 1 mini protease inhibitor cocktail tablets [Roche Applied Science]/ 50 ml) and centrifuged at 14000g for 30 min at 4°C. Protein concentration of the supernatant was measured using Bradford reagent (Bio-Rad Laboratories), before mixing 10

ug of protein 2x laemmli buffer (63 mM Tris-HCl, pH 6.8, 10% glycerol, 5% 2-mercaptoethanol, 3.5% sodium dodecyl sulfate) and heating at 60°C for 10 minutes. Denatured protein was separated using a 4–15% Mini-PROTEAN® TGX™ Precast Gel (Bio-Rad Laboratories). Proteins were transferred to a PVDF membrane (Bio-Rad) using a Trans Blot Turbo (Bio-Rad) protein transfer system. Membranes were stained with Ponceau S to assess equal loadings and imaged for density measurements in ImageJ (http://imagej.nih.gov/ij/; NIH; Bethesda, MD). After Ponceau red destaining, the blots were blocked with 2% dry milk in TBST (50 mM Tris-HCl, pH 7.4, 200 mM NaCl, 0.1% Tween) overnight at 4°C and five times washed with TBST. Bco1 was detected using a 1:3000 dilution of a polyclonal mouse IgG antibody raised against the Atlantic salmon proteins epitope sequence (KVPDTTAGDKAN) by Abmart (NJ, USA). The blots were incubated with primary antibody in 2% dry milk in TBST overnight at 4°C, before being washed five times in TBST. Signal was detected by incubation with an alkaline phosphatase conjugated secondary goat anti-mouse IgG antibody (ThermoFisher) diluted 1:1000 for 1 hour at room temperature in TBST with 2% dry milk. After five times washing with x TBST and alkaline phosphatase buffer (0.1 M Tris-Cl, 50mM MgCl2, 0.1% Tween 20), the blots were stained with NBT/BCIP solution (Sigma-Aldrich), rinsed with water and dried. Images were captured and density measurements were normalized against the Ponceau red image. To verify the specificity of antibody binding, primary antibody was incubated overnight at 4°C with a 10X molar excess of synthetic epitope peptide. The neutralized primary antibody was then used in side-by-side comparisons with untreated antibody.

Immunofluorescent microscopy

For immunofluorescent microscopy tissues were sampled from the same fish pool as used for the western blotting protein quantification. Freeze substituted (Paper I), paraplast (Sigma-Aldrich;

St Louis, MO) embedded intestine tissues (8 µm in thickness) of red and pale-fleshed Atlantic salmon were used for immunofluorescence assay. For antigen retrieval, slides were boiled in an autoclave at 95°C in antigen-retrieval buffer (10 mM Tris-base; pH 8.6, 1 mM EDTA, 0.05% SDS) for 30 minutes, after which slides in the solution were cooled down to room temperature. The tissue sections were blocked in 4% dry milk powder in 1 x TBST for 30 min followed by overnight incubation at 4°C with anti-Bco1 antibody. The primary antibody was detected by Alexa Fluor® 647 conjugated secondary goat anti-mouse IgG antibody (Thermo Fisher Scientific). Several washes in TBST followed each step. DAPI (Sigma-Aldrich) was used for nuclear counterstaining. Samples were imaged on a Leica TCS LSI-III). Immunofluorescence was evaluated by applying excitation and emission filters adapted for the Alexa Fluor® 647 fluorochromes, recommended by the manufacturer. ImageJ was used for image analysis and processing.

mRNA sequencing

The fish used for the transcriptome analyses did not originate from the same fish pool as used for the western blotting protein quantification and immunofluorescence, due to the fish shortage. However, the same rs863785818 SNP was used as criteria to select five red and six pale-fleshed individuals for the analysis.

Total RNA (RIN> 9.5) was extracted from freeze substituted (Paper I) 300 µm vibratome sliced intestine tissues, using Quiagen RNeasy kit (Qiagen, Germany). Eleven samples were used to produce libraries using an Illumina TruSeq stranded mRNA kit (Illumina, California, USA) manufacturer's instructions with the following slight modifications: (i) 2µg input RNA, (ii) incubation for 25 s (vs. 8 min) at the "elute, fragment and prime" step, and (iii) using a cDNA:bead ratio of 1:0.7 ratio (vs. 1:1) after adapter ligation and PCR step. Libraries were

quantified using a Qubit® 2.0 Fluorometer and the Qubit® dsDNA BR Assay kit (Invitrogen™, Thermo Fisher, Massachusetts) and profiled using a 2100 BioAnalyzer system with the DNA High Sensitivity kit (Agilent Technologies, California) before being diluted to 10 nM and equal volumes being combined into a single pool. Sequencing was performed on a MiSeq machine (Illumina, California) with a v3 reagent kit, generating 2 x 300 paired-end reads.

Bioinformatics

RNA sequencing files were processed in the following manner: (i) Illumina adaptors were removed and the sequences were quality-trimmed using cutadapt (v1.8.1 with Python 2.7.8) specifying the options: -q 20 -O 8 --minimum-length 40. (ii) Trimmed reads were mapped to the Atlantic salmon genome (GenBank Accession number: GCA_0002333375.4) using STAR (v2.4.2a) [28]. (iii) Read alignments, recorded in BAM format were subsequently used to count uniquely mapped reads per gene using the HTseq-count.py script (v0.6.1p1) [29] with the RefSeq genome annotation where unique gene_ids were assigned to gene features. All illumina sequence reads are publicly accessible through the European Nucleotide Archive (http://www.ebi.ac.uk/ena) with the accession PRJEB10297.

Gene expression levels were calculated as counts per million total library counts using the R package edgeR [30]. Total library sizes were normalized to account for bias in sample composition using the trimmed mean of m-values approach. Log-fold expression differences were calculated contrasting samples with red and pale flesh color.

Additionally, read alignments (BAM format) were pooled and subsequently processed to count exonic parts for *bcmo1* according to the process deciphered in the vignette of the R package DEXSeq [31]. In short: RefSeq genome annotation was processed using

dexseq_prepare_annotation.py script before counting exonic features using the dexseq_count.py script.

Recombinant protein production - Gene synthesis

E. coli codon optimized *bco1* (GenBank: NM_001279071.1) and *bco1l* (GenBank: NM_001279074) open reading frames inserted into a pUC57 vector with NcoI and KpnI restriction sites were commercially purchased (GenScript, USA). The resulting pUC57_bco1 and pUC57_bco1l vectors were transformed into chemically competent DH5λ cloning cells (New England Biolabs) for plasmid upscaling using Qiagen Miniprep kit (Qiagen, Valencia, CA, USA).

Recombinant production of Bco1 and Bco1l in *E. coli*

Inserts from pUC57_bco1l and pUC57_bco1 were extracted by cutting with NcoI and KpnI and ligated into six NcoI/KpnI linearized expression vectors: pETM_13, pETM_14 (N-His6, 3C protease site), pETM_22 (N-His6, N- thioredoxin [Trx], 3C protease site), pETM_33 (N-His6, N-glutathione S-transferase [32] GST, 3C protease site), pETM_44 (N-His6, N-maltose binding protein [MBP], 3C protease site), and pETZZ_1a (N-His6, N-ZZ, 3C protease site) (EMBL, Heidelberg, Germany). After transformation into DH5λ cells, positive colonies were grown, plasmid DNA were isolated (Qiagen Miniprep kit) and the expression vectors sequenced using pBR3_forward primer (5'-TCCCCATCGGTGATGTC-3') and pET-24a_reverse (5'-GGGTTATGCTAGTTATTGCTCAG-3').

Resulting expression vectors containing correct inserts were transformed for expression into BL21 CodonPlus(DE3)-RIL chemically competent cells (Novagen). A 5 ml LB (Sigma-Aldrich), with 50 ug/ml kanamycin starter culture was incubated overnight at 37°C with shaking. Then, 4 ml of LB broth with 50 µg/ml kanamycin was inoculated with 200 µl starter culture and grown

in 24-well deep-well plates. Three expression conditions were tested: Autoinduction with the autoinduciton media (Sigma-Aldrich) overnight at 25°C (Sigma-Aldrich), induction by isopropyl-β-D-thiogalactopyranoside (IPTG) (Sigma-Aldrich) at 25°C for 4 hours and IPTG induction at 18°C overnight. IPTG induced cultures were preincubated at 37°C until OD600 reached 0.6 and cooled down before addition of IPTG to final concentration of 0.2 mM. The cultures were then incubated at 18°C for ~18 additional hours. Alternatively, IPTG was added to a final concentration of 0.5 mM, followed by incubation at 25°C for four hours. Cells were harvested by centrifugation at 4000 g for 20 min at 4°C. Five ml of lysis buffer (50mM Tris-HCl, pH 8.0; 250 mM NaCl; 20 mM imidazole, 1 EDTA-free protease inhibitor cocktail [Roche Diagnosis, Mannheim, Germany]/ 50 ml; 10 mg/ml chicken lysozyme [Sigma-Aldrich] and 1 ul/ml benzonase nuclease HC [Novagen]) was added per gr of pellet, followed by repeated rounds of freeze-thaw cycles. Soluble and insoluble parts were separated by centrifugation at 15000 g at 4°C for 30 min. A sample of the soluble (supernatant) was collected for SDS-PAGE gel analysis. Purification of soluble Bco1 and Bco1l proteins was carried out on Ni-NTA Agarose in case of His-tagged proteins (Qiagen, Germany) or Glutathione Sepharose 4B (GE Healthcare Life Sciences) for GST-tagged proteins. Eluates were sampled for SDS-PAGE gel analysis. Expression and purification of proteins expressed from different constructs and under different conditions were determined by SDS-PAGE.

Constructs that demonstrated good protein production were used in upscaled production.

Large scale recombinant protein production and purification in *E. coli*

Based on the protein solubility screen in the small scale expression, up-scaled production of soluble recombinant proteins was carried out using the optimal combination of vector and induction conditions previously identified. We chose two *E. coli* constructs for recombinant *bco1*

expression (pETM-MBP and pETM-ZZ) and overnight expression with 0.2 mM IPTG at 18°C. Due to the poor solubility, none of *bco1l* constructs was chosen for *E. coli* recombinant large scale expression. Briefly, 1 L fresh LB-kanamycin in 5 L baffled flask was inoculated with 10 ml starter culture. Cell pellets from five flasks were prepared per construct and lysed as described above, with the exception of using sonication on ice instead of freeze-thaw cycles. The lysate was centrifuged at 40 000 rpm for 30 min at 4°C (Beckman Coulter Optima L-90K Ultracentrifuge) and the supernatant was transferred to chilled 50 ml tubes. Purification was performed on an Akta purifier 10 (GE Healthcare) using HisTrap HP (GE Healthcare) or GSTrap columns (GE Healthcare), pre-equilibrated with lysis buffer. After flow-through collection, Bco1 or Bco1l were eluted using a gradient of 20 to 300 mM imidazole in ice cold buffer at flow rate of 0.5 ml/min. Eluted fractions were pooled, digested with 3C protease and the purification step was repeated as above, but this time flow through was collected and pooled together for ion exchange chromatography. Before being loaded onto a HiTrap Q HP column (GE Healthcare Life) for ion exchange, fractions containing enzyme were pooled together and buffer exchanged by dialysis to ion exchange running buffer (50 mM TrisCl, pH 7.0; 50 mM NaCl). Bco1/Bco1l were eluted from the IEX column with a gradient of 50 mM to 1 M NaCl at a flow rate of 0.4 mL/min and fractions containing the purified proteins were pooled, mixed with 10% glycerol and snap frozen in liquid nitrogen.

Recombinant Bco1 and Bco1l using a baculovirus expression system

Linearized *bco1* and *bco1l* inserts were ligated into a NcoI/KpnI digested both pFastBac HT A plasmid (N-His6, TEV protease cleavage site) (ThermoFisher) and pFastBacM30a (N-GST, pre protease cleavage site) (EMBL, Heidelberg, Germany). The resulting constructs were used to produce baculovirus in DH10BAC bacteria following the manufacturer's instructions

(ThermoFisher, Bac-to-Bac handbook). For initial testing of protein expression, either 5ml, 2ml or 1ml of high titer P3 baculovirus was added to 50 ml Sf9 starter cultures at a density of 1x106 cells/ml in 250 ml baffled flasks, and the cells were shaken at 27°C and rotated at 115 rpm. Serum-free Sf-900 III SFM (Gibco) was employed as growth media. After 72 h cells were harvested by centrifugation and stored at -80°C until further use.

Several constructs showed satisfactory amount of eluted proteins (Bco1: pFastBac-bco1 and pFastBacM30a-bco1 and Bco1l: pFastBacM30a-bco1l) and were expressed and purified on a large scale. For this 20 ml baculovirus was added to 1 L Sf9 cells (1x10ex6 cell density) in a 5 L baffled flask and expression was carried for 72h. Cell pellets were resuspended in 10 ml PBS, pH 7.4 containing 1 EDTA-free protease inhibitors tablet (Roche Applied Science)/ 50 ml. Then, cells were disrupted with Dounce homogenization, sampled for SDS-PAGE and the proteins were purified and analyzed same as described for the *E. coli* expression system.

Enzymatic assays

Frozen *E. coli* cells transfected with recombinant plasmid or Sf9 cell pellets infected with *bco1/bco1l* baculovirus (5 g) were resuspended in 20 ml sample buffer containing 200 mM NaCl, 20 mM Tricine pH 7.5, 1 mM dithiothreitol (DTT, Roche) and one Complete EDTA free Protease inhibitor Cocktail Tablet (Roche). Lysis of *E. coli* cells was performed by sonication on ice, at amplitude level 50, with 30 sec pulse, 30 sec break and repeated three times. Sf9 cells were homogenized manually using a 2 ml dounce homogenizor containing. The lysate was centrifuged at 40 000 rpm for 30 min at 4°C (Beckman Coulter Optima L-90 Ultracentrifuge) and the supernatant collected. For testing enzyme activity in the presence of detergents (tetraethylene glycol monooctyl ether [C8E4], hexaethylene glycol monooctyl ether [C8E8], n-octyl-β-D-

thioglucopyranoside [OTG], n-dodecyl-β-D-maltopyranoside [DDM], 3-[(3-cholamidopropyl) dimethylammonio]-1-propanesulfonate [CHAPS]) were added to the supernatant and samples were incubated on ice for 10 min before the enzymatic assays were performed according to published protocols [33, 34]. The extraction of β-carotene and retinoids from *E. coli* and HPLC analysis was performed as described in [10], with the difference that recombinant plasmids were kanamycin resistant and the expression was induced by adding IPTG to a final concentration 0.5 mM. To test cleavage products in zeaxanthin accumulating *E. coli* we followed the procedure from [15].

Expression of Bco1 and Bco1l constructs in carotenoid producing *E. coli*

Bco1 or *bco1l* expression vectors were transformed into *E. coli* BL21 cells carrying expression plasmids for β-carotene or zeaxanthin biosynthesis. The transformed *E. coli* were grown overnight at 37°C on LB solid medium containing 25 µg/mL kanamycin and 35 µg/mL chloramphenicol. Selected colonies were picked into 5 mL LB medium containing 25 µg/mL kanamycin and 35 µg/mL chloramphenicol and grown at 37°C with shaking until the OD600 was ~0.6. Expression of *bco1* or *bco1l* was induced by adding IPTG to a final concentration of 1 mM. After growing the cultures for an additional 3–5 h, they were then streaked out on LB agar with 25 µg/mL kanamycin and 35 µg/mL and incubated at 25 °C for 2–3 days in darkness. Carotenoid cleavage activity was visualized qualitatively by the lack of accumulated carotenoids which results in the absence of the yellow color characteristic of non-transformed control cells. The bacteria on the plates were then collected for HPLC analysis.

Homology modeling of salmon Bco1 and Bco1l

The multiple sequence alignment of Bco1 (and Atlantic salmon Bco1l) sequences from different species was carried out with the ClustalW program (http://www.ebi.ac.uk/clustalw/) and used as the input for the ESPript program, version 2.1 (http://prodes.toulouse.inra.fr/ESPript/cgi-bin/ESPript.cgi) for multiple sequence alignment representation. The three-dimensional structures of salmon Bco1 and Bco1l were generated through SWISS-PROT using RPE65 (PDB 3fsn.1.a) as the template, while PyMol (Schrödinger, LLC) was used for viewing.

Results

Distribution of Bco1 in Atlantic salmon intestine

Western blots showed the presence of a single band of the expected molecular size (~60-kDa, deduced from the Bco1 sequence) using the Bco1 antibody (Fig. 1A). Further, a peptide competition assay was performed and the resulting blot verified that the signal was lost when the primary antibody was incubated with the corresponding immunizing peptide (Fig. 1B).

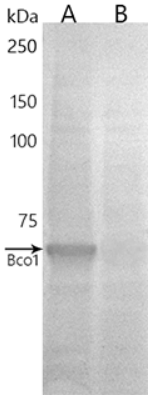

Figure 1. Western blot analysis of total protein lysate from Atlantic salmon intestine using (A) mouse anti-salmon Bco1 IgG polyclonal antibody or (B) the same antibody preincubated with Bco1 blocking

peptide. Absence of the band in B indicates specificity of the antibody for Bco1 in the Atlantic salmon intestine.

Thus, immunoblotting provided solid evidence that *bco1* is transcribed and translated into protein in the intestine of Atlantic salmon. Quantitative western blotting, in which the amounts of Bco1 between the red and pale-fleshed fish (according to the genotypes of the rs863785818 SNP) were compared showed two-fold higher abundance of Bco1 in the pale fish (Fig. 2).

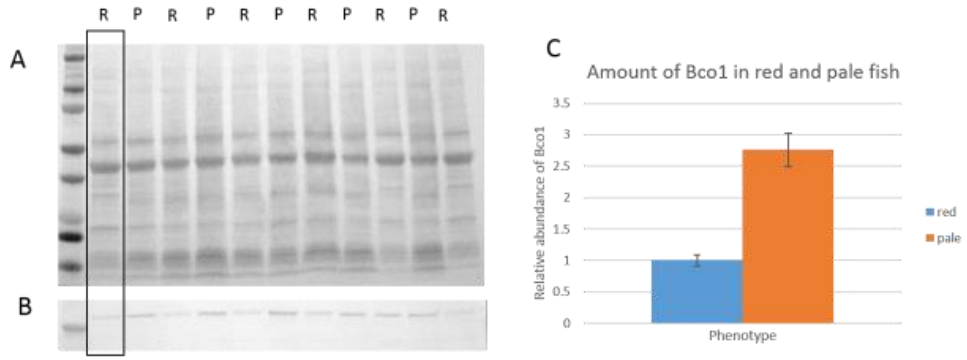

Figure 2. Quantitative western blot analysis of Bco1 protein in red-fleshed (R) and pale-fleshed (P) Atlantic salmon (according to the genotypes of the rs863785818 SNP). (A) Total protein from R and P fish stained with Ponceau red. (B) Western blots of Bco1 in R and P Atlantic salmon intestine. (C) Proportions of Bco1 protein levels in R and P fish. Results are expressed as mean ± SEM. Western blot band intensities were normalized vs. total protein band intensities on the Ponceau stained blots.

Subcellular distribution of Bco1 in intestine was investigated by immunofluorescence using the same anti-Bco1 antibody and revealed that the Bco1 is a cytosolic enzyme. More intense staining

was apparent in the apical part of the enterocytes, but Bco1 was also present in goblet cells and to a lesser extent throughout the basolateral area of the intestinal villi (Fig. 3A). Also, Bco1 was more abundant in pale than in red fish, judged by the signal strength for Bco1, which is in line with the western blotting (Fig. 3 A and B).

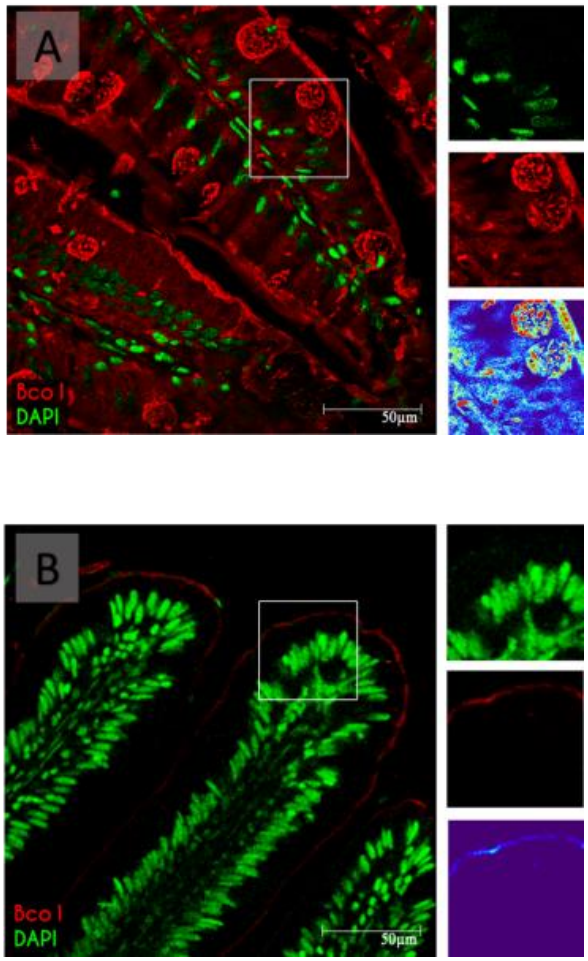

Figure 3. Immunofluorescence images displaying subcellular localization of Bco1 (red) and nuclear staining with DAPI (green) in (A) pale and (B) red-fleshed Atlantic salmon intestine. Staining revealed Bco1 is a cytosolic enzyme, localized to the apical membrane of enterocytes, also abundant in goblet cells

openings and to the lesser extent throughout the basolateral area. Bco1 is more abundant in pale than in red fish, judged by the signal strength for Bco1. Tissue was freeze substituted, paraffin embedded and microtome sliced at 10 μm. Scale bar 50 μm.

Seven antibodies against various epitopes specific to Bco1l were tested without success, despite extensive protocol adjustments such as different lysis buffers, blocking agents, dilutions, incubation times and temperatures. Thus, information about the Bco1l protein expression and distribution in intestine remains unknown.

Transcriptome analysis

We used RNA sequencing to compare intestinal transcription of fish displaying either red or pale flesh color (N=11). In total we identified 10 genes as significantly differentially expressed (DE, Fig. 4A) but this list did not include *bco1* or *bcol1*. We used gene set enrichment analysis (GSEA) to analyze the data from red-fleshed vs. pale-fleshed fish. The method showed significant enrichment of lipid-metabolism related genes in red-fleshed fish ($p < 0.05$).

Five different *bco1* splice variants exist: XM_014175230, XM_014175231, XM_014175233, XM_014175234 and NM_001279071, each coding for a different protein with predicted protein length of 527, 514, 521, 526 and 522 aa. Overall sequence identity is high, but important differences exist. We utilized the RNAseq dataset to inspect *bco1* transcription variant expression in the salmon intestine by counting reads within different exon [31], as well as counting the exon spanning reads. High expression of exon 15 together with low expression of exon 9 indicate that NM_001279071 is the highest expressed *bco1* splice variant in the salmon intestine. Our conclusion was further corroborated by the exon spanning reads (Fig. 4). For this reason, only NM_001279071 was used for gene synthesis and recombinant protein synthesis.

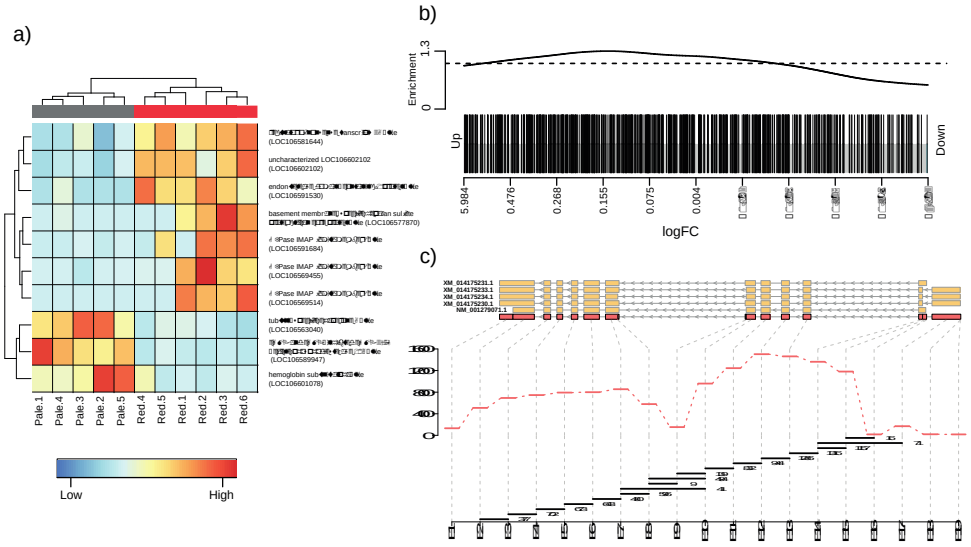
a)
b)
c)
Enrichment
1.3
0
Up
Down
5.984
0.476
0.268
0.155
0.075
0.004
logFC
Pale.1
Pale.4
Pale.3
Pale.2
Pale.5
Red.4
Red.5
Red.1
Red.2
Red.3
Red.6
Low
High
XM_014175231.1
XM_014175233.1
XM_014175234.1
XM_014175230.1
NM_001279071.1

Figure 4. (A) Heatmap showing intestinal expression of the 10 differential expressed genes. (B) Barcode plot showing enrichment of lipid-metabolism related genes in samples with red filet color. (C) Transcript plot indicating exon usage for *bco1*. The exon structure of the five different *bco1* transcripts is shown in orange. The 19 exon derived from the overlap of all five transcripts (representing the counting bins) are shown in red. Read counts for the different exon are shown as red bars. The black bars indicate the reads spanning from one exon to another. Start and end point of the horizontal lines indicate which exons are joined, the number to the right shows the exon-spanning read counts.

Protein purification and *in vitro* enzyme testing

First, small scale expression test was carried using constructs with different solubility tags fused to the *bco1/bco1l* coding sequence and under different expression conditions, because it is not uncommon to observe that overexpressed recombinant proteins are inactive, either due to an incorrect three-dimensional conformation or the formation of inclusion bodies. The expression of recombinant proteins in both *E. coli* and insect cells, was very efficient. However, insoluble proteins were largely rendered, with the limited amount of eluted proteins (Fig. 5 & Fig. 6). Similar difficulties were reported when CCO proteins from orthologues species were produced [35], confirming that production of recombinant Bco1 and Bco1l is challenging.

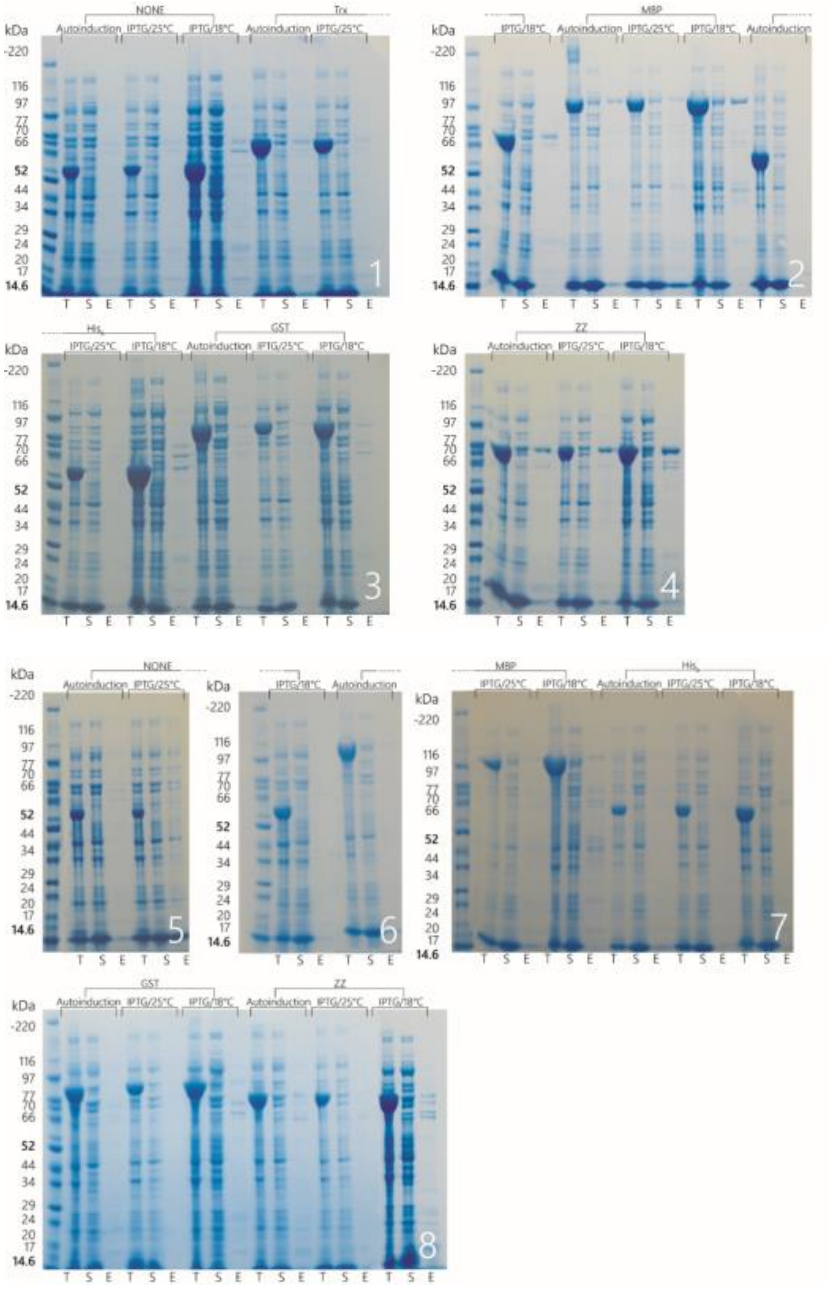
NONE
Trx
Autoinduction
IPTG/25°C
IPTG/18°C
kDa
-220
116
97
77
70
66
52
44
34
29
24
20
17
14.6
T S E
1
MBP
2
His6
GST
3
ZZ
4
5
6
7
8

Figure 5. SDS-PAGE analysis (Coomassie staining) of (1-4) Bco1 and (5-8) Bco1l proteins with fused tags, expressed in *E. coli*. Reading from left to right, the first lane shows the protein ladder (kDa). The next each three lanes show the total (T), supernatant (S) and resin elution (E) fractions under different expression conditions (autoinduction, IPTG induction at 25C for 4 hours, IPTG induction at 18C overnight), and with different tags fused to the coding sequence (None, Trx: thioredoxin, MBP: maltose-binding protein, His6: hexahistidine, GST: glutathione S-transferase, ZZ: Z domain of Staphylococcal protein .

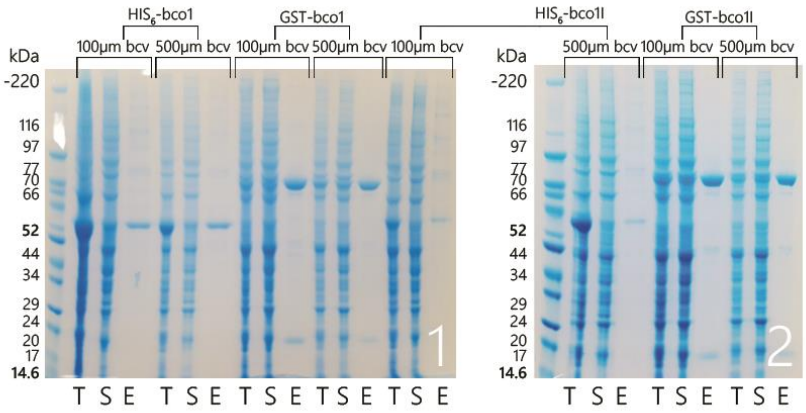

Figure 6. SDS-PAGE analysis (Coomassie staining) of Bco1 and Bco1l proteins fused to His6 (hexahistidine) or GST (glutathione S-transferase), expressed in Sf9 cells. Reading from left to right, the first lane shows the protein ladder (kDa). The next each three lanes show the total (T), supernatant (S) and resin elution (E) fractions, 72h post-infection with 100 ul or 500 ul baculovirus per 50 mL starter culture Sf9 cells (1x106 cell density).

Further, only constructs and the expression conditions that yielded sufficient soluble Bco1/Bco1l protein were used for the large scale expression and protein purification. *Bco1* was expressed in *E. coli* and insect cells, while for the *bco1l* only insect cells were used. Proteins were purified to apparent homogeneity (Fig. 7A). Western blotting analysis confirmed the presence of Bco1 (Fig. 7B), while Bco1l was confirmed by MS (data not shown), due to the lack of a specific antibody.

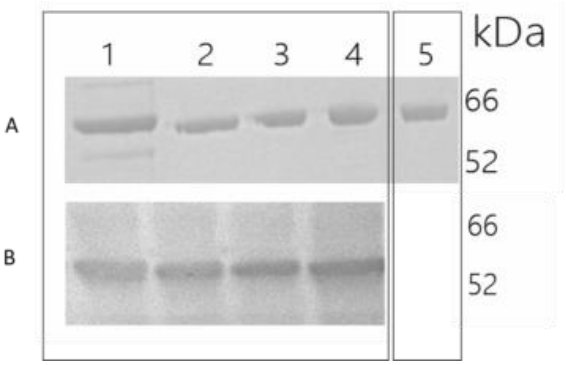

Figure 7. SDS-PAGE (Coomassie staining) (A) and Western blot (B) of purified recombinant proteins from large scale expression experiment. Reading from left to right, lane 1: Bco1 from pETM-MBP-bco1; lane 2: Bco1 from pETM-ZZ-bco1; lane 3: Bco1 from pFastBac HTa-bco1; lane 4: Bco1 from pFastBacM30a-bco1; lane 5: Bco1l from pFastBacM30a-bco1l. Western blotting for eluted Bco1l is missing due to the lack of a specific anti-Bco1l antibody.

Purified Bco1 and Bco1l protein were tested in an *in vitro* enzyme assay based on the previously published method for BCO1 https://www.ncbi.nlm.nih.gov/pubmed/8638938[36]. However, HPLC analysis revealed that neither Bco1 nor Bco1l cleave β-carotene, astaxanthin and lycopene substrates, further indicating the lack of activity of the purified Bco1 and Bco1l *in vitro* (data not shown). Because other members of the non-heme iron oxygenase family require detergents for either their solubilization (RPE65 [37]) or crystallization (ACO [38]) we also tested salmon recombinant Bco1 and Bco1l in the presence of several different detergents (tetraethylene glycol monooctyl ether (C8E4), hexaethylene glycol monooctyl ether (C8E8), n-octyl-β-D-thioglucopyranoside (OTG), n-dodecyl-β-D-maltopyranoside (DDM), 3-[(3-cholamidopropyl) dimethylammonio]-1-propanesulfonate (CHAPS)]. However, addition of detergents failed to improve enzyme activities (data not shown).

Cell based carotenoid cleavage assay

To further investigate activities of Bco1 and Bco1l we utilized an *E. coli* test system, previously used successfully to characterize CCOs [9, 13, 39-42]. This test system offered the advantage of combining β-carotene/zeaxanthin biosynthesis, and potential cleavage by carotene dioxygenases, in one organism. β-carotene or zeaxanthin producing *E. coli* were transfected with *bco1* or *bco1l* expression vector and the cleavage products were analyzed on HPLC [9, 13, 39-41]. pETM plasmids with *bco1*/*bco1l* coding sequences fused to Trx, MBP, His6 or ZZ tag were tested by following the established protocol [10]. If the bacterium remained yellow after transfection it indicates enzyme inactivity, if the color disappears it indicates a functional enzyme. Potential cleavage products from the enzyme reaction were determined by HPLC (Table 3).

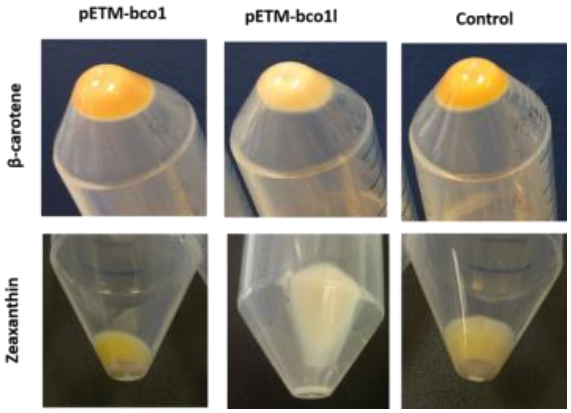

Table 3. Pellets of *E. coli* synthesizing β-carotene (upper row) or zeaxanthin (bottom row). The bacteria were transformed with plasmids containing salmon *bco1* (pETM-bco1) coding sequence, *bco1l* (pETM-bco1l) coding sequence or an empty vector (pETM-control).

Bco1 showed no cleavage activity, as both β-carotene and zeaxanthin producing *E. coli* cells transfected with *bco1* plasmids remained yellow. Corresponding HPLC chromatograms also confirmed absence of Bco1 cleavage products (Fig. 8 & Fig. 9).

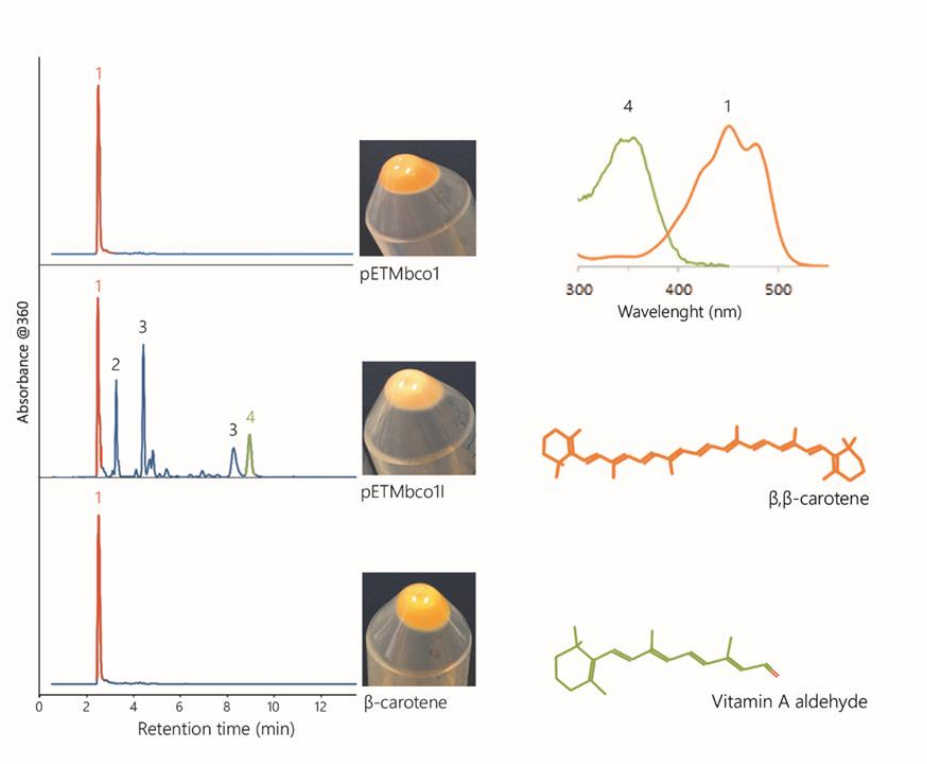

Figure 8. HPLC profiles of carotenoids and retinoids formed in β-carotene producing *E. coli* transformed with plasmids (pETM-MBP-bco1) for expression of salmon *bco1* cDNA or with (pETM-His6-bco1l) for the expression of *bco1l*. β-carotene producing *E. coli* transformed with an empty vector (pETM-MBP) was used as negative control. The scale bars indicate absorbance of 0.01 at 360 nm. Peaks corresponding to UV/Vis absorption spectra for individual compounds are shown in the upper right panels. Peaks corresponding to major compounds are denoted with numbers 1: β-carotene, 2: retinyl-ester, 3: All-trans-

Retinal oxime (syn and anti), 4: All-trans-Retinal. Cell pellets and structures of identified carotenoids are shown in the lower-right panel.

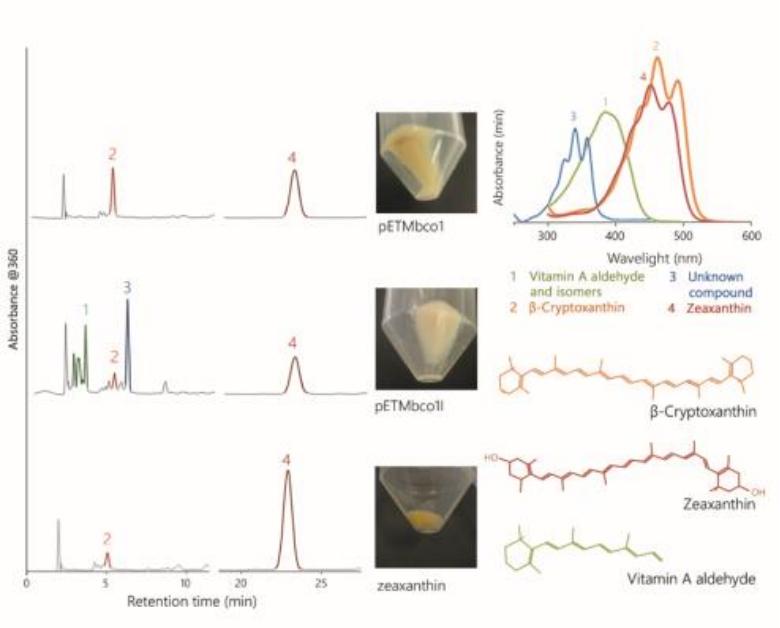

Figure 9. HPLC profiles (full chromatograms) of carotenoids and retinoids formed in zeaxanthin producing *E. coli* transformed with the plasmids (pETM-MBP-bco1) for the expression of salmon *bco1* or with (pETM-His6-bco1l) for the expression of *bco1l*. Zeaxanthin producing *E. coli* transformed with an empty vector (pETM-MBP) was used as control. The insert box of the panels to the left show enlarged chromatograms. Peaks corresponding to UV/Vis absorption spectra for individual compounds are shown in the upper right panels. Peaks corresponding to major detected compounds are denoted with numbers 2: β-cryptoxanthin, 4: zeaxanthin. Cell pellets and structures of the identified carotenoids are shown in the lower-right panel.

Differently from Bco1, Bco1l showed cleavage activity in both strains. First, β-carotene producing *E. coli* faded the yellow color when expressing *bco1l* and the HPLC chromatograms revealed the formation of retinal at the expense of β-carotene (Fig. 8). Results were similar when plasmids containing *bco1l* were expressed in zeaxanthin producing *E. coli* (Fig. 9): faded pellet color and retinaldehyde shown as cleavage product by HPLC. Spectra of the cleavage products of zeaxanthin producing cells transfected with *bco1* plasmids indicated that they either result from lycopene cleavage (which is a precursor for zeaxanthin in the pathway) or are oxidized 3-hydroxy-retinal (thus zeaxanthin cleavage products). To distinguish between these two possibilities and determine exact substrate specificity of Bco1, additional analysis such as mass-spectrometry should be performed. Thus, the biosynthetic precursors of zeaxanthin might already be converted by Bco1l when expressed in this *E. coli* strain. Hence, the zeaxanthin-producing *E. coli* did not provide a robust test system to characterize substrate specificity of Bco1l, but it confirmed its 15, 15' cleavage activity. The two experiments strongly suggested that Atlantic salmon Bco1l has 15, 15' oxygenase activity, while the activity of Atlantic salmon Bco1 remains elusive.

Sequence and structure comparison of salmon Bco1 and Bco1l

Multiple sequence alignment of Bco1 and Bco1l proteins of salmon with other species (Fig. 10) show that the two salmon proteins are highly conserved, although the salmon sequences have shorter C-terminal parts than BCO1 in the other species. In orthologues BCO1 the four Fe (II) binding histidines together with the five acidic residues were proposed as part of the catalytic center essential for enzyme function, and are completely conserved in both salmon proteins (Fig. 10).

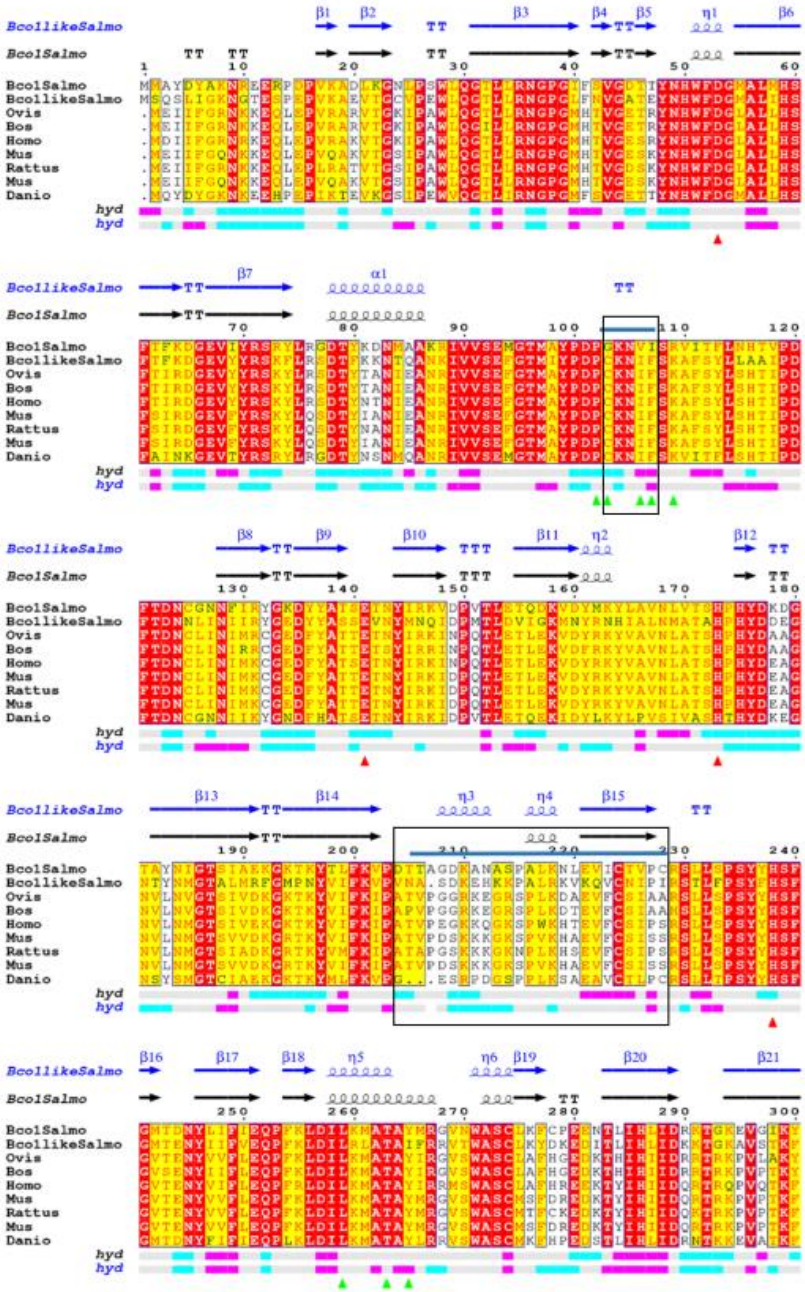
BcollikeSalmo
BcolSalmo
BcolSalmo
BcollikeSalmo
Ovis
Bos
Homo
Mus
Rattus
Mus
Danio
hyd
hyd

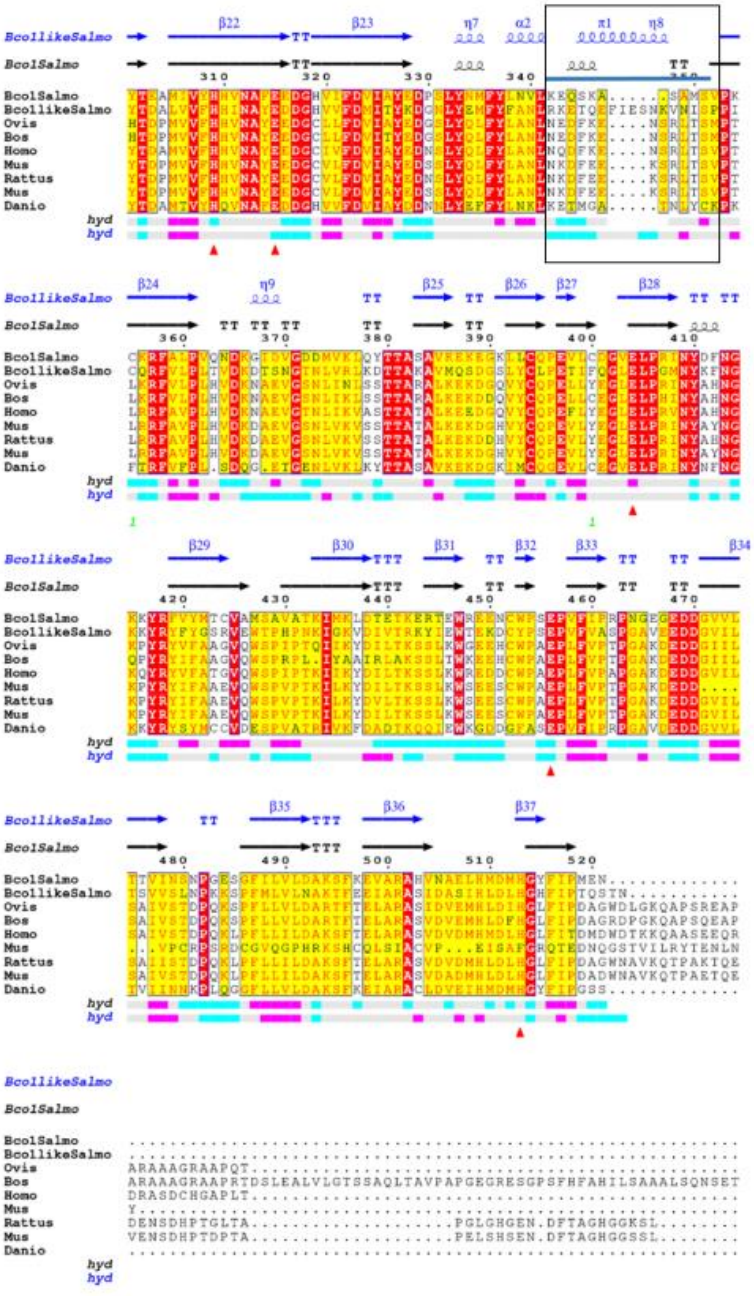
BcollikeSalmo
BcolSalmo
Ovis
Bos
Homo
Mus
Rattus
Danio
hyd
hyd

Figure 10. Multiple sequence alignment of Atlantic salmon Bco1 and Bco1l protein sequences against BCO1s' from different species, generated with ClustalW and ESpript. Similar residues are shown in yellow background, residues strictly conserved have red background, while the amino acid residues with different properties are white. Histidine residues and acidic residues vital for enzyme function are marked with red triangles. Residues composing hydrophobic patch are marked with green triangles. Residues showing differences between Bco1 and Bco1l models are boxed. Secondary structures of salmon Bco1 and Bco1l are illustrated on top: helices with squiggles, beta strands with arrows, turns with TT letters. Symbols below blocks of sequences show the relative hydropathy of Bco1 (upper) and Bco1l (bottom) sequence (hydrophobic as pink, intermediate as gray and hydrophilic and cyan).

Although the two salmon Bco1 enzymes are highly similar, Bco1 shows higher divergence than Bco1l, compared to consensus of conserved residues. The divergent amino acids include proposed substrate binding positions (F51, F93, E140, F307, Y326, S139, T141, Y235) and the hydrophobic patch forming residues at the entrance to the active tunnel in human BCO1 (P101, I105, K108, T262, C102, F106, L258, Y264) [43] (marked with the green triangles in Fig. 10) might underlie deviating functions of the two salmon Bco1 paralogs. In Bco1l T141 and Y236 diverged to V and F, while in Bco1 F93 and F307 diverged to M and Y, respectively. Bco1 differs at the following positions from Bco1l: C102G, I105V, F106I and K108R, while Bco1l at Y2645. Further, we compared 3D models of salmon Bco1 and Bco1l, and inspected diverged residues. For homology model making we used the crystal structure of bovine RPE65 as a template [44]. High similarities (40.1% for both Bco1/Bco1l) and identities of template sequences (40.04% for Bco1l and 39.36% for Bco1) with the RPE65 yielded reliable homology model, which was additionally supported by 0.70 Global Model Quality Estimates (GMQE) score. The overall structures of Bco1 and Bco1l exhibited substantial overlap (Fig. 11). The regions which do not

align between the two models (Fig. 12) correspond to the regions with diverged residues between Bco1 and Bco1l and are located at the proteins' periphery, not close to the proposed enzymes' active sites.

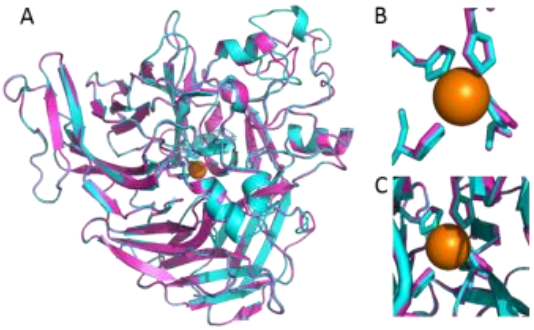

Figure 11. (A) Overlay cartoon view of predicted and spatially aligned Atlantic salmon Bco1 (purple) and Bco1l (cyan) structures, modeled with SWISS-MODEL program based on related RPE65 template 3fsn.1A (2.14 Å). (B) The iron cofactor, shown as an orange sphere, is directly coordinated by four histidine residues. (C) Iron cofactor with all the surrounding amino acid residues. For viewing PyMol was used.

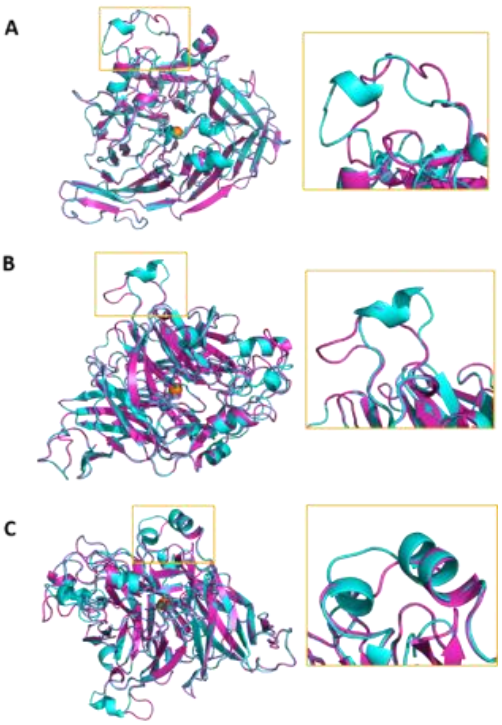

Figure 12. Regions of misalignment between predicted 3D Bco1 and Bco1l models.

Discussion

There has been a discussion about the molecular mechanisms explaining the red muscle of salmonids. It is well known that the color mainly originates from the red carotenoid pigment astaxanthin, but it is not well understood how astaxanthin is taken up and metabolized in salmonids and why there is such large variation between and within species. A QTL affecting flesh color in salmon was identified in the chromosomal region containing the *bco1* and *bco1l* genes [4]. The same study revealed differential expression of the two genes between red and pale fish using qPCR, providing additional evidence that these CCO might be important determinants

of salmon flesh pigmentation. Studies on various vertebrate CCO enzymes have shown they can cleave carotenoids such as β-carotene, astaxanthin and lutein. Detrimental mutations in some of these genes have caused yellow/orange coloration of various tissues in chicken, cow and sheep due to accumulation of carotenoids [21, 45, 46].

Why Atlantic salmon maintained two actively transcribed *bco1* and *bco1l* genes is not clear. Here, we functionally tested *bco1* and *bco1l*, and the corresponding gene products (proteins) in order to reveal how they influence carotenoid metabolism in the small intestine of Atlantic salmon. Western blotting demonstrated that the *bco1* gene is translated into protein in salmon intestine and that the Bco1 is two-folds more abundant in the intestine of pale compared to the red-fleshed fish. Immunofluorescence staining of Bco1 in sections of salmon intestine tissue indicated that Bco1 is a cytosolic enzyme, distributed across the enterocyte, with the strongest immunoreactivity in subapical region, close to the membranes of the apical surface of absorptive epithelial cells. This distribution is in line with what has been observed for human BCO1 [47, 48] and such spatial distribution ensures efficient cleavage of carotenoids absorbed into the enterocytes.

BCO1 in humans and mice is expressed in liver and adipose tissue, placenta, yolk sac and the embryo [9, 47, 49-52]. The expression in different tissues suggests that BCO1 might have additional roles like lipid homeostasis regulation [15-17]. A possible link of salmon astaxanthin pigmentation to lipid metabolism is indicated by the prevalence of carotenoids in lipid droplets in these animals [53]. A remarkable portion of astaxanthin may be esterified with fatty acids [54], probably conferring the antioxidant protection of storage lipids [55]. Free astaxanthin also incorporates into cell membranes, where it reduces lipid peroxidation while preserving membrane structure [56]. In order to check if astaxanthin and lipid metabolism in salmon are

linked, we analyzed RNAseq data using gene set enrichment analysis (GSEA) method. We focused on *a priori* defined set of genes assigned to lipid metabolism in Atlantic salmon and the results revealed that lipid-metabolism related genes, including those involved in lipid raft and lipid droplet formation, lipogenesis and cholesterol biosynthesis and membrane cell signaling were enriched in red-fleshed fish ($p<0.05$). Thus, the link between astaxanthin and lipid metabolism is supported by our results. GSEA analyze was appointed because it focuses on data at the level of gene sets, which is very beneficial since cellular processes often affect sets of genes acting in concert. Salmon flesh pigmentation is a result of interactions between genomic, proteomic and metabolomics factors, with animal characteristics such as age and nutrition playing an important role. This illustrates the challenge to identify DE genes between the two groups and explains why neither *bco1* nor *bco1l* were not among the 10 DE genes between the red and pale-flesh groups. However, results from [22] and the western blot protein quantification and immunofluorescence data from this study support that Bco1 protein is more abundant in red-fleshed than in pale-fleshed fish.

The Atlantic salmon genome has recently been sequenced [57] and the current gene annotation indicates the existence of five *bco1* isoforms. Judged by our RNAseq data, *bco1* NM_001279071 transcript was the most abundant in the intestine, while the other four (XM_014175230, XM_014175231, XM_014175233, XM_014175234) were detected at very low levels. Thus, we do not expect that other than *bco1* NM_001279071 variant is largely involved in carotenoid metabolism in salmon intestine.

Both western blotting and immunofluorescence showed different Bco1 abundance between the red and pale-fleshed fish. Differential Bco1 abundance between the red and pale-fleshed fish suggests that both Bco1 and Bco1l are active enzymes, perhaps with different substrate specificities, which also explains the retention of the two functional *bco1* paralogs. Since Bco1

was two folds more abundant it suggests that it cleaves astaxanthin. To study enzyme substrate preferences and their functions in carotenoid metabolic pathways we produced Atlantic salmon Bco's in *E. coli* and baculovirus expression systems. Purified recombinant Bco1 or Bco1l did not show *in vitro* activity when tested on β-carotene, astaxanthin and lycopene substrates.

Since the recombinant enzymes failed to show any *in vitro* activity, we also tested their activities *in vivo*, by expressing *bco1*/*bco1l* in *E. coli* strains engineered to produce β-carotene or zeaxanthin. Bco1l had clear 15, 15'-oxygenase activity on β-carotene and zeaxanthin, while Bco1 did not show any cleavage activity on either pigment. The observed activity of salmon Bco1l is consistent with the previous results for the orthologous beta-carotene oxygenase 1 in human, mouse, rat and chicken. Although Bco1 failed to cleave the substrate *in vivo*, it is also expected to be a functional protein in Atlantic salmon, since the protein was abundantly expressed according to the western blot and immunofluorescence analyses. Inspection of the Bco1 sequence showed that the four key histidine residues required for enzyme activity in orthologues enzymes are conserved in both Bco1 and Bco1l. Bco1 has diverged more than Bco1l in regions proposed to be essential for enzyme function (blue triangles, Fig. 10), including Cys102 → Gly, Ile105 → Val and Phe106 → Ile substitutions (yellow triangles in Fig. 10), but all of these changes are conservative, and are not likely to cause loss of Bco1 function. To further investigate the putative differences in structures of salmon Bco1 and Bco1l, we modeled salmon Bco1 and Bco1l using the crystal structure of bovine RPE65 as a template. The two models are highly similar and both have highly conserved structure in the active site domain. Poor alignment between Bco1 and Bco1l was only observed at the three periphery regions, which in orthologues BCO1 were suggested to be involved in substrate binding, indicating that Bco1 and Bco1l are likely to have identical cleavage mechanism, but they may differ in substrate specificities.

Based on all the results it is indicative to propose that the retention of the two *bco1* paralogs in Atlantic salmon is an adaptation to increased variability of dietary carotenoids in aquatic environment through the subspecialization and diverged substrate specificities of Bco1 and Bco1l enzymes.

Mammals have β-caroten as a dominant carotenoid in their diet, which is then converted into vitamin A with the activity of BCO1. However, in salmonid diet astaxanthin is the most abundant carotenoid, with β-carotene and other carotenoids present at remarkably lower levels. Thus, the yet unknown metabolic pathway of vitamin A synthesis in Atlantic salmon from astaxanthin could occur by the Bco1 activity, while Bco1l might regulate the cleavage of the other carotenoids.

In summary, we have shown that salmon Bco1l is an active carotenoid oxygenase, with 15,15'-oxygenase activity. The function of Bco1 remains elusive, as it did not show any cleavage activity when tested *in vitro* or in cell based cleavage assays. However, Bco1 was expressed as a cytosolic enzyme in enterocytes, which incites that it is an active CCO enzyme, but in the present study we failed to purify it in its active form. Also, sequence analysis and structure prediction of Bco1 and Bco1l indicated that the both enzymes probably have same cleavage mechanism, but divergent substrate specificities. The obvious next step is therefore to optimize conditions for producing active salmon Bco1 and Bco1l and test their substrate specificities *in vitro*, astaxanthin being the most important one. Tagging proteins at the C-terminus, instead of N-terminus of *bco1*/*bco1l*, and adding divalent iron during protein expression might be useful to fulfil such goals, as it was shown in some earlier studies on human BCO1 [8-10, 13, 58]. Alternatively, refolding of inclusion bodies might result in properly folded and active enzymes.

References

1. Chimsung, N., et al., *Effects of dietary cholesterol on astaxanthin transport in plasma of Atlantic salmon (Salmo salar).* Comp Biochem Physiol B Biochem Mol Biol, 2013. **165**(1): p. 73-81.
2. Odegard, J., et al., *Genomic prediction in an admixed population of Atlantic salmon (Salmo salar).* Front Genet, 2014. **5**: p. 402.
3. Baranski, M., T. Moen, and D.I. Vage, *Mapping of quantitative trait loci for flesh colour and growth traits in Atlantic salmon (Salmo salar).* Genetics Selection Evolution, 2010. **42**.
4. Sodeland M, H.H., Torgersen J, Moen T, Kjøglum, S, Våge DI, Lien S, *Gene and genome duplications allowed for the evolution of the characteristic red color of salmon flesh* 2016.
5. Biesalski, H.K., et al., *Conversion of beta-carotene to retinal pigment.* Vitam Horm, 2007. **75**: p. 117-30.
6. dela Sena, C., et al., *The Human Enzyme That Converts Dietary Provitamin A Carotenoids to Vitamin A Is a Dioxygenase.* Journal of Biological Chemistry, 2014. **289**(19): p. 13661-13666.
7. Hessel, S., et al., *CMO1 deficiency abolishes vitamin A production from beta-carotene and alters lipid metabolism in mice.* Journal of Biological Chemistry, 2007. **282**(46).
8. Lindqvist, A. and S. Andersson, *Biochemical properties of purified recombinant human beta-carotene 15,15'-monooxygenase.* J Biol Chem, 2002. **277**(26): p. 23942-8.
9. Redmond, T.M., et al., *Identification, expression, and substrate specificity of a mammalian beta-carotene 15,15'-dioxygenase.* J Biol Chem, 2001. **276**(9): p. 6560-5.
10. von Lintig, J. and K. Vogt, *Filling the gap in vitamin A research. Molecular identification of an enzyme cleaving beta-carotene to retinal.* J Biol Chem, 2000. **275**(16): p. 11915-20.
11. Wyss, A., et al., *Cloning and expression of beta,beta-carotene 15,15'-dioxygenase.* Biochem Biophys Res Commun, 2000. **271**(2): p. 334-6.
12. Hu, K.Q., et al., *The biochemical characterization of ferret carotene-9 ', 10 '-monooxygenase catalyzing cleavage of carotenoids in vitro and in vivo.* Journal of Biological Chemistry, 2006. **281**(28): p. 19327-19338.
13. Kiefer, C., et al., *Identification and characterization of a mammalian enzyme catalyzing the asymmetric oxidative cleavage of provitamin A.* Journal of Biological Chemistry, 2001. **276**(17): p. 14110-14116.
14. Amengual, J., et al., *A mitochondrial enzyme degrades carotenoids and protects against oxidative stress.* FASEB J, 2011. **25**(3): p. 948-59.
15. Lee, S.A., et al., *Cardiac dysfunction in beta-carotene-15,15 '-dioxygenase-deficient mice is associated with altered retinoid and lipid metabolism.* American Journal of Physiology-Heart and Circulatory Physiology, 2014. **307**(11): p. H1675-H1684.
16. Palczewski, G., et al., *Genetic dissection in a mouse model reveals interactions between carotenoids and lipid metabolism.* Journal of Lipid Research, 2016. **57**(9): p. 1684-1695.
17. Shete, V. and L. Quadro, *Mammalian Metabolism of beta-Carotene: Gaps in Knowledge.* Nutrients, 2013. **5**(12): p. 4849-4868.

18. Borel, P., et al., *Genetic variants in BCMO1 and CD36 are associated with plasma lutein concentrations and macular pigment optical density in humans.* Annals of Medicine, 2011. **43**(1): p. 47-59.
19. Lietz, G., et al., *Single Nucleotide Polymorphisms Upstream from the beta-Carotene 15,15 '-Monoxygenase Gene Influence Provitamin A Conversion Efficiency in Female Volunteers.* Journal of Nutrition, 2012. **142**(1): p. 161s-165s.
20. Le Bihan-Duval, E., et al., *Detection of a Cis [corrected] eQTL controlling BCMO1 gene expression leads to the identification of a QTG for chicken breast meat color.* PLoS One, 2011. **6**(7): p. e14825.
21. Vage, D.I. and I.A. Boman, *A nonsense mutation in the beta-carotene oxygenase 2 (BCO2) gene is tightly associated with accumulation of carotenoids in adipose tissue in sheep (Ovis aries).* Bmc Genetics, 2010. **11**.
22. Helgeland, H., et al., *The evolution and functional divergence of the beta-carotene oxygenase gene family in teleost fish-Exemplified by Atlantic salmon.* Gene, 2014. **543**(2): p. 268-274.
23. Gross, J. and P. Budowski, *Conversion of Carotenoids into Vitamins A1 and A2 in 2 Species of Freshwater Fish.* Biochemical Journal, 1966. **101**(3): p. 747-&.
24. Katsuyama, M. and T. Matsuno, *Carotenoid and Vitamin-a, and Metabolism of Carotenoids, Beta-Carotene, Canthaxanthin, Astaxanthin, Zeaxanthin, Lutein and Tunaxanthin in Tilapia Tilapia-Nilotica.* Comparative Biochemistry and Physiology B-Biochemistry & Molecular Biology, 1988. **90**(1): p. 131-139.
25. Moren, M., T. Naess, and K. Hamre, *Conversion of beta-carotene, canthaxanthin and astaxanthin to vitamin A in Atlantic halibut (Hippoglossus hippoglossus L.) juveniles.* Fish Physiology and Biochemistry, 2002. **27**(1-2): p. 71-80.
26. Schiedt, K., et al., *Absorption, Retention and Metabolic Transformations of Carotenoids in Rainbow-Trout, Salmon and Chicken.* Pure and Applied Chemistry, 1985. **57**(5): p. 685-692.
27. Yamashita, E., S. Arai, and T. Matsuno, *Metabolism of xanthophylls to vitamin A and new apocarotenoids in liver and skin of black bass, Micropterus salmoides.* Comparative Biochemistry and Physiology B-Biochemistry & Molecular Biology, 1996. **113**(3): p. 485-489.
28. Dobin, A., et al., *STAR: ultrafast universal RNA-seq aligner.* Bioinformatics, 2013. **29**(1): p. 15-21.
29. Anders, S., P.T. Pyl, and W. Huber, *HTSeq-a Python framework to work with high-throughput sequencing data.* Bioinformatics, 2015. **31**(2): p. 166-169.
30. Robinson, M.D., D.J. McCarthy, and G.K. Smyth, *edgeR: a Bioconductor package for differential expression analysis of digital gene expression data.* Bioinformatics, 2010. **26**(1): p. 139-140.
31. Anders, S., A. Reyes, and W. Huber, *Detecting differential usage of exons from RNA-seq data.* Genome Res, 2012. **22**(10): p. 2008-17.
32. D'Ambrosio, D.N., R.D. Clugston, and W.S. Blaner, *Vitamin A metabolism: an update.* Nutrients, 2011. **3**(1): p. 63-103.
33. Maeda, T., et al., *Dietary 9-cis-beta,beta-carotene fails to rescue vision in mouse models of leber congenital amaurosis.* Mol Pharmacol, 2011. **80**(5): p. 943-52.
34. Oberhauser, V., et al., *NinaB combines carotenoid oxygenase and retinoid isomerase activity in a single polypeptide.* Proc Natl Acad Sci U S A, 2008. **105**(48): p. 19000-5.

35. dela Sena, C., et al., *Substrate Specificity of Purified Recombinant Chicken -Carotene 9,10-Oxygenase (BCO2).* Journal of Biological Chemistry, 2016. **291**(28): p. 14609-14619.
36. Nagao, A., et al., *Stoichiometric conversion of all trans-beta-carotene to retinal by pig intestinal extract.* Archives of Biochemistry and Biophysics, 1996. **328**(1): p. 57-63.
37. Kiser, P.D. and K. Palczewski, *Membrane-binding and enzymatic properties of RPE65.* Progress in Retinal and Eye Research, 2010. **29**(5): p. 428-442.
38. Sui, X.W., et al., *Analysis of Carotenoid Isomerase Activity in a Prototypical Carotenoid Cleavage Enzyme, Apocarotenoid Oxygenase (ACO).* Journal of Biological Chemistry, 2014. **289**(18): p. 12286-12299.
39. Garcia-Limones, C., et al., *Functional characterization of FaCCD1: A carotenoid cleavage dioxygenase from strawberry involved in lutein degradation during fruit ripening.* Journal of Agricultural and Food Chemistry, 2008. **56**(19): p. 9277-9285.
40. Schwartz, S.H., X.Q. Qin, and M.C. Loewen, *The biochemical characterization of two carotenoid cleavage enzymes from Arabidopsis indicates that a carotenoid-derived compound inhibits lateral branching.* Journal of Biological Chemistry, 2004. **279**(45): p. 46940-46945.
41. Schwartz, S.H., X.Q. Qin, and J.A.D. Zeevaart, *Characterization of a novel carotenoid cleavage dioxygenase from plants.* Journal of Biological Chemistry, 2001. **276**(27): p. 25208-25211.
42. Sun, Z., et al., *Cloning and characterisation of a maize carotenoid cleavage dioxygenase (ZmCCD1) and its involvement in the biosynthesis of apocarotenoids with various roles in mutualistic and parasitic interactions.* Planta, 2008. **228**(5): p. 789-801.
43. Kim, Y.S., C.S. Park, and D.K. Oh, *Hydrophobicity of residue 108 specifically affects the affinity of human beta-carotene 15,15'-monooxygenase for substrates with two ionone rings.* Biotechnology Letters, 2010. **32**(6): p. 847-853.
44. Kiser, P.D., et al., *Crystal structure of native RPE65, the retinoid isomerase of the visual cycle.* Proc Natl Acad Sci U S A, 2009. **106**(41): p. 17325-30.
45. Jlali, M., et al., *Nutrigenetics of carotenoid metabolism in the chicken: a polymorphism at the beta,beta-carotene 15,15'-mono-oxygenase 1 (BCMO1) locus affects the response to dietary beta-carotene.* British Journal of Nutrition, 2014. **111**(12): p. 2079-2088.
46. Berry, S.D., et al., *Mutation in bovine beta-carotene oxygenase 2 affects milk color.* Genetics, 2009. **182**(3): p. 923-6.
47. Lindqvist, A. and S. Andersson, *Cell type-specific expression of beta-carotene 15,15 '-mono-oxygenase in human tissues.* Journal of Histochemistry & Cytochemistry, 2004. **52**(4): p. 491-499.
48. Raghuvanshi, S., et al., *Cellular localization of beta-carotene 15,15' oxygenase-1 (BCO1) and beta-carotene 9',10' oxygenase-2 (BCO2) in rat liver and intestine.* Arch Biochem Biophys, 2015. **572**: p. 19-27.
49. Kim, Y.K., et al., *beta-Carotene and its cleavage enzyme beta-carotene-15,15'-oxygenase (CMOI) affect retinoid metabolism in developing tissues.* FASEB J, 2011. **25**(5): p. 1641-52.
50. Paik, J., et al., *Expression and characterization of a murine enzyme able to cleave beta-carotene. The formation of retinoids.* J Biol Chem, 2001. **276**(34): p. 32160-8.
51. von Lintig, J., et al., *Towards a better understanding of carotenoid metabolism in animals.* Biochim Biophys Acta, 2005. **1740**(2): p. 122-31.

52. Wang, Z., et al., *beta-Carotene-vitamin A equivalence in Chinese adults assessed by an isotope dilution technique.* Br J Nutr, 2004. **91**(1): p. 121-31.
53. Van der Veen, I.T., *Costly carotenoids: a trade-off between predation and infection risk?* Journal of Evolutionary Biology, 2005. **18**(4): p. 992-999.
54. Snoeijs, P. and N. Haubner, *Astaxanthin dynamics in Baltic Sea mesozooplankton communities.* Journal of Sea Research, 2014. **85**: p. 131-143.
55. Sommer, F., et al., *Astaxanthin in the calanoid copepod Calanus helgolandicus: dynamics of esterification and vertical distribution in the German Bight, North Sea.* Marine Ecology Progress Series, 2006. **319**: p. 167-173.
56. McNulty, H.P., et al., *Differential effects of carotenoids on lipid peroxidation due to membrane interactions: X-ray diffraction analysis.* Biochimica Et Biophysica Acta-Biomembranes, 2007. **1768**(1): p. 167-174.
57. Lien, S., et al., *The Atlantic salmon genome provides insights into rediploidization.* Nature, 2016. **533**(7602): p. 200-+.
58. Schwartz, S.H., et al., *Specific oxidative cleavage of carotenoids by VP14 of maize*. Science, 1997. **276**(5320): p. 1872-1874.

Paper III

Online image, retrieved June 2017, from http://www.fisheries.noaa.gov

A missense mutation in the *abcg2-1a* gene (ATP-binding cassette sub-family G member 2) is strongly associated with muscle color in Atlantic salmon (*Salmo salar*)

Nina Zoric[1], Thomas Moen[2], Sven Arild Korsvoll[2], Sissel Kjøglum[2], Nina Santi[2], Sigbjørn Lien[1], Dag Inge Våge[1] and Jacob Torgersen[2*]

[1]Centre for Integrative Genetics (CIGENE), Department of Animal and Aquacultural Sciences (IHA), Faculty of Biosciences (BIOVIT), Norwegian University of Life Sciences (NMBU), P.O. Box 5003, N-1432 Ås, Norway.

[2]AquaGen, Postboks 1240, 7462 Trondheim, Norway.

[*]Corresponding author

Abstract

Both diet and genetics affect the red muscle color of Atlantic salmon. Improving the knowledge about genetic variations underlying this trait would allow for more precise selection and improved quality of farmed Atlantic salmon. In this study we identified a region on ssa02 (chromosome 2) containing SNPs strongly associated with salmon flesh coloration. Fine mapping of this region identified a missense mutation (rs863939997) in an ATP binding cassette subfamily G member 2 (*abcg2-1a*). This SNP causes an amino acid substitution in amino acid position 230 (Asn230Ser), and is located in the proximity of an ATP binding site in the D-loop which is involved in protein activation. Abcg2 is a known exporter of lipophilic molecules, and we suggest that Abcg2-1a is involved in salmon flesh coloration by translocating astaxanthin from enterocytes to the intestinal lumen, thus limiting the astaxanthin availability for muscle deposition. The Abcg2-1a protein was 2.5 folds more abundant in the pale-fleshed fish than in red-fleshed fish, supporting that Abcg2-1a plays a role in intestinal astaxanthin uptake.

Introduction

Astaxanthin deposition in the muscle of most salmonids, including Atlantic salmon (*Salmo salar*), leads to the characteristic red muscle color. The pigment originates from crustacean-rich diets in the wild, whereas astaxanthin is supplemented through a formulated diet in salmon farming. Pigment content in muscle depends upon uptake and metabolism in the gastrointestinal tract and liver, as well as uptake and deposition in muscle cells. The final muscle deposition varies between the salmonid species, with sockeye salmon (*Oncorhynchus nerka*) and Atlantic salmon reaching high and relatively low concentrations, respectively [1]. Increasing dietary astaxanthin above 70 mg/kg diet does not improve retention in Atlantic salmon [2-4]. However, in experiments where astaxanthin has been injected intraperitoneally to avoid the intestinal barrier, Atlantic salmon has achieved muscle redness similar to sockeye salmon [5, 6]. http://onlinelibrary.wiley.com/doi/10.1111/j.1365-2095.1995.tb00022.x/fullThese observations suggest that the intestinal absorptive processes may limit the muscle retention of dietary astaxanthin.

Substantial genetic variation associated with flesh color has been reported in Atlantic salmon, with heritability estimates ranging between 0.1-0.6 (reviewed in [7]). Previous genome-wide association studies (GWAS) have identified a region on ssa26 strongly associated with salmon flesh color [8, 9]. Fine mapping of the genomic region tied this QTL to a region containing two beta-carotene oxygenase genes, *bco1* and *bco1l*. The encoded enzyme regulates carotenoid metabolism via symmetrically cleaving provitamin-A carotenoids into two vitamin A molecules [10].

The intestinal uptake and transport of carotenoids and fatty acids in the blood serum are closely linked, and seem to be similar for all vertebrates [11-13]. Upon feeding, carotenoids are

dissolved in the dietary lipids and solubilized within mixed micelles, in which they form esters. The mixed micelles are subsequently taken up by enterocytes in the intestinal lining. In the enterocytes, provitamin- A carotenoids can be enzymatically cleaved into vitamin A, while intact carotenoids are reassembled with fatty acids into chylomicrons. The chylomicrons are released into the blood circulation and transported to various tissues, including muscle. Carotenoids that hydrolyze from the chylomicrons, and bind to the actomyosin complex of the muscle fibers, cause the red flesh coloration [11, 14]. Thus, critical processes defining Atlantic salmon flesh coloration are intestinal absorption, enzymatic cleavage in intestine or liver, muscle deposition, and excretion. Among these, the uptake mechanisms in intestinal and muscle cells have been predicted to be particularly important by mathematical modelling of the carotenoid metabolism [15].

In this study we identified a region on ssa02 with SNPs significantly associated with flesh color by a genome wide association study (GWAS). Identification of additional polymorphisms in this region, identified by Illumina sequencing, revealed a missense mutation in an ATP binding cassette subfamily G member 2 (*abcg2*), possibly the causative polymorphism. Different Abcg2 protein expression between red and pale salmon supported the hypothesis that this gene contributes to the unique red flesh color of Atlantic salmon.

Materials and methods

Phenotyping and genotyping

Altogether 8180 individuals from the four year-classes (2005, 2008, 2011, and 2012) of the AquaGen breeding population was included in the genome wide association studies (GWAS)

(2891, 1847, 1963, and 1479 animals, respectively). Fillet color was analyzed in four independent test rounds two years after hatching (Table 1).

Table 1. Sample/data sets

Year class = year of hatching for the samples in question; Genotyping technol. = technology (and marker density) used for genotyping the data set; No. animals = number of animals having been genotyped and phenotyped ('offspring'); No. FS groups = number of full-sibling groups represented by genotyped and phenotyped animals; No. fathers and No. mothers = number of fathers and mothers of the phenotyped and genotyped animals; No. markers = number of DNA polymorphisms genotyped.

Data set	Year class	Genotyping technol.	No. animals	No. FS groups	No. fathers	No. mothers	No. markers	Mean weight (g)
1	2005	Illumina 6k	2891	265	177	141	5650	2845
2	2008	Illumina 6k	1847	308	241	242	4423	3024
3	2010	Affymetrix 220k	1963	99	68	69	219,998	3853
4	2012	Affymetrix 56k	1479	567	118	111	55,567	2636

In all four test iterations, fillet color was measured on the Norwegian Quality Cut (NQC) part of the fillet. In 2007 and in 2013, fillet color was measured using a QVision Analyser from TOMRA Solution (Asker, Norway), a spectrophotometer which measures absorption/reflection at 400-1200 nm wavelengths (visible and near-infrared part of spectrum). In 2010, fillet color was measured using Photofish technology (currently owned by AKVA Group; Bryne, Norway), which is based on image analysis of photographs taken under standardized conditions (i.e. inside a closed box with constant light). In 2014, fillet color was measured using a Foss XDS Near-Infrared Spectrophotometer (Foss, Denmark). Irrespective of the method, the fillet color measurements were converted to units of mg astaxhantin per kg of fillet, based on previous correlations between HPLC and spectrophotometric/Photofish measurements. Within each of the four test rounds, all fillet color measurements were done under similar conditions. Tissue samples for genotyping (from skeletal muscle, liver, or heart) were taken from a random subset of phenotyped animals (a random subset with regard to fillet colour). DNA was extracted from these tissues using a standard method (using the DNAeasy 96 kit from QIAGEN, following the protocol supplied by QIAGEN).

Individuals from year class (yc) 2005 and 2008 were genotyped using a 6K custom design iSelect SNP-array from Illumina (San Diego, CA, USA) developed in-house at CIGENE [16]. The samples were genotyped following standard protocols for iSelect SNP-arrays, provided by Illumina.

Year class 2011 was genotyped using a custom Axiom array from Affymetrix (San Diego, CA, USA). The SNPs on this array were identified through whole genome sequencing of 29 Atlantic salmon from the AquaGen breeding nucleus in addition to three double haploid

(androgenetically derived) Atlantic salmon. The SNP array contained 198,998 SNPs that were polymorphic in yc 2011. Genotyping was done according to the Axiom 2.0 Assay Manual Workflow User Guide (http://media.affymetrix.com/support/downloads/manuals/axiom_2_assay_manual_workflow_prepguide.pdf). Genotype calling was done using the Affymetrix Power Tools programs (http://www.affymetrix.com/estore/partners_programs/programs/developer/tools/powertools.affx), according to "best practices" recommendations from Affymetrix (http://media.affymetrix.com/support/downloads/manuals/axiom_best_practice_supplement_user_guide.pdf). Year class 2012 was genotyped using a custom Axiom array from Affymetrix, containing 55,567 SNPs polymorphic in yc 2012. The bulk of DNA polymorphisms on this array constituted a subset of the SNPs genotyped on yc 2011, but 3,719 were novel, i.e. not on the SNP chip used for genotyping yc 2011.

Genome-wide association study

In order to identify QTLs for fillet color, the data set corresponding to individual year classes were analyzed using a linear mixed model in the DMU software [17]. Each SNP was analyzed individually. The dependent variable was mg astaxanthin in muscle, derived as described above. The linear mixed model was an animal model containing the fixed effect of the animal's sex, the fixed regression on the animal's round weight (weight before slaughter), and the random regression on the number of copies of allele A carried by the animal (allele A being one of the two alleles present at the SNP).

LD analysis

We used the following procedure in order to identify additional DNA polymorphisms in linkage disequilibrium (LD) with the best tag-SNP for a particular QTL (here, 'in LD with' means that alleles at the DNA polymorphism in question had a squared correlation coefficient (r2) to alleles at the tag-SNP equal to 0.3 or more). DNA polymorphisms in LD with the tag-SNP were identified as follows: 54 Atlantic salmon originating from AquaGen year classes 1998, 1999, 2000, 2001, and 2005, were whole-genome sequenced on Illumina HighSeq 2000, producing paired-end reads (2x100 bp) to an average genome coverage of 18x (range 8x to 32x, assuming a genome size of 3.0 billion base pairs). The reads were aligned to the reference sequence of ssa02 (GenBank identifier = NC_027301.1) using BWA mem version 0.7.10-r789 [18]. SNPs and short indels were identified using Freebayes version 0.9.'i15-1 [19] to filter away low-quality variants, using run-time parameters –use-mapping-quality and –min-mapping-quality 1, in addition to 'vcffilter -f "QUAL > 20"'. The SNP-detection pipeline also returned genotypes on the 54 animals, for all identified DNA polymorphisms. SNPs and short indels were annotated using SnpEff version 4.0e [20]. The SnpEff annotation database was based on the CIGENE annotation version 2.0 [16]. DNA polymorphisms in sufficiently strong LD with the tag SNP were identified by PLINK v1.9 (https://gigascience.biomedcentral.com/articles/10.1186/s13742-015-0047-8) (options --r2 -ld-snp <tag-SNP-name> --chr-set 29 --no-xy --ld-window 999999999 --ld-window-kb 500).

Identification of putative causal polymorphism

Output from the LD analysis was manually investigated for candidate genes involved in astaxanthin metabolism and for potential underlying causal polymorphisms, using the

annotation described above. One megabase on each side of the best tag-SNP (rs159406379) for the fillet colour QTL on ssa02, was searched for DNA polymorphisms that fulfilled the following criteria: 1) a moderate to high (equal to or above 0.3) squared correlation coefficient to the tag SNP, 2) variant impact value HIGH, MODERATE or MODIFIER according to SnpEff [20], 3) a location within a gene subjectively assessed to be a plausible candidate gene for fillet color. The 29 most promising DNA polymorphisms were genotyped on the iPlex genotyping system from Agena Bioscience (San Diego, USA). Primers for genotyping were constructed using Agena's Assay Design Suite v2.0 (https://www.agenacx.com/Tools). The SNPs were genotyped in the material from yc 2005, and each SNP was tested individually for association to fillet color, using DMU as described above.

Western blotting

Quantification of Abcg2 was carried out to assess differences between specimens homozygous at a putative functional polymorphism (rs863939997) on ssa02 (n=7 individuals with red T allele and n=12 individuals with pale C allele). Of the selected fish, other QTLs affecting astaxanthin metabolism were accounted for by keeping those genotypes at those QTL identical. Approximately 30 mg of mid-intestine, just after the pyloric caeca, was lysed in 100 µl of RIPA buffer (150 mM NaCl, 50 mM Tris-HCl (pH 7.4), 1.0% Triton, 1% sodium deoxycholate, 0.1% SDS, 10 mM EDTA and protease inhibitor Complete Ultra Tablets (Roche, Switzerland). A 4-15% SDS PAGE gel (Mini Protean TGX, Biorad, CA USA) was loaded with 20 µg of proteins before separation and blotting onto PVDF membranes (Biorad). Quantification of total protein transferred to the PVDF membrane was achieved by ponceau red staining [21]. After imaging, the membranes were destained (0.1% NaOH) and blocked in 1 x TBST (Tris buffered saline with 0.05% Tween-20) with 2% dry milk. A primary Abcg2 antibody (Cell signaling #4477)

was applied to the membrane (2000x dilution in 1 x TBST with 1% dry milk) and subjected to cold microwave incubation for 10 min [22]. After extensive washing in 1 x TBST, a 10 min cold microwave incubation with an AP-conjugated secondary antibody (Sigma) in 1 x TBST washing and development with NBT/BCIP solution (Thermo Fisher), the membrane was dried and imaged. The amount of intestinal Abcg2 was assessed by measuring band intensities using ImageJ (https://imagej.nih.gov/ij/), after which the values were normalized against total protein (Ponceau red).

Xenobiotics analysis

Members of the Abc transporter family are important eliminators of harmful substances from the intestine and other tissues [23]. As the QTL reported here potentially restrain enterocyte export of dietary xenobiotics, muscle samples were tested for contaminant content. Briefly, NQC (Norwegian quality cut) homogenates were prepared from 20 homozygous fish of each genotype. Two pools of each genotype consisting of muscle tissue from 10 specimens were then thoroughly mixed and prepared for analysis. The four samples were frozen at -80^{o}C and shipped on dry ice to NIFES in Norway for contaminant analysis (https://www.nifes.no/).

Atlantic salmon *abcg2* genes

The Atlantic salmon genome was explored for *abcg2* paralogues using text mining of the NCBI database, as well as Blast analysis with NM_001173655.1 as a query. Combined, the searches identified nine different *abcg2* genes (Table 2). Corresponding transcripts and protein

sequences were aligned using Unipro UGENE (http://ugene.unipro.ru/download.html), to assess variations among the transcripts and investigate functional domains, respectively. For the latter, human ABCG2 annotation was used as a consensus sequence (Protein identifier).

Table 2. Overview of *abcg2* genes in the Atlantic salmon genome.

* Denotes *abcg2* variant with the missense mutation. FPKM values are from salmobase.org. #Abcg2 proteins containing all functional domains. @ http://web.expasy.org/cgi-bin/compute_pi/pi_tool

Gene	Chr.	Location	GB. acc.	Transcript	FPKM	Protein	Length [aa]	Tissue
*abcg2-1a**	2	71393258..71417739	LOC106595425	-	35	-	633# 70Kda@	Gut
abcg2-1b	2	71393258..71417739	LOC106595425	-	6	-	167	Gut
abcg2-2a	4	5513017..5520053	LOC106602262	XM_014194785.1	<1	XP_014050260.1	282	Skin
abcg2-2b	4	8204041..8213367	LOC106602338	XM_014194916.1	<1	XP_014050391.1	406	Skin, spleen
abcg2-3a	8	16987237..17004315	100380370	NM_001173655.1	4	NP_001167126.1	677#	Gill, heart, spleen
abcg2-4a	18	69164289..69166980	LOC106578184	XM_014156818.1	10	XP_014012293.1	125	Gut
abcg2-4b	18	69238986..69241362	LOC106578186	XM_014156819.1	20	XP_014012294.1	163	Gut
abcg2-4c	18	68703354..68733988	LOC106578162	XM_014156791.1	18	XP_014012266.1	594# 66Kda@	Gut
abcg2-5a	-	Unplaced Scaffold	LOC106591134	XM_014182323.1	-	XP_014037798.1	225	-

Results

GWAS

The GWAS for fillet color in Atlantic salmon revealed three major quantitative trait loci (QTL), one previously described on chromosome 26 [8, 9], one on chromosome 14 and one on ssa02. The QTL was located on ssa02 at about 71 Mbp and was significant or close to significant (Bonferroni corrected for multiple testing) in all 4 year classes (Fig. 1). Therefore, we decided to follow up by fine mapping of the ssa02 QTL in the current paper. Among the SNPs tagging the QTL on ssa02, rs159406379 came out as particularly significant in year classes 2005 and 2008. Unfortunately the Affymetrix assay for rs159406379 did not work out, leaving us with no genotypes on the SNP for year classes 2011 and 2012. Still, the striking significance levels of rs159406379 in yc 2005 and 2008 (Fig. 1) led us to consider rs159406379 as the best tag SNPs for the QTL on ssa02.

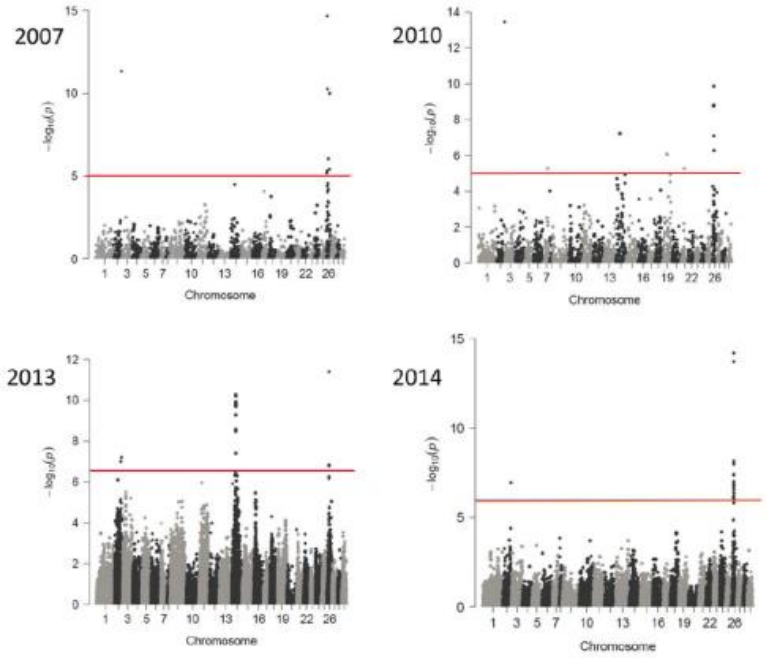

Figure 1. Manhattan plots from GWAS experiments performed on four different year classes. The red horizontal lines correspond to significance threshold when multiple testing is taken into account (Bonferroni correction).

Linkage disequilibrium (LD) analyses - identification of putative causal variants

Illumina-sequencing of 29 individual AquaGen animals revealed 828,122 putative polymorphisms on ssa02. These SNPs were screened for LD with the best tag SNP for the QTL on ssa02 (rs159406379), and a number of high-LD SNPs were identified in an *abcg2* gene located ~30 kb upstream of the SNP (Fig. 2).

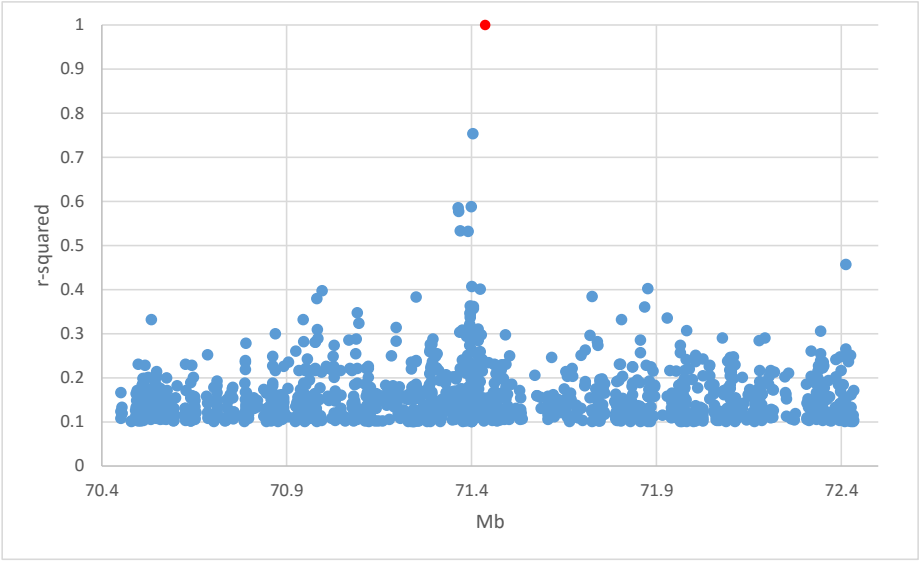

Figure 2. Pair-wise linkage disequilibrium (r2) between best original tag-SNP for the fillet color QTL on chromosome 2 (ESTNV_25199_261, dbSNP ID rs159406379, red dot) and other SNP located ± 1Mb from the best tag-SNP. Positions are relative to the sequence of Atlantic salmon chromosome 2 (GenBank ID NC_027301.1).

The most apparent hit was a high-scoring missense mutation (rs863939997, $r^2 = 0.75$) in LOC106595425, hereafter called *abcg2-1a*. A paralogue of *abcg2-1a*, *abcg2-1b*, locates just upstream of *abcg2-1a*. In the NCBI salmon genome assembly, both paralogues are annotated as a single pseudogene (GCA_000233375.4). In this assembly, *abcg2-1a* appears to lack the most 5' exons. RNAseq data was used to identify the missing exons of *abcg2-1a* by manual curation and the analysis confirmed that *abcg2-1a* and *abcg2-1b* are unique neighboring genes. *Abcg2-1b* is a truncated paralogue, lacking several exons encoding the functional domains in the middle region and encoding a 167 aa long protein.

Sequenom MassArray iPlex analysis

The rs863939997 (NC_027301.1_71404326) missense mutation was genotyped on the GWAS material from yc 2005, resulting in a regression p-value of 5.33×10^{-14}. The mean fillet color levels (mg astaxhantin/kg muscle, ± standard error) of individuals that were homozygous for the red allele, heterozygous, and homozygous for the pale allele were 7.09 ± 0.04, 6.88 ± 0.04 and 6.66 ± 0.08, respectively. The identified missense mutation was more strongly associated to fillet color than any other DNA polymorphism located on ssa02, including the originally best tag-SNP (rs159406379).

Abcg2-1a activity in QTL salmon

To evaluate a possible connection between the Abcg2-1a and salmon flesh coloration and address the effect of the missense mutation (Ser230 in pale salmon and Asn230 in red salmon), we examined intestinal protein abundance in homozygous specimens. The normalized western blots showed that the intestine of pale salmon described 2.5 fold higher Abcg2-1a abundance compared to the red phenotype (Fig. 3).

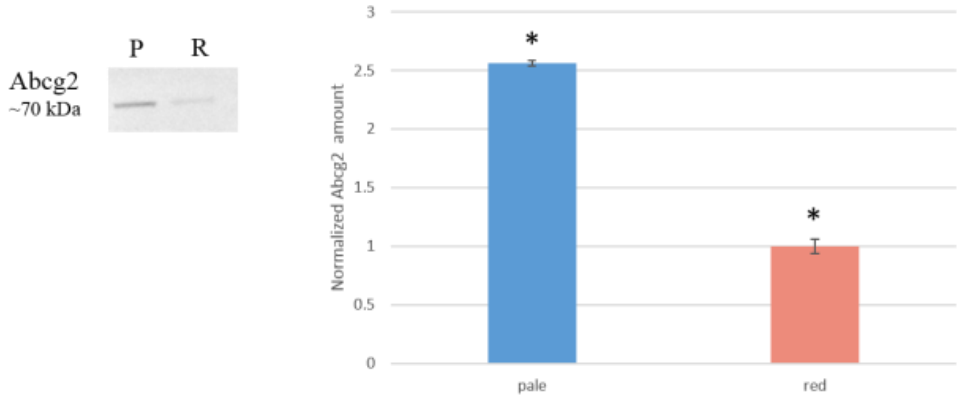

Figure 3. Western blot quantification of Abcg2-1a in intestine of pale-fleshed (P) and red-fleshed (R) salmon. Values are mean±SEM. Data are presented as a ratio of Abcg2-1a to total protein load measured by ponceau. Values are means ± standard error mean. * significant difference at $P < 0.05$. Images shown for one pale-fleshed and one red-fleshed fish sample.

Atlantic salmon *abcg2* genes

We investigated the *abcg2* gene family in the Atlantic salmon genome using publicly available genomic sequences (salmobase.org and NCBI). Our text mining and BLAST analyses revealed that the salmon genome most likely harbors 9 *abcg2* genes (Fig. 3). The missense mutation highly associated with flesh coloration is located within *abcg2-1a* at ~71 MB, a region which also contains the *abcg2-1b* gene. Although no high-resolution structural data are available for ABCG2, homology models have been built [35, 37], proposing that ABCG2 consists of one nucleotide binding domain (NBD): Walker A/P loop, Q-Loop, ABC signature motif, Walker B, D-Loop, H-Loop/switch region, ATP binding sites, and a transmembrane domain (TMD) comprising of six transmembrane regions. Based on this, we found that salmon *abcg2-1a* encodes a full-length Abcg2 protein with all functional domains, while *abcg2-1b* encodes only

the exon for Q-loop in NBD and the very last transmembrane domain in TMD. In addition to *abcg2-1a*, *abcg2-3a* at ssa08 and *abcg2-4c* at ssa18 also encode full-length proteins, whereas the other six paralogues encode truncated proteins. Of all *abcg2* genes, *abcg2-1a* is most abundantly expressed (35 FPKM), in intestine.

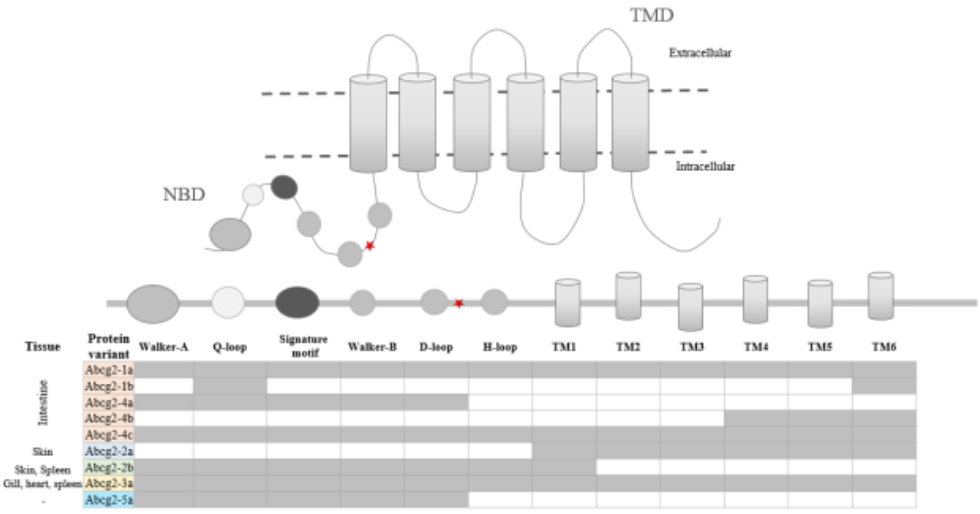

Figure 3. Illustration of the proposed ABCG2 structure with the subdomains specified in the top figure. The bottom table shows subdomain organization of nine Abcg2 salmon variants. Grey and white boxes corresponds to presence and absence of the subdomains, respectively. Red star denotes hypothetical location of residue S230N in Abcg2-1a. NBD: Nucleotide binding domain; TMD: Transmembrane domain.

Discussion

The intense red color of salmon filet is a desired attribute among consumers, and improving muscle redness while minimizing variation is a goal for the salmon industry. Muscle retention of

astaxanthin is low and considerable individual variation in flesh coloration exists [11], so there is large potential for genetic improvement of muscle pigmentation. Previous GWAS studies on Atlantic salmon have identified a QTL for fillet color on ssa26 [11,[9]], and in the current study we identified two additional QTLs, one on ssa02 and one on ssa14. Here we followed up the QTL on ssa02 by fine mapping.

The rs159406379 on ssa02 came out as highly significant in our study. The LD analysis using this SNP as a tag, and subsequent verification by genotyping, revealed that this polymorphism is unique, being the only SNP with a high linkage disequilibrium to the *abcg2-1a* missense mutation (rs863939997). Therefore, the two above-mentioned SNPs are the only SNPs associated with muscle redness on ssa02, which may explain why the ssa02 QTL has not been identified in earlier studies.

An apparent question is how rs863939997 located in *abcg2-1a* affects astaxanthin content in muscle. The encoded protein belongs to the ABC transporters, a family of proteins known to facilitate export of a wide range of molecules across the cell membrane. Abcg2 is best known for its role in protection against xenobiotic molecules, including chemotherapeutic drugs (reviewed in [24]). Extensive studies have shown that mammalian ABCG2 is abundantly expressed in the intestine, where it is an important transporter that limits the absorption of a broad range of ingested compounds [25]. In Atlantic salmon, *abcg2-1a* is highly expressed in the intestine and it is possible that uptake of lipophilic molecules such as astaxanthin is controlled by Abcg2-1a. Although we show genetic association between ABC subfamily genes and carotenoid metabolism, it remains unclear how the *Abcg2* polymorphism affect carotenoid status.

In humans, β-carotene and lutein availability were associated with polymorphisms in ABCA1 and ABCG5 [26, 27]. Also, astaxanthin enhanced ABCA1 and ABCG1 expression in

macrophages [28] and β-carotene exerted a partially inhibitory effect on ABCG2 efflux function [29]. A possible mechanism of how the missense mutation in the Abcg2-1a influence flesh color in Atlantic salmon is therefore through transporter efficiency. In order to elucidate this, a western blot was carried out on intestinal tissue from salmon with different QTL genotypes. The results indeed showed a difference between genotypes, where the pale genotype showed a 2.5 fold increased in Abcg2-1a protein over the salmon with the red genotype.

One could then speculate if the mutation in Abcg2-1a affects export efficiency, and to compensate for lower activity of the Asn230 variant, the protein is produced in larger amounts. Abcg2 orthologue alignment (Ensembl.org) show that among 18 mammalian and teleost species, the position corresponding to Atlantic salmon Asn230Ser, the asparagine residue is highly conserved. The Asn230Ser mutation in salmon locates within the NBD, in the proximity of D-loop, which is involved in Mg·ATP binding and transporter activation [30-32] and thus possibly also affecting transporter activity. Asn230 and Ser230 Abcg2-1a protein variants might have different efficiency to transport hydrophobic substrates, such as astaxanthin, which may explain the functional effect of the missense mutation on the flesh coloration.

A protective role of ABC transporters in fish has already been known as they were found to eliminate various endogenous and exogenous toxic molecules from the cells, such as cadmium and certain types of insecticides, rhodamine, heavy metals and BaP [33-40]. Increased astaxanthin levels could come at the cost of increased xenobiotics content. In order to answer this we conducted a contaminant analysis of muscle tissue from fish with or without rs863939997. No significant differences in contaminant content between the genotypes were detected. However, the levels of contaminants were very low for both genotypes, which could possibly mask a genotype effect.

We describe a QTL on ssa02 for muscle redness in Atlantic salmon. By fine mapping we identified a missense mutation in the *abcg2-1a* gene which causes an Asn230Ser polymorphism in the gene product. Abcg2-1a protein was 2.5-fold more abundant in the intestine of pale compared to red-fleshed fish, supporting that Abcg2-1a has a role in carotenoid metabolism, most likely by translocating astaxanthin from enterocytes to the intestinal lumen.

References

1. Rajasingh, H., et al., *Why are salmonids pink?* Canadian Journal of Fisheries and Aquatic Sciences, 2007. **64**(11): p. 1614-1627.
2. Forsberg, O.I. and A.G. Guttormsen, *A pigmentation model for fanned Atlantic salmon: Nonlinear regression analysis of published experimental data.* Aquaculture, 2006. **253**(1-4): p. 415-420.
3. Torrissen, O.J., et al., *Astaxanthin deposition in the flesh of Atlantic Salmon, Salmo salar L., in relation to dietary astaxanthin concentration and feeding period.* Aquaculture Nutrition, 1995. **1**(2): p. 77-84.
4. Torrissen, O.J., *Pigmentation of Salmonids - Factors Affecting Carotenoid Deposition in Rainbow-Trout (Salmo-Gairdneri).* Aquaculture, 1985. **46**(2): p. 133-142.
5. Ytrestoyl, T. and B. Bjerkeng, *Intraperitoneal and dietary administration of astaxanthin in rainbow trout (Oncorhynchus mykiss) - Plasma uptake and tissue distribution of geometrical E/Z isomers.* Comparative Biochemistry and Physiology B-Biochemistry & Molecular Biology, 2007. **147**(2): p. 250-259.
6. Ytrestoyl, T. and B. Bjerkeng, *Dose response in uptake and deposition of intraperitoneally administered astaxanthin in Atlantic salmon (Salmo salar L.) and Atlantic cod (Gadus morhua L.).* Aquaculture, 2007. **263**(1-4): p. 179-191.
7. Garcia de Leaniz, C., et al., *A critical review of adaptive genetic variation in Atlantic salmon: implications for conservation.* Biol Rev Camb Philos Soc, 2007. **82**(2): p. 173-211.
8. Baranski, M., T. Moen, and D.I. Vage, *Mapping of quantitative trait loci for flesh colour and growth traits in Atlantic salmon (Salmo salar).* Genet Sel Evol, 2010. **42**: p. 17.
9. Sodeland M, H.H., Torgersen J, Moen T, Kjøglum, S, Våge DI, Lien S, *Gene and genome duplications allowed for the evolution of the characteristic red color of salmon flesh* 2016.
10. Shete, V. and L. Quadro, *Mammalian metabolism of beta-carotene: gaps in knowledge.* Nutrients, 2013. **5**(12): p. 4849-68.
11. Aas, G.H., et al., *Blood appearance, metabolic transformation and plasma transport proteins of (14)C-astaxanthin in Atlantic salmon (Salmo salar L.).* Fish Physiology and Biochemistry, 1999. **21**(4): p. 325-334.
12. Clevidence, B.A. and J.G. Bieri, *Association of Carotenoids with Human Plasma-Lipoproteins.* Methods in Enzymology, 1993. **214**: p. 33-46.
13. Parker, R.S., *Carotenoids .4. Absorption, metabolism, and transport of carotenoids.* Faseb Journal, 1996. **10**(5): p. 542-551.
14. Saha, M.R., et al., *Development of a method to assess binding of astaxanthin to Atlantic salmon Salmo salar L. muscle proteins.* Aquaculture Research, 2005. **36**(4): p. 336-343.
15. Rajasingh, H., et al., *Carotenoid dynamics in Atlantic salmon.* BMC Biol, 2006. **4**: p. 10.
16. Lien, S., et al., *The Atlantic salmon genome provides insights into rediploidization.* Nature, 2016. **533**(7602): p. 200-+.
17. Madsen P, S.P., Su G, Damgaard LH, Thomsen H, Labouriau R *DMU-a package for analyzing multivariate mixed models.*, in *In Proceedings of the 8th World Congress on Genetics Applied to Livestock Production:* . 2006: Belo Horizonte.

18. Li, H. and R. Durbin, *Fast and accurate short read alignment with Burrows-Wheeler transform.* Bioinformatics, 2009. **25**(14): p. 1754-60.
19. G, G.E.a.M., *Haplotype-based variant detection from short-read sequencing.* . arXiv: 1207.3907v2 [q-bio.GN], 2012.
20. Cingolani, P., et al., *A program for annotating and predicting the effects of single nucleotide polymorphisms, SnpEff: SNPs in the genome of Drosophila melanogaster strain w1118; iso-2; iso-3.* Fly (Austin), 2012. **6**(2): p. 80-92.
21. Thacker, J.S., et al., *Total protein or high-abundance protein: Which offers the best loading control for Western blotting?* Analytical Biochemistry, 2016. **496**: p. 76-78.
22. Grutzner, N., et al., *Cold Microwave-Enabled Protein Detection and Quantification.* Methods Mol Biol, 2015. **1314**: p. 207-17.
23. Arana, M.R., et al., *Physiological and pathophysiological factors affecting the expression and activity of the drug transporter MRP2 in intestine. Impact on its function as membrane barrier.* Pharmacological Research, 2016. **109**: p. 32-44.
24. Horsey, A.J., et al., *The multidrug transporter ABCG2: still more questions than answers.* Biochemical Society Transactions, 2016. **44**: p. 824-830.
25. Gutmann, H., et al., *Distribution of breast cancer resistance protein (BCRP/ABCG2) mRNA expression along the human GI tract.* Biochem Pharmacol, 2005. **70**(5): p. 695-9.
26. Borel, P., et al., *A Combination of Single-Nucleotide Polymorphisms Is Associated with Interindividual Variability in Dietary beta-Carotene Bioavailability in Healthy Men.* Journal of Nutrition, 2015. **145**(8): p. 1740-1747.
27. Herron, K.L., et al., *The ABCG5 polymorphism contributes to individual responses to dietary cholesterol and carotenoids in eggs.* J Nutr, 2006. **136**(5): p. 1161-5.
28. Iizuka, M., et al., *Astaxanthin enhances ATP-binding cassette transporter A1/G1 expressions and cholesterol efflux from macrophages.* J Nutr Sci Vitaminol (Tokyo), 2012. **58**(2): p. 96-104.
29. Teng, Y.N., et al., *beta-carotene reverses multidrug resistant cancer cells by selectively modulating human P-glycoprotein function.* Phytomedicine, 2016. **23**(3): p. 316-323.
30. Gaudet, R. and D.C. Wiley, *Structure of the ABC ATPase domain of human TAP1, the transporter associated with antigen processing.* Embo Journal, 2001. **20**(17): p. 4964-4972.
31. Ramaen, O., et al., *Structure of the human multidrug resistance protein 1 nucleotide binding domain 1 bound to Mg2+/ATP reveals a non-productive catalytic site.* Journal of Molecular Biology, 2006. **359**(4): p. 940-949.
32. Zaitseva, J., et al., *A molecular understanding of the catalytic cycle of the nucleotide-binding domain of the ABC transporter HlyB.* Biochemical Society Transactions, 2005. **33**: p. 990-995.
33. Chen, J., et al., *A tweezers-like motion of the ATP-binding cassette dimer in an ABC transport cycle.* Molecular Cell, 2003. **12**(3): p. 651-661.
34. Sarkadi, B., et al., *ABCG2 - a transporter for all seasons.* Febs Letters, 2004. **567**(1): p. 116-120.
35. Bard, S.M., *Multixenobiotic resistance as a cellular defense mechanism in aquatic organisms.* Aquatic Toxicology, 2000. **48**(4): p. 357-389.
36. Ferreira, M., J. Costa, and M.A. Reis-Henriques, *ABC transporters in fish species: a review.* Frontiers in Physiology, 2014. **5**.

37. Nakagawa, H., et al., *Ubiquitin-mediated proteasomal degradation of non-synonymous SNP variants of human ABC transporter ABCG2.* Biochem J, 2008. **411**(3): p. 623-31.
38. Verdon, G., et al., *Crystal structures of the ATPase subunit of the glucose ABC transporter from Sulfolobus solfataricus: nucleotide-free and nucleotide-bound conformations.* J Mol Biol, 2003. **330**(2): p. 343-58.
39. Allen, J.D., S.C. Jackson, and A.H. Schinkel, *A mutation hot spot in the Bcrp1 (Abcg2) multidrug transporter in mouse cell lines selected for Doxorubicin resistance.* Cancer Res, 2002. **62**(8): p. 2294-9.
40. Honjo, Y., et al., *Acquired mutations in the MXR/BCRP/ABCP gene alter substrate specificity in MXR/BCRP/ABCP-overexpressing cells.* Cancer Res, 2001. **61**(18): p. 6635-9.

ISBN: 978-82-575-1437-2
ISSN: 1894-6402

Norwegian University
of Life Sciences

Postboks 5003
NO-1432 Ås, Norway
+47 67 23 00 00
www.nmbu.no